(12) FC

AFCRL-TR-76-0023
PHYSICAL SCIENCES RESEARCH PAPERS, NO. 654

An Invariant Imbedding, Orders-of-Scattering Approach to Particle Transport in a Slab

JOHN C. GARTH
STANLEY WOOLF

14 January 1976

This research was partially sponsored by the Defense Advanced Research Projects Agency under ARPA Order No. 2180.

SOLID STATE SCIENCES LABORATORY PROJECT 5621
AIR FORCE CAMBRIDGE RESEARCH LABORATORIES
HANSCOM AFB, MASSACHUSETTS 01731

AIR FORCE SYSTEMS COMMAND, USAF

BEST
AVAILABLE COPY

Qualified requestors may obtain additional copies from the Defense Documentation Center. All others should apply to the National Technical Information Service.

Unclassified

SECURITY CLASSIFICATION OF THIS PAGE (When Data Entered)

REPORT DOCUMENTATION PAGE

READ INSTRUCTIONS BEFORE COMPLETING FORM

14

1. REPORT NUMBER: AFCRL-TR-76-0023, AFCRL-PSRP-654

2. GOVT ACCESSION NO.

3. RECIPIENT'S CATALOG NUMBER

4. TITLE (and Subtitle): 6 AN INVARIANT IMBEDDING, ORDERS-OF-SCATTERING APPROACH TO PARTICLE TRANSPORT IN A SLAB.

5. TYPE OF REPORT & PERIOD COVERED: Scientific. Interim.

6. PERFORMING ORG. REPORT NUMBER: PSRP. No. 654

7. AUTHOR(s): 10 John C. Garth, Stanley Woolf*

8. CONTRACT OR GRANT NUMBER(s): 9 Physical sciences research papers

9. PERFORMING ORGANIZATION NAME AND ADDRESS: Air Force Cambridge Research Laboratories (LQ), Hanscom AFB, Massachusetts 01731

10. PROGRAM ELEMENT, PROJECT, TASK AREA & WORK UNIT NUMBERS: 61102F, 56210905 — 12 177p.

11. CONTROLLING OFFICE NAME AND ADDRESS: Air Force Cambridge Research Laboratories (LQ), Hanscom AFB, Massachusetts 01731

12. REPORT DATE: 11 13 January 1976

13. NUMBER OF PAGES: 166

14. MONITORING AGENCY NAME & ADDRESS (if different from Controlling Office): 16 AF-5621

15. SECURITY CLASS. (of this report): Unclassified

15a. DECLASSIFICATION/DOWNGRADING SCHEDULE

16. DISTRIBUTION STATEMENT (of this Report)

Approved for public release; distribution unlimited.

15 ARPA Order-2180

17. DISTRIBUTION STATEMENT (of the abstract entered in Block 20, if different from Report): 17 562109

18. SUPPLEMENTARY NOTES

*Stanley Woolf is employed by Arcon Corporation, Wakefield, Massachusetts. This work was partially sponsored by the Defense Advanced Research Projects Agency under ARPA Order 2180.

19. KEY WORDS (Continue on reverse side if necessary and identify by block number)

Invariant imbedding
Transport theory
Orders-of-scattering
Electron-phonon scattering

20. ABSTRACT (Continue on reverse side if necessary and identify by block number)

A novel, simplified approach to particle transport in slabs is given. The number of particles transmitted and reflected by a slab of finite thickness is obtained as a function of the number of collisions the particles receive. This "orders-of-scattering" solution is facilitated by an invariant imbedding approach which leads to a set of integral recursion relations between transmitted and reflected particle currents. Solutions are given for both one-dimensional and three-dimensional transport in slabs for an arbitrary anisotropic scattering law.

DD FORM 1 JAN 73 1473 EDITION OF 1 NOV 65 IS OBSOLETE

Unclassified

SECURITY CLASSIFICATION OF THIS PAGE (When Data Entered)

1/B

411 500

20. (Cont.)

For comparison, the one-dimensional Boltzmann equation for isotropic scattering is formulated and the orders-of-scattering solution found numerically. A Monte Carlo calculation for orders-of-scattering is also described. These methods provide a valuable numerical check on the invariant imbedding solution, but they also demonstrate the greater computing efficiency of the new method. Finally, numerical solutions for three different cases of anisotropic scattering are given, including application to the case of electron-phonon scattering in solids.

Preface

The authors of this report wish to thank Dr. William L. Filippone of the Department of Nuclear Engineering at the University of Lowell, Lowell, Massachusetts for his valuable suggestions and encouragement. As part of a research program on electron transport in insulating solids, this work was partially supported under ARPA Order 2180 by the Material Science Office of the Defense Advanced Research Projects Agency. The cooperation and assistance of Mr. John Pustaver of the Analysis and Simulation Branch (SUYA) is also gratefully acknowledged.

Contents

Contents

Illustrations

Tables

An Invariant Imbedding, Orders-of-Scattering Approach to Particle Transport in a Slab

1. INTRODUCTION

Invariant imbedding theory has been applied extensively to particle transport problems, especially in nuclear particle shielding calculations. The theory was originated by Ambarzumian[1] in 1943 as a means of estimating reflection of light by foggy media. A later adaptation for use in particle transport calculations was developed by Bellman, Kalaba, and Wing[2] in 1960. Since that time, Bellman,[3] Mingle,[4] and others have applied invariant imbedding theory extensively to describe radiative transfer in slabs, most often for radiation shielding and dosimetry calculations. A principal advantage of the invariant imbedding approach is that it is a direct calculation of the current of particles emerging from a scattering medium and does not require the calculation of the particle flux at all points within the medium. Conventional invariant imbedding calculations have the disadvantage that they often prove to be computationally burdensome, hence their practicality has been somewhat limited. The word "conventional" is applied here to denote the

(Received for publication 13 January 1976)

1. Ambarzumian, V.A. (1942) Soviet Astron. AJ, 19:1.
2. Bellman, R., Kalaba, R., and Wing, G.M. (1960) J. Math. Phys. 1:280.
3. Bellman, R., Kalaba, R., and Prestrud, M.C. (1963) Invariant Imbedding and Radiative Transfer in Slabs of Finite Thickness, American Elsevier, New York.
4. Mingle, J.O. (1967) Nucl. Sci. Eng. 28:177.

class of calculations which at once include all orders of scattering, zero to infinity, and for which the dependent variable, the particle current, is an explicit function of particle energy, position, and direction of motion. For this reason invariant imbedding has not been extensively applied to such problems as slowing down of neutrons and electrons in scattering media. This has not proven to be a serious handicap at high energies where continuous slowing down theory can be applied. At low energies, however, the success achieved by alternative methods is not nearly as formidable. Prominent among these alternatives are methods spanning the wide range of sophistication from the direct solution of the Boltzmann equation to Monte Carlo calculations. The Boltzmann approach consists of a flux calculation, which even for the case of isotropic scattering is not trivial. For scattering other than isotropic, spherical harmonic expansions can be performed on either the differential or integral form of the Boltzmann equation. This approach becomes impractical when the scattering anisotropy extends beyond first order. At the other extreme, Monte Carlo calculations, while providing a relatively certain means of achieving the solution in most cases, can be costly when high accuracy is required.

A class of particle transport problems exists for which a variation of the invariant imbedding method seems most appropriate. This situation can arise when the average energy of a particle can be reasonably well correlated with the number of collisions it has undergone in the course of transport through a scattering medium. For these cases a method for calculating emergent nth scattered particle currents from scattering media has been developed which combines an orders-of-scattering formulation with the familiar invariant imbedding method.[5*] The equations for the transmitted and reflected current are evolved through the consideration of the dependence of the nth scattered current on the lower order scattered currents. The final expressions for these currents assume the form of coupled integral incursion relations expressing the interdependence of the currents of the various scattering orders. In the sections that follow, these invariant imbedding recursion relations will first be developed for the simple one-dimensional case or rod model, and then for the case of angle-dependent particle transport in a slab geometry. In the former case comparisons are made with the exact analytic result for the total transmitted and reflected currents obtained from the classical rod model, and for the case of scattering in a slab geometry, the results are compared with those obtained by two independent methods, the solution of the one-dimensional Boltzmann equation

---

5. Mingle, J.O. (1972) J. Math. Anal. Appl. 38:53.

*Mingle[5] developed an orders-of-scattering theory for isotropic scattering based on an expansion of infinite order transmitted and reflected currents in terms of their finite order components. He applied this formulation to the determination of critical multiplication factors in the slab geometry.

for isotropic scatter and a Monte Carlo calculation. The application of the orders-of-scattering invariant imbedding method, henceforth to be referred to as "OOSII", to anisotropic scattering situations is then demonstrated for three cases, strong anisotropy such as encountered in the elastic scattering of neutrons from hydrogen, mild anisotropy such as encountered in the elastic scatter of neutrons from carbon nuclei, and extreme anisotropy such as can occur in the scattering of low energy (hot) electrons by phonons, a process for which a screened Rutherford cross section has been proposed on the basis of empirical observations.[6]

2. SCATTERING IN ONE DIMENSION

2.1 Development of Current Equations

It is first appropriate to develop the OOSII equations for the simplest geometrical case, that of one-dimensional scattering, or as many authors term it,[7] the rod model. Adoption of this approach is advantageous for several reasons, the most notable of which are:

(1) The geometric simplification allows for the development of the basic equations without the complicating presence of angular variables which would tend to obscure the fundamental logic; and

(2) The results obtained can be compared with well-known analytical results, thus providing verification of both the basic equations and the numerical means for their solution.

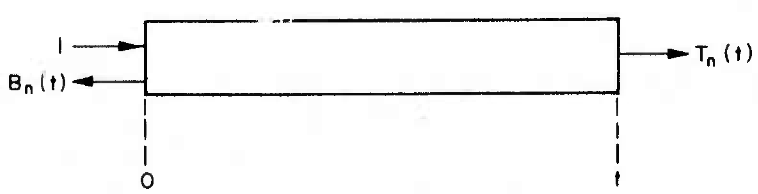

Figure 1. The One-Dimensional Geometry

6. Garth, J.C., Parke, N.G., and DeStefano, T.H. (1974) Bull. Am. Phys. Soc., Ser. II, 19 No. 3:232.

7. Wing, G.M. (1962) An Introduction to Transport Theory, John Wiley and Sons, Inc., New York.

If a unit particle current is injected into the left end of a rod of length t (Figure 1, then the quantities $T_n(t)$ and $B_n(t)$ can be defined such that

$$\left\{\begin{matrix} T_n(t) \\ B_n(t) \end{matrix}\right\} \text{ is the}$$

$$\left\{\begin{matrix} \text{transmitted} \\ \text{reflected} \end{matrix}\right\} \quad \text{particle current emerging from the}$$

$$\left\{\begin{matrix} \text{right} \\ \text{left} \end{matrix}\right\} \quad \text{end of the rod of length t after n interactions.}$$

First, to be considered is the case of forward scattering alone. If the current $T_n(t)$ for a rod of length t after n interactions is known, then the transmitted current emergent from a rod of length t+dt after n interactions consisting of scattering in the forward direction alone is

$$T_n(t+dt) = T_n(t)\left[1 - \frac{dt}{\lambda}\right] + f\,T_{n-1}(t)\,\frac{dt}{\lambda}\,, \tag{1}$$

where λ is the scattering mean-free-path, and f is the probability of scatter in the forward direction. The first term on the right represents the transmitted current emergent from the rod of length t after n interactions which then escapes unscattered through the increment of length dt (Figure 2a). The probability of no interaction occurring in dt is $(1-dt/\lambda)$. The second term represents the transmitted current emergent from the rod of length t after n-1 interactions which then undergoes one more interaction in dt with probability dt/λ (Figure 2b). This nth interaction is a forward scattering with probability f. Rearrangement of the terms in Eq. (1) gives

$$T_n(t+dt) - T_n(t) = \left[-T_n(t) + f\,T_{n-1}(t)\right]\frac{dt}{\lambda} \tag{2}$$

or

$$\frac{dT_n}{dt} = \frac{1}{\lambda}\left[-T_n(t) + fT_{n-1}(t)\right]\,. \tag{3}$$

Making use of the identity

$$\frac{d}{dt}\left[e^{t/\lambda}\,T_n(t)\right] = e^{t/\lambda}\,\frac{dT_n}{dt} + \frac{1}{\lambda}\,e^{t/\lambda}T_n(t)\,, \tag{4a}$$

or

$$\frac{dT_n}{dt} = e^{-t/\lambda} \frac{d}{dt}\left(e^{t/\lambda} T_n(t)\right) - \frac{1}{\lambda} T_n(t) , \tag{4b}$$

it is found that

$$\frac{d}{dt}\left(e^{t/\lambda} T_n(t)\right) = e^{t/\lambda} \frac{f}{\lambda} T_{n-1}(t) . \tag{5a}$$

Integration over the rod length yields

$$e^{t/\lambda} T_n(t) - T_n(o) = \frac{f}{\lambda} \int_o^t e^{x/\lambda} T_{n-1}(x)\, dx , \tag{5b}$$

subject to the conditions

$$T_n(0) = 0, \; n \leq 1 , \tag{6a}$$

and

$$T_o(t) = e^{-t/\lambda} , \tag{6b}$$

so that the emergent transmitted current is given by

$$T_n(t) = \frac{f}{\lambda} e^{-t/\lambda} \int_o^t e^{x/\lambda} T_{n-1}(x) dx . \tag{7}$$

Upon inspection of the first few T_n solutions, it becomes apparent that the general expression for $T_n(t)$ is

$$T_n(t) = e^{-t/\lambda} \frac{f^n \left(\frac{t}{\lambda}\right)^n}{n!} , \tag{8}$$

from which it can be seen that for the special case where $f = 1$, $T_n(t)$ is Poisson distributed.

At this point the one dimensional scattering picture is incomplete since backscatter has not yet been considered. The situation where backscatter gives rise to a contribution to the transmitted current can be examined by considering the following: a particle first survives $n-m-1$ $(0 \leq m \leq n-1)$ interactions in $(0, t)$, as shown in Figure 2c, thus giving rise to a transmitted current at t of $T_{n-m-1}(t)$. A single backscatter then occurs in the interval dt with probability $b(dt/\lambda)$, where b is the

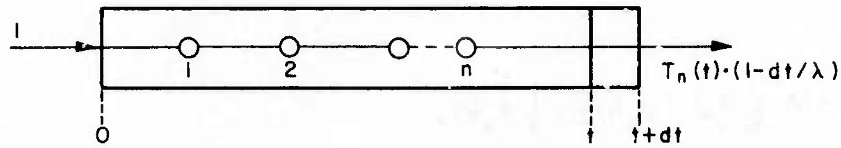

Figure 2a. Transmission Following n Interactions in (0, t)

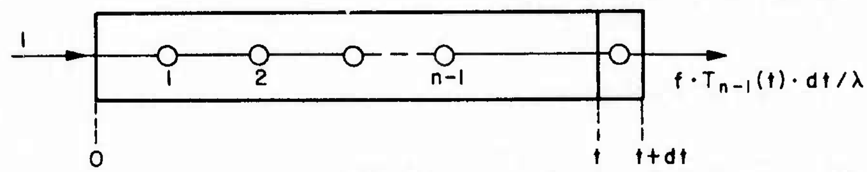

Figure 2b. Transmission Following n-1 Interactions in (0, t) and One Forward Scatter in dt

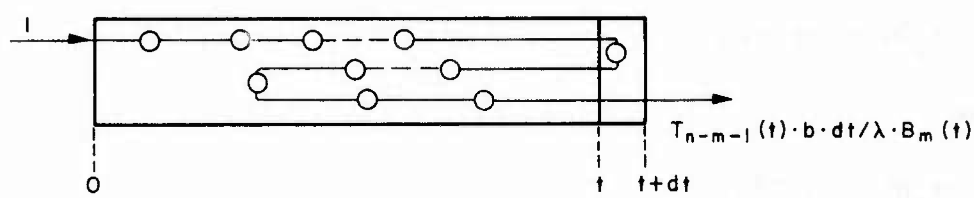

Figure 2c. Transmission Following n-m-1 Interactions in (0, t), a Single Backscatter in dt and a Reflection from (0, t) in the Forward Direction after m Interactions

probability of backscatter given that an interaction takes place in dt with probability (dt/λ). The particle, having returned to (0, t), is then backscattered out of t after m interactions. The number of such backscattered particles is $B_m(t)$, and the total number of interactions occurring in the course of the trajectory is $(n-m-1)+m+1 = n$. The possibility of the particle having a second collision in the interval dt can be ignored since the joint probability that a particle suffers two collisions in dt in the same trajectory is proportional to $(dt)^2$ and is therefore negligible. The transmitted current contribution due to backscatter is then

$$b\sum_{m=1}^{n-1} B_m(t)\, T_{n-m-1}(t)\, \frac{dt}{\lambda}\ .$$

The summation is necessary to account for all possible combinations of events which may result in a transmission after n interactions. The extreme cases occur when m=1 and m=n-1. In the first instance the particle enters dt after having been

transmitted through (0, t) with n-2 interactions. The single backscatter occurs in dt, and then another single backscatter out of (0, t) takes place. When m=n-1, the particle enters dt unscattered in (0, t), undergoes the single backscatter in dt, and is subsequently backscattered out of (0, t) after n-1 interactions.

When the backscatter contribution is added to Eq. (1), the transmitted current emergent from a rod of length t+dt after n interactions is

$$T_n(t+dt) = T_n(t)\left[1 - \frac{dt}{\lambda}\right] + f\,T_{n-1}(t)\,\frac{dt}{\lambda} + \frac{b}{\lambda}\sum_{m=1}^{n-1} B_m(t)\,T_{n-m-1}(t)\,dt\,. \tag{9}$$

As was done for the case of forward scattering alone, application of the appropriate integrating factor leads to

$$T_n(t) = \frac{f}{\lambda}e^{-t/\lambda}\int_0^t e^{x/\lambda}\,T_{n-1}(x)\,dx + \frac{b}{\lambda}e^{-t/\lambda}\sum_{m=1}^{n-1}\int_0^t e^{x/\lambda}\,B_m(x)\,T_{n-m-1}(x)\,dx\,. \tag{10}$$

In order that useful solutions of Eq. (10) may be obtained, a similar recursion formula must be derived for the reflected current $B_n(t)$.

If the reflected current for a rod of length t is known, then the expression for the reflected current from a rod of length t+dt as a result of having undergone n interactions can be written as

$$B_n(t+dt) = B_n(t) + b\sum_{m=0}^{n-1} T_{n-m-1}(t)\,T_m(t)\,\frac{dt}{\lambda}\,, \tag{11}$$

where b is defined as in Eq. (10). The first term on the right, $B_n(t)$, represents the reflected current from (0, t) after n interactions (Figure 3a). The second term is the total of contributions to the reflected current resulting from single backscatter in dt (Figure 3b). Each contribution in this sum consists of three factors. The current due to a particle which first survives n-m-1 interactions to be transmitted through (0, t) is $T_{n-m-1}(t)$. A single backscatter occurs in dt with probability $b(dt/\lambda)$, and the particle then survives m interactions to be transmitted through the interval (0, t) in the reverse direction, giving rise to a current $T_m(t)$. The total of interactions for this term is (n-m-1)+m+1 = n, and the extreme cases for the values of m occur when m=0 (no scattering during the first trajectory segment) and when m=n-1 (no scattering on the return segment). Rearrangement of the terms of Eq. (11) in a manner similar to that for the transmission case yields

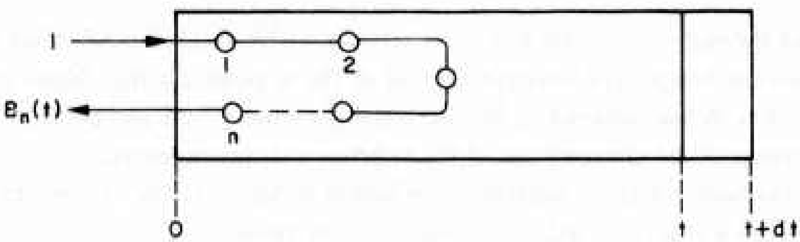

Figure 3a. Reflection Following n Interactions in (0, t)

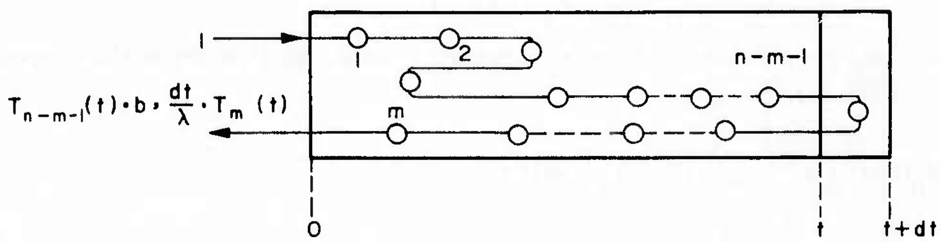

Figure 3b. Reflection Following n-m-1 Interactions in (0,t), a Single Backscatter in dt, and a Back Transmission from (0,t) after m Interactions

$$\frac{dB_n}{dt} = \frac{b}{\lambda} \sum_{m=0}^{n-1} T_{n-m-1}(t)\, T_m(t) \, , \tag{12}$$

or upon integration

$$B_n(t) = \frac{b}{\lambda} \sum_{m=0}^{n-1} \int_0^t T_{n-m-1}(x)\, T_m(x)\, dx \, , \tag{13}$$

subject to the conditions

$$B_n(0) = 0 \, , \tag{14a}$$

$$B_o(t) = 0 \, . \tag{14b}$$

2.2 Solution of the One-Dimensional Current Equations

Equations (10) and (13), together with the initial conditions of Eq. (6) and Eq. (14), form the following set of coupled integral recursion relations:

$$T_n(t) = \frac{f}{\lambda} e^{-t/\lambda} \int_o^t e^{x/\lambda} T_{n-1}(x)dx + \frac{b}{\lambda} e^{-t/\lambda} \sum_{m=1}^{n-1} \int_o^t e^{x/\lambda} B_m(x) T_{n-m-1}(x)dx \,, \tag{10}$$

$$B_n(t) = \frac{b}{\lambda} \sum_{m=0}^{n-1} \int_o^t T_{n-m-1}(x)\, T_m(x)\, dx \,, \tag{13}$$

$$T_n(0) = 0 \,, \qquad n \leq 1 \,, \tag{6a}$$

$$T_o(t) = e^{-t/\lambda} \,, \tag{6b}$$

$$B_n(0) = 0 \,, \tag{14a}$$

$$B_o(t) = 0 \,. \tag{14b}$$

Although it is possible to obtain exact solutions for all orders of scattering, such an analytical approach becomes impractical beyond n=3. The expressions for T_n and B_n are listed below for $n \leq 3$.

$$T_o(t) = e^{-t/\lambda} \,, \tag{15a}$$

$$T_1(t) = e^{-t/\lambda}\, f \frac{t}{\lambda} \,, \tag{15b}$$

$$T_2(t) = e^{-t/\lambda} \left[\frac{f^2 t^2}{2\lambda^2} + \frac{b^2 t}{2\lambda} - \frac{b^2}{4} \left(1 - e^{-2t/\lambda}\right) \right] \,, \tag{15c}$$

$$T_3(t) = e^{-t/\lambda} \frac{f^3 t^3}{6\lambda^3} + \frac{fb^2}{2} \left(t^2/\lambda^2 + t/2\lambda - 1\right) + \frac{fb^2}{2} \left(1 - \frac{3}{2} \frac{t}{\lambda}\right) e^{-2t/\lambda} \,, \tag{15d}$$

$$B_1(t) = \frac{b}{2} \left[1 - e^{-2t/\lambda}\right] \,, \tag{16a}$$

$$B_2(t) = \frac{fb}{2} \left[1 - (1 + 2t/\lambda)\, e^{-2t/\lambda} \right] \,, \tag{16b}$$

$$B_3(t) = \frac{f^2 b}{2} - \frac{f^2 b}{2} \left(2\, t^2/\lambda^2 + 2\frac{t}{\lambda} + 1\right) e^{-2t/\lambda} + \frac{b^3}{8} \frac{t}{\lambda} e^{-2t/\lambda} + \frac{b^3}{8} \left(1 - e^{-4t/\lambda}\right) \,. \tag{16c}$$

Numerical solutions for Eqs. (10) and (13) were obtained for values of n up to 40 by means of a semi-analytical method based on the assumption that the T_n and

B_n could be considered piecewise linear. If an appropriate integration interval (t_1, t_2) could be found over which the approximation holds, then integrals of the type occurring in Eqs. (10) and (13) could be readily evaluated. The linearity assumptions are

$$\left.\begin{aligned} T_n(x) &\doteq m_T^n\, x + b_T^n \qquad &(17a)\\ \text{and} & \\ B_n(x) &\doteq m_B^n\, x + b_B^b \qquad &(17b) \end{aligned}\right\} \quad (t_1 \le x \le t_2),$$

where m_T^n and m_B^n are the slopes over the interval (t_1, t_2) for the nth scattered transmitted and reflected currents, respectively, and b_T^n and b_B^n are the corresponding intercepts at $x = t_1$. There are three distinct integral forms present in Eqs. (10) and (13), which under the above assumptions, are readily evaluated. That is

$$\int_{t_1}^{t_2} e^{x/\lambda}\, T_\ell(x)\, dx \doteq \lambda e^{x/\lambda} \left[m_T^\ell (x - \lambda) + b_T^\ell \right] \Bigg|_{t_1}^{t_2}, \tag{18a}$$

$$\int_{t_1}^{t_2} e^{x/\lambda}\, T_\ell(x)\, B_k(x)\, dx \doteq \lambda e^{x/\lambda} \Big[m_T^\ell\, m_B^k (x^2 - 2\lambda x + 2\lambda^2) + (m_B^k\, b_T^\ell + m_T^\ell\, b_B^k)(x - \lambda) + b_T^\ell\, b_B^k \Big] \Bigg|_{t_1}^{t_2}, \tag{18b}$$

$$\int_{t_1}^{t_2} T_\ell(x)\, T_k(x)\, dx \doteq \left[m_T^\ell\, m_T^k \frac{x^3}{3} + (m_T^\ell\, b_T^k + m_T^k\, b_T^\ell) \frac{x^2}{2} + b_T^\ell\, b_T^k\, x \right] \Bigg|_{t_1}^{t_2}. \tag{18c}$$

Since exact expressions were available for $T_n(t)$ and $B_n(t)$ up to $n=3$, the approximate method of solution was employed only for values of $n \geq 4$.

A computer code was written to solve the system of recursion relations. Slopes and intercepts for the first three orders of scattering were readily available from the exact expressions. The computer program was written in such a way as to compute the currents for all orders of scattering, up to $n=40$, in one pass for each increment of rod length. Computations were made of T_n and B_n for 51 values of rod length ranging from $t=0.0$ to $t=10.0$ mean-free-paths in steps of 0.2 mfp. It was found that an integration interval of 0.004 mfp proved adequate to satisfy the piecewise linearity assumption. This was verified by a comparison of the computational results for the case where $f=1$, $b=0$, with exact answers obtained by

evaluation of the Poisson distribution. Additional verification was obtained by comparison of the current totals for other values of f and b over the first 40 orders of scattering with exact expressions obtained for the totals over all orders by the "classical" method of solution for the rod model. The values of the three integral forms of Eqs. (18 a, b, c) were accumulated from one step in t to the next, eliminating the necessity of starting the integration from t=0 for each rod length of interest.

Plots of the computational results are given in Figures 4 through 9. The transmission and reflection current curves are plotted vs order of scattering for rods ranging in length from 1 to 10 mfp in steps of 1 mfp (the scattering mean-free-path was assumed constant for all collision orders) and for the following values of the scattering probability:

(1) f=0.5, b=0.5 --- Figures 4a, b
(2) f=0.6, b=0.4 --- Figures 5a, b
(3) f=0.7, b=0.3 --- Figures 6a, b
(4) f=0.8, b=0.2 --- Figures 7a, b
(5) f=0.9, b=0.1 --- Figures 8a, b
(6) f=1.0, b=0.0 --- Figure 9a

and

(7) Poisson distribution curves --- Figure 9b.

The last set, Figures 9a and b, are included for the purposes of comparison. Only cases of conservative scattering (f+b=1) were considered, although this was not a necessary restriction.

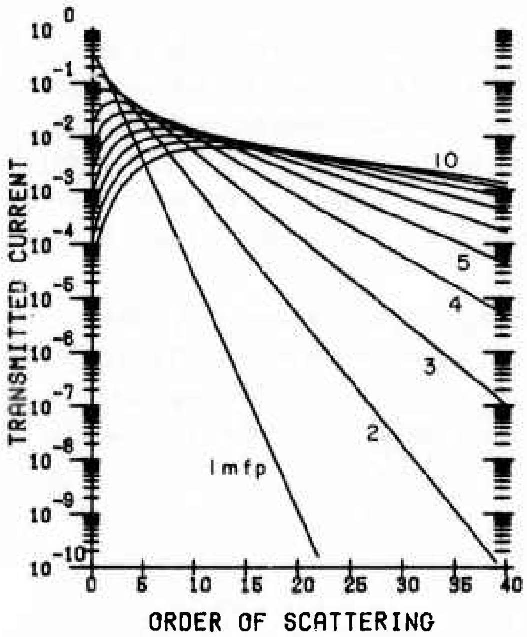

Figure 4a. Transmitted Current vs Order of Scattering for 10 Rod Lengths: f=0.5

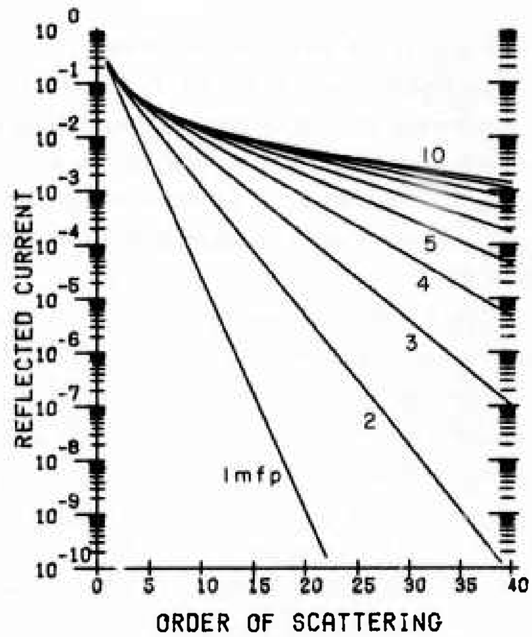

Figure 4b. Reflected Current vs Order of Scattering for 10 Rod Lengths: f=0.5

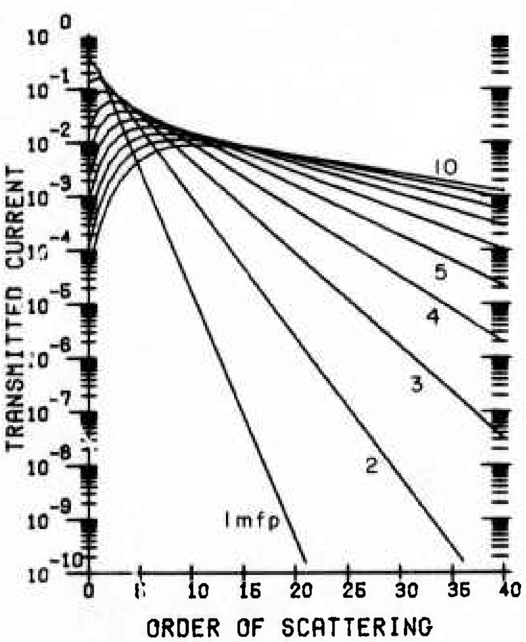

Figure 5a. Transmitted Current vs Order of Scattering for 10 Rod Lengths: f=0.6

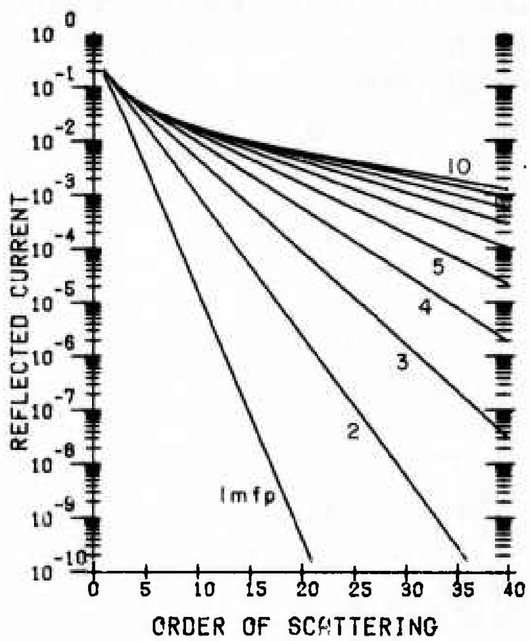

Figure 5b. Reflected Current vs Order of Scattering for 10 Rod Lengths: f=0.6

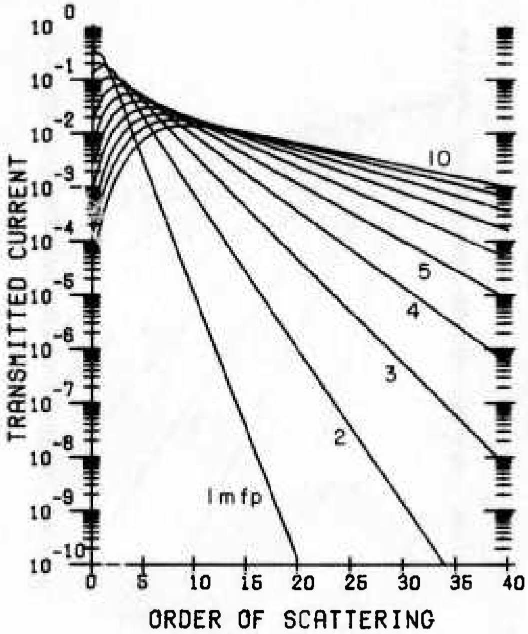

Figure 6a. Transmitted Current vs Order of Scattering for 10 Rod Lengths: f=0.7

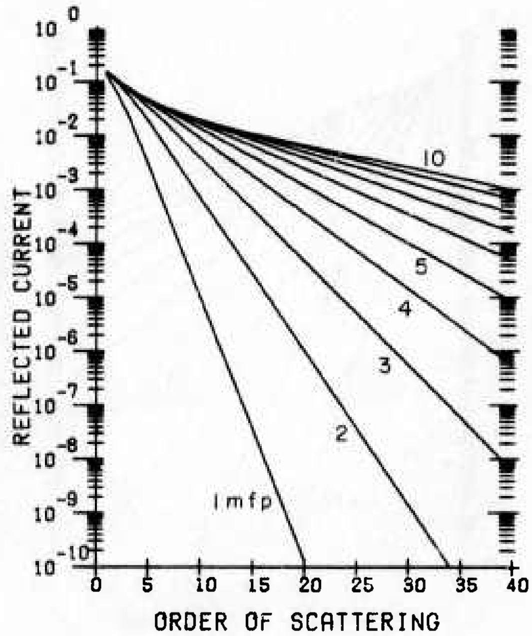

Figure 6b. Reflected Current vs Order of Scattering for 10 Rod Lengths: f=0.7

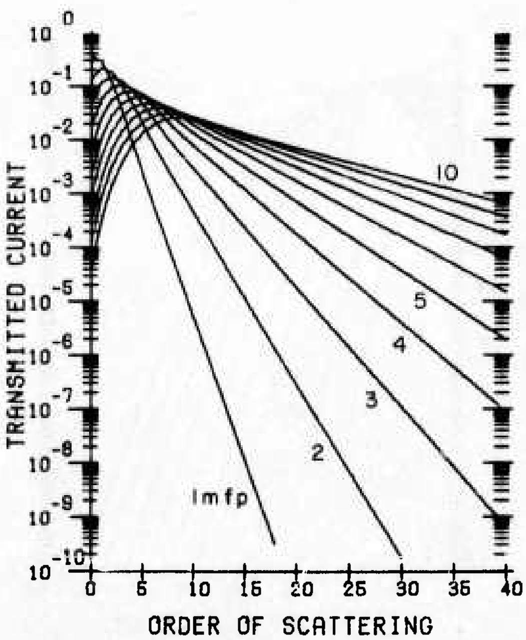

Figure 7a. Transmitted Current vs Order of Scattering for 10 Rod Lengths: f=0.8

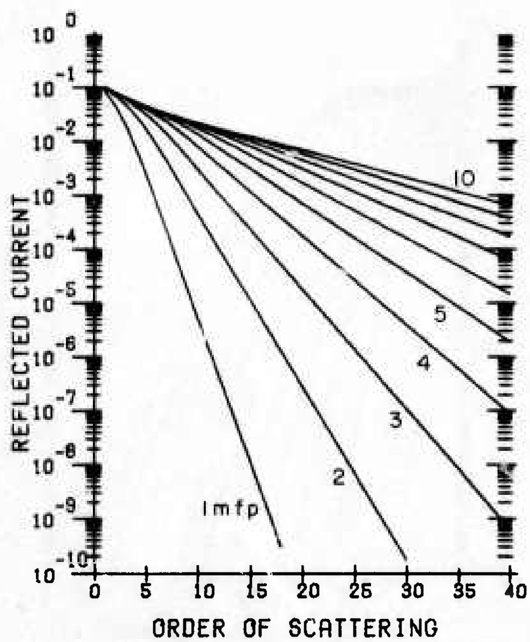

Figure 7b. Reflected Current vs Order of Scattering for 10 Rod Lengths: f=0.8

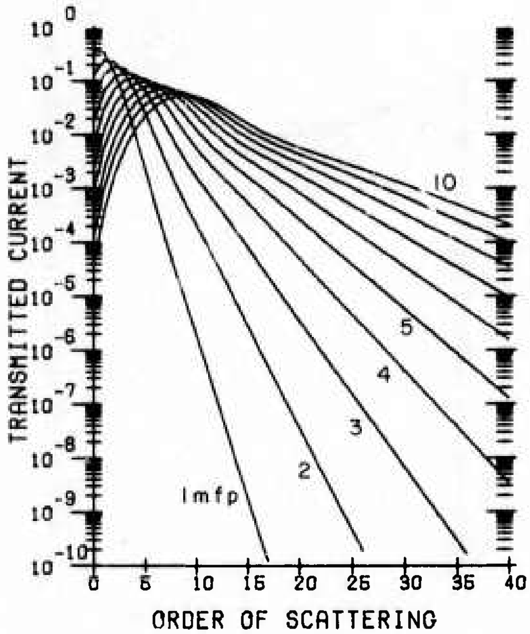

Figure 8a. Transmitted Current vs Order of Scattering for 10 Rod Lengths: f=0.9

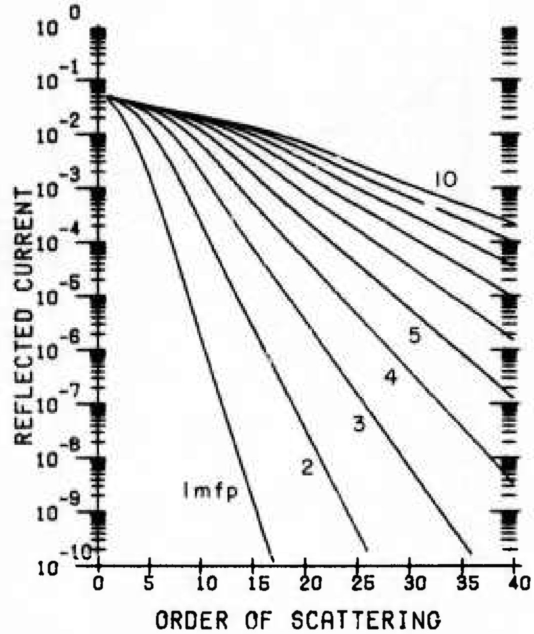

Figure 8b. Reflected Current vs Order of Scattering for 10 Rod Lengths: f=0.9

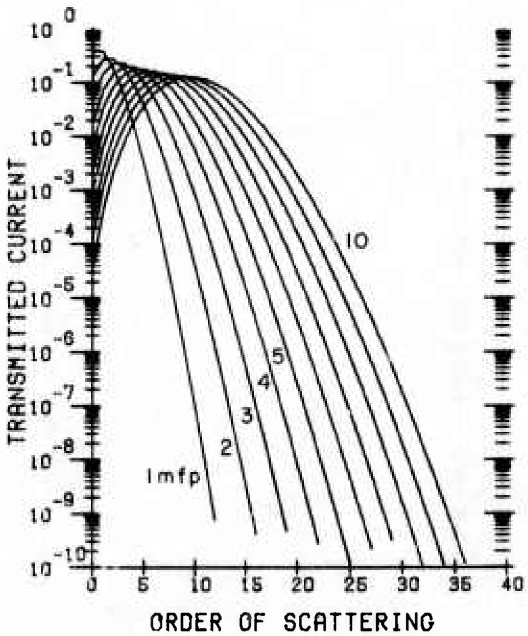

Figure 9a. Transmitted Current vs Order of Scattering for 10 Rod Lengths: f=1.0

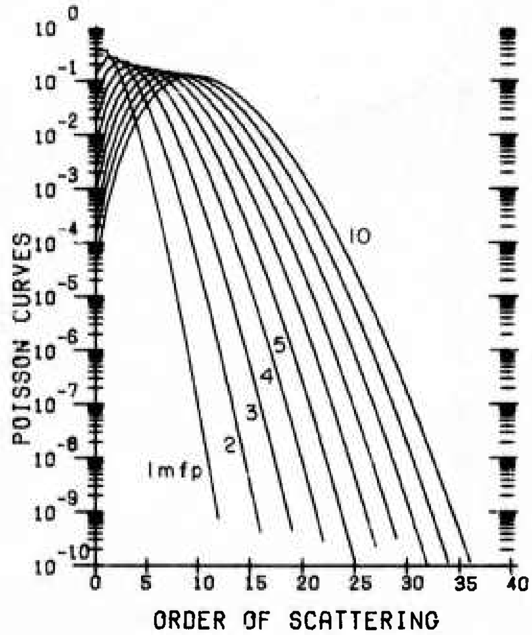

Figure 9b. Poisson Curves Plotted vs Order of Scattering

2.3 Comparison of One-Dimensional Results with those Obtained Using the Classical Treatment of the Rod Model

An independent means of testing the validity of the OOSII one-dimensional results can be found in the classical treatment of the rod model.[7] Simple expressions for the total (infinite order) transmitted and reflected currents can be readily obtained which, when evaluated, should yield results which agree closely with the totals of the finite order currents up to 40 orders, at least for the shorter rod lengths. Determination of the total currents according to the classical treatment proceeds as follows:

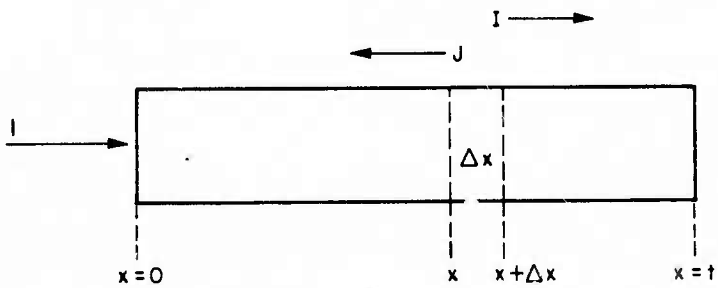

Figure 10. Classical Rod Model Geometry

Let there be an incident current of 1 particle entering a rod of length t at x=0 (Figure 10). Let there be defined two particle currents at the interior point x such that I(x) is the total particle current moving to the right at x, and J(x) is the total particle current moving to the left at x. The boundary conditions are

$$I(0) = 1, \tag{19a}$$

$$J(t) = 0. \tag{19b}$$

The probability of a collision occurring in the interval Δx is

$$\frac{\Delta x}{\lambda} + O(\Delta x),$$

where λ is the scattering mean-free-path, as before. The probability of forward scatter, f, and backscatter, b, are defined as before. Then the number of particles moving to the right undergoing a collision in Δx is

$$f\, I(x) \frac{\Delta x}{\lambda} + O(\Delta x)^2 .$$

The number of particles moving to the right undergoing no collision in Δx is

$$(1 - \frac{\Delta x}{\lambda}) I(x) + O(\Delta x)^2 .$$

In addition, particles moving to the left may have a collision in Δx resulting in backscatter to the right. The number of such backscattered particles is

$$b J(x+\Delta x) \frac{\Delta x}{\lambda} + O(\Delta x)^2 .$$

If these are added together, the total right-moving current at $x+\Delta x$ is

$$I(x+\Delta x) = I(x) + I(x) \frac{\Delta x}{\lambda} (f-1) + b J(x+\Delta x) \frac{\Delta x}{\lambda} ,$$

or

$$\frac{dI}{dx} = \frac{f-1}{\lambda} I(x) + \frac{b}{\lambda} J(x) . \tag{20}$$

Similary, for the left-moving current, the number moving to the left undergoing a collision in Δx is

$$f J(x+\Delta x) \frac{\Delta x}{\lambda} + O(\Delta x)^2 .$$

The uncollided left-moving current is

$$(1 - \frac{\Delta x}{\lambda}) J(x+\Delta x) + O(\Delta x)^2 .$$

and the backscattered contribution from the right-moving current is

$$b I(x) \frac{\Delta x}{\lambda} + O(\Delta x)^2 .$$

When these are added together, the total left-moving current is

$$J(x) = J(x+\Delta x) + (f-1) J(x+\Delta x) \frac{\Delta x}{\lambda} + b I(x) \frac{\Delta x}{\lambda} ,$$

or

$$-\frac{dJ}{dx} = \frac{f-1}{\lambda} J(x) + \frac{b}{\lambda} I(x) . \tag{21}$$

The system of coupled equations, Eqs. (20) and (21) together with the boundary conditions of Eqs. (19a, b), can be readily solved, particularly for the case where f+b= 1. Differentiation of Eq. (20) and substitution of Eq. (21) for dJ/dx yields the following second-order differential equation for I(x);

$$\frac{d^2I}{dx^2} + (b^2 - (f-1)^2)\, I = 0 \,, \tag{22}$$

which for the case of conservative scattering leads to

$$\frac{d^2I}{dx^2} = 0 \,. \tag{23}$$

Therefore, I(x) may be written in the form

$$I(x) = \alpha x + \beta \,, \tag{24}$$

where α and β are undetermined constants.
A similar procedure applied to Eq. (21) yields the same form for the left-moving current:

$$J(x) = \gamma x + \delta \,. \tag{25}$$

Application of the boundary conditions of Eqs. (19a, b) to Eqs. (24) and (25) eliminates two of the unknowns. That is

$$I(0) = 1 \rightarrow \beta = 1 \,, \tag{26}$$

$$J(t) = 0 \rightarrow \gamma t = -\delta \,. \tag{27}$$

Substitution of Eq. (19b) into Eqs. (20) and (21) provides a set of differential boundary conditions to eliminate the two remaining constants as follows:

$$\left.\frac{dI}{dx}\right|_t = \frac{(f-1)}{\lambda}\, I(t) \rightarrow \alpha = \frac{f-1}{\lambda-(f-1)t} \,, \tag{28}$$

$$\left.\frac{dJ}{dx}\right|_t = -\frac{b}{\lambda}\, I(t) \rightarrow \gamma = \frac{-b}{\lambda-(f-1)t} \,. \tag{29}$$

With the constants now determined, the expressions for I(x) and J(x) may be rewritten as

$$I(x) = 1 - \frac{bx}{1+bt}, \tag{24}$$

$$J(x) = \frac{b(t-x)}{1+bt}. \tag{25}$$

The forward current at the boundary x=t, I(t), and the reflected current at x=0, J(0), should correspond to the summation of the transmitted and reflected currents obtained by means of the OOSII method. That is

$$\sum_{n=0}^{\infty} T_n(t) = \frac{1}{1+bt} \tag{30}$$

and

$$\sum_{n=1}^{\infty} B_n(t) = \frac{bt}{1+bt}. \tag{31}$$

The extent to which these relations hold for currents up to 40 orders is demonstrated in Tables 1a, 1b, 2a, and 2b where comparisons are given for the cases where f=0.5, b=0.5, (Tables 1a, 1b) and f=0.8, b=0.2 (Tables 2a, 2b). Except for large values of t, the agreement seems to be very close.

Table 1a. Comparison of Scattered Current Totals to 40 Orders with Infinite Order Exact Values: Transmission; f=0.5, b=0.5

Rod Length (mfp)	$\sum_{n=1}^{40} T_n$	Infinite Order T, Exact Value
.2	.903601837E-01	.903601560E-01
.4	.163013362E+00	.163013287E+00
.6	.220419247E+00	.220419133E+00
.8	.264956889E+00	.264956750E+00
1.0	.299787375E+00	.298787225E+00
1.2	.323805938E+00	.323805788E+00
1.4	.341638473E+00	.341638330E+00
1.6	.353659169E+00	.353659038E+00
1.8	.361017019E+00	.361016901E+00
2.0	.364664820E+00	.364664717E+00
2.2	.365387405E+00	.365387318E+00
2.4	.363827571E+00	.363827501E+00
2.6	.360509072E+00	.360509030E+00
2.8	.355856580E+00	.355856604E+00
3.0	.350212730E+00	.350212932E+00
3.4	.336995398E+00	.336997100E+00
3.8	.322448476E+00	.322456814E+00
4.2	.307554964E+00	.307585068E+00
4.6	.292891789E+00	.292978467E+00
5.0	.278767022E+00	.278976339E+00
5.4	.265313991E+00	.365753689E+00
5.8	.252556973E+00	.253382702E+00
6.2	.240457427E+00	.241873008E+00
6.6	.228946132E+00	.231197771E+00
7.0	.217944629E+00	.221310340E+00
8.0	.192211091E+00	.199664537E+00
9.0	.168413724E+00	.181694772E+00
10.0	.146227483E+00	.166621267E+00

Table 1b. Comparison of Scattered Current Totals to 40 Orders with Infinite Order Exact Values: Reflection; f=0.5, b=0.5

Rod Length (mfp)	$\sum_{n=1}^{40} B_n$	Infinite Order B, Exact Value
.2	.909091190E-01	.909090909E-01
.4	.166666744E+00	.166666667E+00
.6	.230769352E+00	.230769231E+00
.8	.285714438E+00	.285714286E+00
1.0	.333333505E+00	.333333333E+00
1.2	.375000182E+00	.375000000E+00
1.4	.411764892E+00	.411764706E+00
1.6	.444444632E+00	.444444444E+00
1.8	.473684396E+00	.473684211E+00
2.0	.500000183E+00	.500000000E+00
2.2	.523809704E+00	.523809524E+00
2.4	.545454720E+00	.545454545E+00
2.6	.565217548E+00	.565217391E+00
2.8	.583333433E+00	.583333333E+00
3.0	.599999932E+00	.600000000E+00
3.4	.629628074E+00	.629629630E+00
3.8	.655164232E+00	.655172414E+00
4.2	.677389412E+00	.677419355E+00
4.6	.696883183E+00	.696969697E+00
5.0	.714076562E+00	.714285714E+00
5.4	.729290196E+00	.729729730E+00
5.8	.742764177E+00	.743589744E+00
6.2	.754682138E+00	.756097561E+00
6.6	.765190373E+00	.767441860E+00
7.0	.774412199E+00	.777777778E+00
8.0	.792546283E+00	.800000000E+00
9.0	.804897162E+00	.818181818E+00
10.0	.812919116E+00	.833333333E+00

Table 2a. Comparison of Scattered Current Totals to 40 Orders with Infinite Order Exact Values: Transmission; f=0.8, b=0.2

Rod Length (mfp)	$\sum_{n=1}^{40} T_n$	Infinite Order T, Exact Value
.2	.142807731E+00	.142807708E+00
.4	.255605948E+00	.255605880E+00
.6	.344045625E+00	.344045507E+00
.8	.412740162E+00	.412740001E+00
1.0	.465454086E+00	.465453892E+00
1.2	.505257617E+00	.505257401E+00
1.4	.534653264E+00	.534653036E+00
1.6	.555679470E+00	.555679240E+00
1.8	.569995455E+00	.569995229E+00
2.0	.578950646E+00	.578950431E+00
2.2	.583641486E+00	.583641286E+00
2.4	.584957904E+00	.584957722E+00
2.6	.583621320E+00	.583621159E+00
2.8	.580215719E+00	.580215578E+00
3.0	.575213051E+00	.575212932E+00
3.4	.561864894E+00	.561864825E+00
3.8	.545811009E+00	.545811046E+00
4.2	.528482270E+00	.528482684E+00
4.6	.510779756E+00	.510781498E+00
5.0	.493256344E+00	.493262053E+00
5.4	.476236853E+00	.476252650E+00
5.8	.459897250E+00	.459935408E+00
6.2	.444316761E+00	.444399141E+00
6.6	.429512231E+00	.429674115E+00
7.0	.415460937E+00	.415754785E+00
8.0	.383288421E+00	.384279922E+00
9.0	.354521771E+00	.357019447E+00
10.0	.328172142E+00	.333287933E+00

Table 2b. Comparison of Scattered Current Totals to 40 Orders with Infinite Order Exact Values: Reflection; f=0.8, b=0.2

Rod Length (mfp)	$\sum_{n=1}^{40} B_n$	Infinite Order B, Exact Value
.2	.384615524E-01	.384615385E-01
.4	.740741126E-01	.740740741E-01
.6	.107142918E+00	.107142857E+00
.8	.137931112E+00	.137931034E+00
1.0	.166666755E+00	.166666667E+00
1.2	.193548482E+00	.193548387E+00
1.4	.218750099E+00	.218750000E+00
1.6	.242424343E+00	.242424242E+00
1.8	.264705985E+00	.264705882E+00
2.0	.285714390E+00	.285714286E+00
2.2	.305555661E+00	.305555556E+00
2.4	.324324432E+00	.324324324E+00
2.6	.342105373E+00	.342105263E+00
2.8	.358974470E+00	.358974359E+00
3.0	.375000113E+00	.375000000E+00
3.4	.404762010E+00	.404761905E+00
3.8	.431818218E+00	.431818182E+00
4.2	.456521428E+00	.456521739E+00
4.6	.479165051E+00	.479166667E+00
5.0	.499994432E+00	.500000000E+00
5.4	.519215124E+00	.519230769E+00
5.8	.536999035E+00	.537037037E+00
6.2	.553489208E+00	.553571429E+00
6.6	.568803791E+00	.568965517E+00
7.0	.583039640E+00	.583333333E+00
8.0	.614393258E+00	.615384615E+00
9.0	.640359588E+00	.642857143E+00
10.0	.661550993E+00	.666666667E+00

3. SCATTERING IN A SLAB GEOMETRY

3.1 Development of Current Equations

Application of the OOSII method to the one-dimensional scattering problem served not only as a demonstration of the principles of the method, but also as a means of verification of the method of numerical solution of the current equations. Further utility beyond this point, however, is limited except for the possibility of modelling some three-dimensional problems with one-dimensional solutions through the use of some sort of equivalent mean-free-path for curve fitting purposes. Greater practical value for the OOSII method can be demonstrated when applied to three-dimensional problems. The problem of particle transport in slabs is a convenient choice from among the class of physically realistic cases since it is the simplest in the geometric sense, and it relates to a wide variety of physical situations ranging from neutron transport in reactors to laboratory studies of electron transport in thin films.

As in the case of one-dimensional scattering, development of the imbedding equations can begin with consideration of the transmitted current due solely to forward scattering. Let

$$\begin{Bmatrix} T_n(t, \vec{\Omega}, \vec{\Omega}_o) d\Omega \\ B_n(t, \vec{\Omega}, \vec{\Omega}_o) d\Omega \end{Bmatrix} \quad \text{be the}$$

$$\begin{Bmatrix} \text{transmitted} \\ \text{reflected} \end{Bmatrix} \quad \text{particle current emerging from the}$$

$$\begin{Bmatrix} \text{right} \\ \text{left} \end{Bmatrix}$$

face of the slab of thickness t (Figure 11), after n interactions, in the solid angle $d\Omega$ about $\vec{\Omega}$ because of a unit current incident on the left face in the direction Ω_o. Then the transmitted current emergent from a slab of thickness t+dt after n interactions consists of two contributions, the first due to n scatters having occurred in (0, t) (Figure 12a), and the second due to n-1 scatterings in (0, t) followed by the nth scattering in dt (Figure 12b). This is written as

$$\begin{aligned} T_n(t+dt, \vec{\Omega}, \vec{\Omega}_o) d\Omega &= T_n(t, \vec{\Omega}, \vec{\Omega}_o) d\Omega \left[1 - \frac{dt}{\mu \lambda_n} \right] \\ &+ \int_{\mu'=0}^{\mu'=1} d\Omega' \, T_{n-1}(t, \vec{\Omega}', \vec{\Omega}_o) \, f(\vec{\Omega}' \rightarrow \vec{\Omega}) \, d\Omega \, \frac{dt}{\mu' \lambda_{n-1}} , \end{aligned} \tag{32}$$

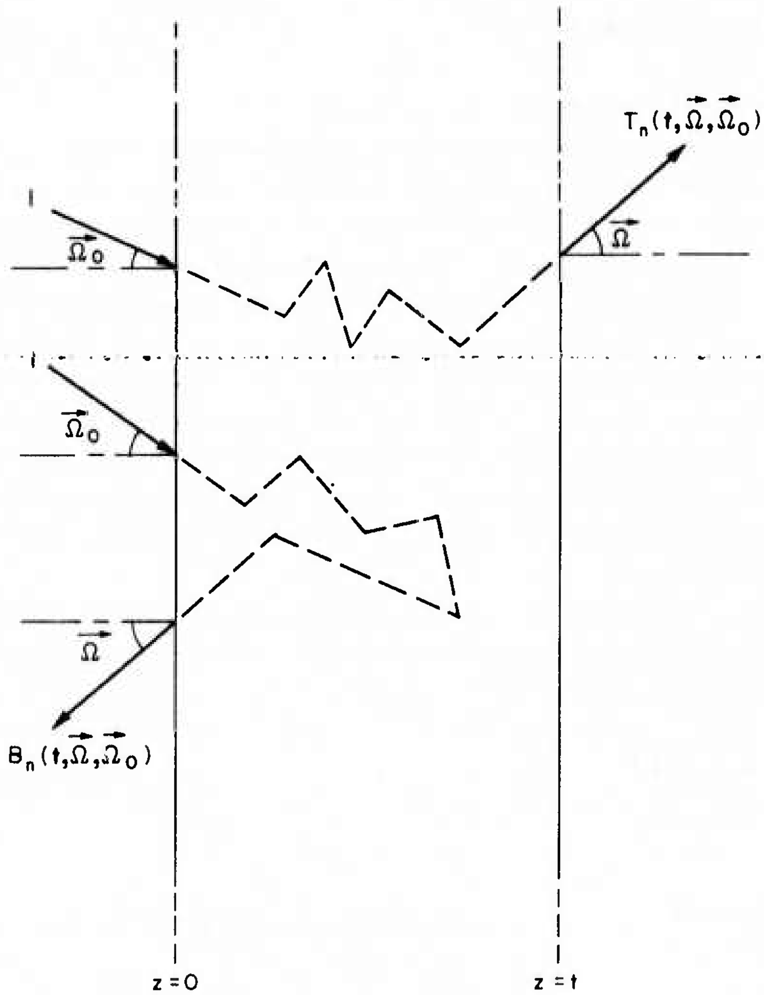

Figure 11. The Slab Geometry

where λ_n is the scattering mean-free-path at the nth collision, μ and μ' are the direction cosines of $\vec{\Omega}$ and $\vec{\Omega}'$, respectively, with respect to the normal to the slab surface (that is, $\vec{\Omega} = \hat{e}_x \sqrt{1-\mu^2} \cos \phi + \hat{e}_y \sqrt{1-\mu^2} \sin \phi + \hat{e}_z \mu$, ϕ being the azimuth about the z-axis), and $f(\vec{\Omega}' \to \vec{\Omega}) d\Omega$ is the probability of scattering from the direction $\vec{\Omega}'$ into the solid angle $d\Omega$ about $\vec{\Omega}$.

The first term on the right is the transmitted current emergent from the slab of thickness t after n interactions, which then escapes unscattered through the incremental thickness dt (Figure 12a). The probability of no interaction occurring in dt is $(1 - dt/\mu\lambda_n)$, where dt/μ is the path length of the incident particle in dt. The second term arises when a particle with incident direction $\vec{\Omega}_o$ is first scattered out

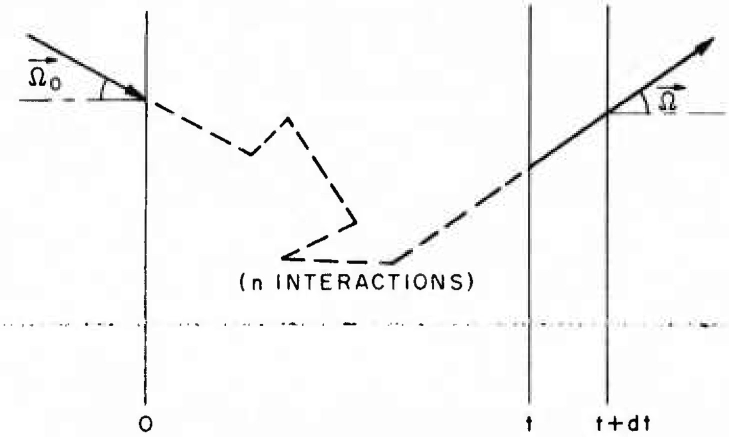

Figure 12a. Transmission Following n Interactions in (0, t)

of (0, t) after n-1 interactions into $d\Omega'$. A further interaction occurs in dt with probability $dt/\mu'\lambda_{n-1}$, where dt/μ' is the path length of the incident particle in dt. This nth interaction is a forward scatter from $\vec{\Omega}'$ into $d\Omega$ with probability $f(\vec{\Omega}'\to\vec{\Omega})d\Omega$ (Figure 12b). The integral over $d\Omega'$ serves to account for all possible intermediate orientations.

Cancellation of the $d\Omega$ factor common to both sides of Eq. (32) and rearrangement of terms gives

$$\frac{T_n(t+dt, \vec{\Omega}, \vec{\Omega}_o) - T_n(t, \vec{\Omega}, \vec{\Omega}_o)}{dt} = -\frac{1}{\mu\lambda_n} T_n(t, \vec{\Omega}, \vec{\Omega}_o)$$
$$+ \frac{1}{\lambda_{n-1}} \int_{\mu'=0}^{\mu'=1} \frac{d\Omega'}{\mu'} f(\vec{\Omega}'\to\vec{\Omega})\, T_{n-1}(t, \vec{\Omega}'\vec{\Omega}_o), \qquad (33)$$

from which the following partial differential equation is derived:

$$\frac{\partial T_n(t, \vec{\Omega}, \vec{\Omega}_o)}{\partial t} = \frac{1}{\mu\lambda_n} T_n(t, \vec{\Omega}, \vec{\Omega}_o)$$
$$+ \frac{1}{\lambda_{n-1}} \int_{\mu'=0}^{\mu'=1} \frac{d\Omega}{\mu'} f(\vec{\Omega}'\to\vec{\Omega})\, T_{n-1}(t, \vec{\Omega}', \vec{\Omega}_o). \qquad (34)$$

In like manner to that of the one-dimensional case, use of the identity

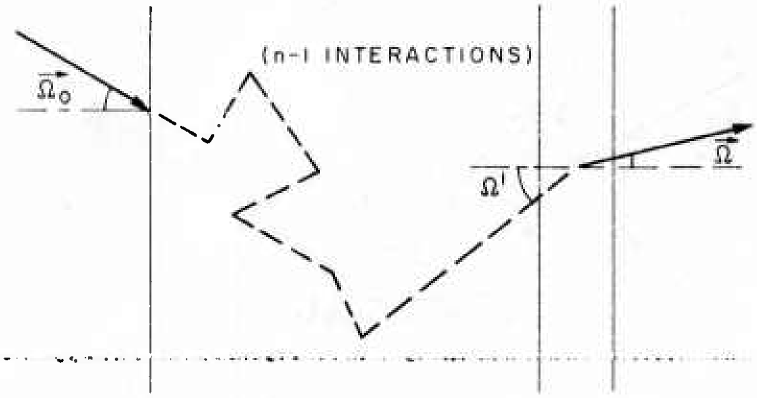

Figure 12b. Transmission Following n-1 Interactions in (0, t) and One Forward Scatter in dt

$$\frac{\partial}{\partial t}\left[e^{t/\lambda\mu}\, T_n(t, \vec{\Omega}, \vec{\Omega}_o)\right] = \frac{1}{\lambda\mu} e^{t/\lambda\mu}\, T_n + e^{t/\lambda\mu}\frac{\partial T_n}{\partial t} \tag{35}$$

leads to

$$\frac{\partial}{\partial t}\left[e^{t/\lambda_n\mu}\, T_n(t, \vec{\Omega}, \vec{\Omega}_o)\right] =$$

$$\frac{e^{t/\lambda_n\mu}}{\lambda_{n-1}} \int_{\mu'=0}^{\mu'=1} \frac{d\Omega'}{\mu'}\, f(\vec{\Omega}' \to \vec{\Omega})\, T_{n-1}(t, \vec{\Omega}', \vec{\Omega}_o)\, , \tag{36}$$

and with the boundary condition that

$$T_n(0, \vec{\Omega}, \vec{\Omega}_o) = 0, \quad n \geq 1\, , \tag{37}$$

integration of Eq. (36) over the slab width yields

$$T_n(t, \vec{\Omega}, \vec{\Omega}_o) =$$

$$\frac{e^{-t/\lambda_n\mu}}{\lambda_{n-1}} \int_{\mu'=0}^{\mu'=1} \frac{d\Omega'}{\mu'}\, f(\vec{\Omega}' \to \vec{\Omega}) \int_o^t dz\, e^{z/\lambda_n\mu}\, T_{n-1}(x, \vec{\Omega}', \vec{\Omega}_o)\, . \tag{38}$$

The contribution of backscatter to the transmitted directional current is determined in much the same way as it is for the one-dimensional case. The description of the multiple scattering process is, however, more complicated due to the

consideration of scattering angles. As before, a particle enters at $z=0$ in the direction $\vec{\Omega}_o$ and survives $n-m-1$ $(0 \leq m \leq n-1)$ interactions in $(0, t)$ (Figure 12c), so that the transmitted directional current entering the incremental thickness dt along the direction $\vec{\Omega}'$ is $T_{n-m-1}(t, \vec{\Omega}', \vec{\Omega}_o)$. The (n-m)th interaction then occurs in dt with probability $dt/\mu'\lambda_{n-m-1}$. The probability of backscatter at this point from the direction $\vec{\Omega}'$ into the solid angle $d\Omega''$ about $\vec{\Omega}''$ is $f(\vec{\Omega}' \to \vec{\Omega}'')d\Omega''$. The particle, once scattered back into $(0, t)$ from dt is, after m interactions, rescattered out of the slab into the solid angle $d\Omega$ about $\vec{\Omega}$. The term describing this combination of events is

$$d\Omega \sum_{m=1}^{n-1} \frac{1}{\lambda_{n-m-1}} \int_{\mu'=0}^{1} T_{n-m-1}(t, \vec{\Omega}', \vec{\Omega}_o) \frac{d\Omega'}{\mu'} \int_{\mu''-1}^{o} f(\vec{\Omega}' \to \vec{\Omega}'') B_m(t, \vec{\Omega}, \vec{\Omega}'') d\Omega'' .$$

The summation covers the range of possible values of m which can contribute to a transmission after n interactions, and the integrals over $d\Omega'$ and $d\Omega''$ account for all possible intermediate orientations.

The addition of this multiple backscatter term to Eq. (32) together with cancellation of the $d\Omega$ factor completes the partial differential equation for the transmitted current:

$$\frac{\partial T_n}{\partial t}(t, \vec{\Omega}, \vec{\Omega}_o) =$$

$$- \frac{1}{\mu\lambda_n} T_n(t, \vec{\Omega}, \vec{\Omega}_o) + \frac{1}{\lambda_{n-1}} \int_{\mu'=0}^{1} \frac{f(\vec{\Omega}' \to \vec{\Omega})}{\mu'} T_{n-1}(t, \vec{\Omega}', \vec{\Omega}_o) d\Omega' \tag{39}$$
$$+ \sum_{m=1}^{n-1} \frac{1}{\lambda_{n-m-1}} \int_{\mu'=o}^{1} T_{n-m-1}(t, \vec{\Omega}', \vec{\Omega}_o) \frac{d\Omega'}{\mu'} \int_{\mu''=-1}^{o} f(\vec{\Omega}' \to \vec{\Omega}'') B_m(t, \vec{\Omega}, \vec{\Omega}'') d\Omega'' .$$

Integration of the above over the slab width results in the following expression for the transmitted directional current:

$$T_n(t, \vec{\Omega}, \vec{\Omega}_o) =$$

$$e^{-t/\mu\lambda_n} \Bigg[\int_{\mu'=0}^{1} \frac{d\Omega'}{\mu'} f(\vec{\Omega}' \to \vec{\Omega}) \int_{o}^{t} \frac{dz}{\lambda_{n-1}} e^{z/\mu\lambda_n} T_{n-1}(z, \vec{\Omega}', \vec{\Omega}_o)$$
$$+ \sum_{m-1}^{n-1} \int_{\mu'=0}^{1} \frac{d\Omega'}{\mu'} \int_{\mu''=-1}^{o} d\Omega'' f(\vec{\Omega}' \to \vec{\Omega}'')$$
$$\times \int_{0}^{t} \frac{dz}{\lambda_{n-m-1}} e^{z/\mu\lambda_n} T_{n-m-1}(z, \vec{\Omega}', \vec{\Omega}_o) B_m(z, \vec{\Omega}, \vec{\Omega}'') \Bigg] . \tag{40}$$

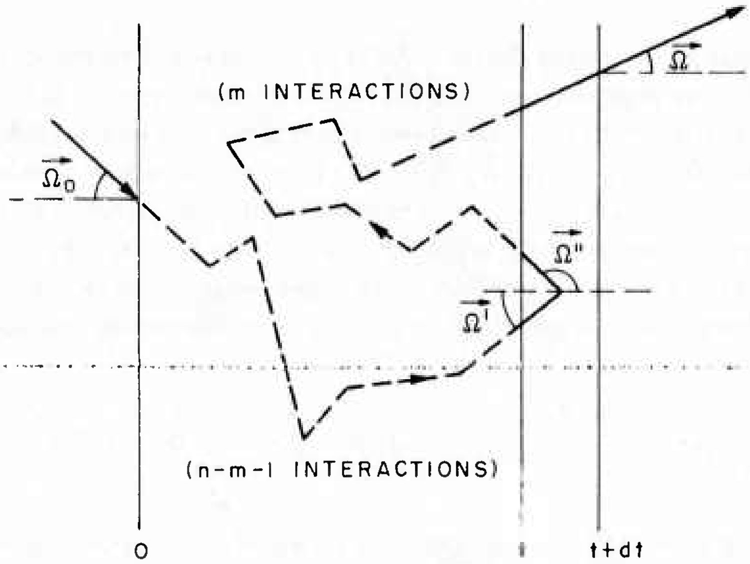

Figure 12c. Transmission Following n-m-1 Interactions in (0, t), a Single Backscatter in dt and a Reflection from (0, t) in the Forward Direction after m Interactions

In order that the set of current equations be complete, a similar expression must be developed for the reflected current. The arguments proceed along the same lines as previously discussed. The reflected current from a slab of thickness t+dt consists of two parts, a portion due to reflection from (0, t) after n interactions, and another portion due to a single backscatter occurring in dt (Figure 13). The resulting expression is

$$B_n(t + dt, \vec{\Omega}, \vec{\Omega}_o) d\Omega = B_n(t, \vec{\Omega}, \vec{\Omega}_o) d\Omega$$

$$+ d\Omega \sum_{m=0}^{n-1} \int_{\mu''=-1}^{o} d\Omega'' T_m(t, \vec{\Omega}, \vec{\Omega}'') \int_{\mu'=0}^{1} d\Omega' \frac{dt}{\mu' \lambda_{n-m-1}}$$

$$\times \ f(\vec{\Omega}' \to \vec{\Omega}'') T_{n-m-1}(t, \vec{\Omega}', \vec{\Omega}_o) . \qquad (41)$$

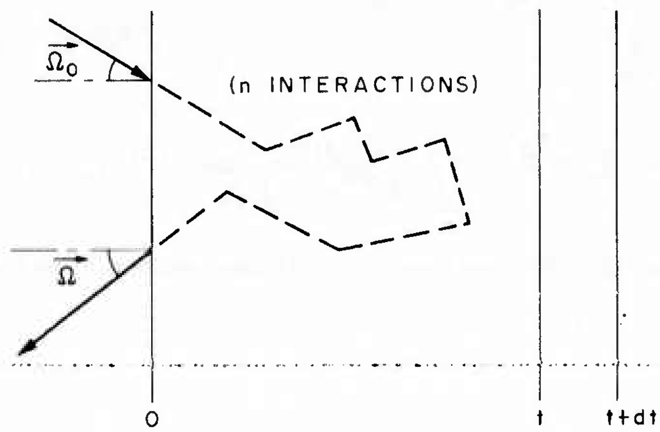

Figure 13a. Reflection Following n Interactions in (0, t)

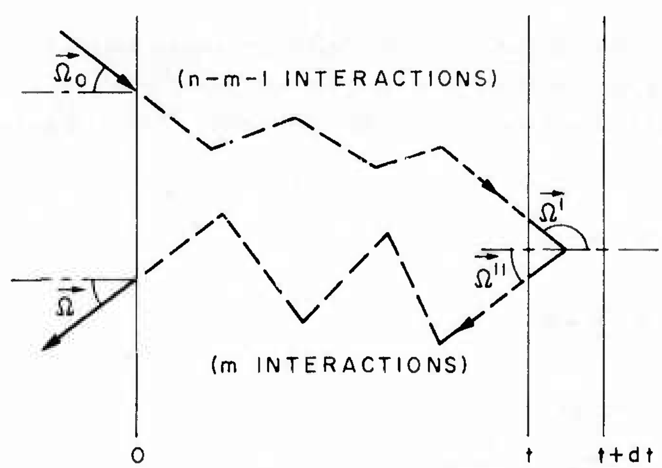

Figure 13b. Reflection Following n-m-1 Interactions in (0, t) a Single Backscatter in dt and a Back Transmission from (0, t) After m Interactions

The significance of the first term of Eq. (41) is obvious from its definition. The second term, once again, is the total of contributions to the reflected current resulting from single backscatter in dt. A particle with incident direction $\vec{\Omega}_o$ is transmitted through (0, t) with exit direction $\vec{\Omega}'$ after n-m 1 interactions. A backscatter into the solid angle $d\Omega''$ about $\vec{\Omega}''$ occurs in dt with probability $f(\vec{\Omega}' \rightarrow \vec{\Omega}'')\cdot d\Omega'' dt/\mu\lambda_{n-m-1}$. The particle is then transmitted back through (0, t) with m interactions occurring during this return trajectory. Rearrangement of the terms of Eq. (41) results in

$$\frac{\partial}{\partial t} B_n(t, \vec{\Omega}, \vec{\Omega}_o) = \tag{42}$$

$$\sum_{m=0}^{n-1} \int_{\mu''=-1}^{o} d\Omega'' T_m(t, \vec{\Omega}, \vec{\Omega}'') \int_{\mu'=0}^{1} \frac{d\Omega'}{\mu \lambda_{n-m-1}} f(\vec{\Omega}' \to \vec{\Omega}'') T_{n-m-1}(t, \vec{\Omega}', \vec{\Omega}_o) .$$

Integration over the slab width provides the final expression for the reflected current:

$$B_n(t, \vec{\Omega}, \vec{\Omega}_o) =$$

$$\sum_{m=0}^{n-1} \int_{o}^{t} \frac{dz}{\lambda_{n-m-1}} \int_{\mu''=-1}^{o} d\Omega'' T_m(z, \vec{\Omega}, \vec{\Omega}'') \int_{\mu'=0}^{1} \frac{d\Omega'}{\mu'} f(\vec{\Omega}' \to \vec{\Omega}'') \times \tag{43}$$

$$T_{n-m-1}(z, \vec{\Omega}', \vec{\Omega}_o) .$$

The above equation combined with Eq. (40) and appropriate boundary and initial conditions constitute the set of coupled integral recursion relations for transmitted and reflected directional currents in the slab geometry. The boundary conditions are

$$T_k(0, \vec{\Omega}, \vec{\Omega}_o) = 0 , \ k > 0 , \tag{44a}$$

$$B_k(0, \vec{\Omega}, \vec{\Omega}_o) = 0 , \ k > 0 , \tag{44b}$$

and the initial conditions are

$$T_o(z, \vec{\Omega}, \vec{\Omega}_o) = e^{-z/\lambda_o \mu} \delta_2(\vec{\Omega} \cdot \vec{\Omega}_o) , \tag{45a}$$

$$B_o(z, \vec{\Omega}, \vec{\Omega}_o) = 0 , \tag{45b}$$

where the three-dimensional delta function $\delta_2(\vec{\Omega} \cdot \vec{\Omega}')$ is defined as

$$\delta_2(\vec{\Omega} \cdot \vec{\Omega}') = \delta(\mu - \mu') \delta(\phi - \phi') . \tag{46}$$

3.2 Solution of the Slab Geometry Current Equations

The equations which form the coupled integral recursion relations for the slab geometry can be rewritten in the following form:

$$\int_0^{2\pi} d\phi_o \int_0^{2\pi} d\phi\, T_n(t, \vec{\Omega}, \vec{\Omega}_o) =$$

$$e^{-t/\lambda_n\mu}\Bigg[\int_0^{2\pi} d\phi_o \int_0^{2\pi} d\phi \int_0^{2\pi} d\phi' \int_0^1 \frac{d\mu'}{\mu'} f(\vec{\Omega}' \to \vec{\Omega}) \int_0^t \frac{dz}{\lambda_{n-1}} e^{z/\lambda_n\mu} T_{n-1}(z, \vec{\Omega}', \vec{\Omega}_o)$$

$$+ \sum_{m=1}^{n-1} \int_0^{2\pi} d\phi_o \int_0^{2\pi} d\phi \int_0^{2\pi} d\phi' \int_0^{2\pi} d\phi'' \int_0^1 \frac{d\mu'}{\mu'} \int_{-1}^{0} d\mu''\, f(\vec{\Omega}' \to \vec{\Omega}'')$$

$$\times \int_0^t \frac{dz}{\lambda_{n-m-1}} e^{z/\lambda_n\mu} T_{n-m-1}(z, \vec{\Omega}', \vec{\Omega}_o)\, B_m(z, \vec{\Omega}, \vec{\Omega}'')\Bigg] \qquad (47)$$

and

$$\int_0^{2\pi} d\phi_o \int_0^{2\pi} d\phi\, B_n(t, \vec{\Omega}, \vec{\Omega}_o) =$$

$$\sum_{m=0}^{n-1} \int_0^{2\pi} d\phi_o \int_0^{2\pi} d\phi \int_0^t \frac{dz}{\lambda_{n-m-1}} \int_0^{2\pi} d\phi'' \int_{-1}^{0} d\mu''\, T_m(z, \vec{\Omega}, \vec{\Omega}'')$$

$$\times \int_0^{2\pi} d\phi' \int_0^1 \frac{d\mu'}{\mu'} f(\vec{\Omega}' \to \vec{\Omega}'')\, T_{n-m-1}(z, \vec{\Omega}', \vec{\Omega}_o) \,. \qquad (48)$$

Since the slab is infinite in extent in the x and y directions, the functions f, T_n, and B_n are invariant under rotations about the z-axis. The integrals over azimuth may then be dispensed with. Given the definition

$$F(\mu, \mu') = \int_0^{2\pi} d\phi \int_0^{2\pi} d\phi'\, F(\vec{\Omega}, \vec{\Omega}') \,, \qquad (49)$$

where F is an arbitrary function of $\vec{\Omega}$ and $\vec{\Omega}'$, Eqs. (47) and (48) then take the following simplified form:

$$T_n(t, \mu, \mu_o) =$$

$$e^{-t/\lambda_n\mu}\Bigg[\int_0^1 \frac{d\mu'}{\mu'} f(\mu' \to \mu) \int_0^t \frac{dz}{\lambda_{n-1}} e^{z/\lambda_n\mu} T_{n-1}(z, \mu', \mu_o) + \sum_{m=1}^{n-1} \int_0^1 \frac{d\mu'}{\mu'}$$

$$\times \int_{-1}^{0} d\mu''\, f(\mu' \to \mu'') \int_0^t \frac{dz}{\lambda_{n-m-1}} e^{\frac{z}{\lambda_n\mu}}\, T_{n-m-1}(z, \mu', \mu_o)\, B_m(z, \mu, \mu'')\Bigg] \,, \qquad (50)$$

$$B_n(t,\mu,\mu_o) = \sum_{m=0}^{n-1} \int_o^t \frac{dz}{\lambda_{n-m-1}} \int_{-1}^{o} d\mu'' T_m(z,\mu,\mu'') \int_o^1 \frac{d\mu'}{\mu'} f(\mu'\to\mu'') T_{n-m-1}(z,\mu',\mu_o)\,, \tag{51}$$

and the boundary and initial conditions become

$$T_k(0,\mu,\mu_o) = 0\,, \quad k > 0\,, \tag{52a}$$

$$B_k(0,\mu,\mu_o) = 0\,, \quad k > 0\,, \tag{52b}$$

$$T_o(z,\mu,\mu_o) = e^{-z/\lambda_o\mu}\,\delta(\mu-\mu_o)\,, \tag{53a}$$

$$B_o(z,\mu,\mu_o) = 0\,. \tag{53b}$$

Exact solutions are possible for the once-scattered currents T_1 and B_1. In fact, knowledge of these solutions is indispensible to the success of the solution scheme to be outlined. Direct substitution of Eq. (53a) into Eq. (50) yields for n=1,

$$\begin{aligned}
T_1(t,\mu,\mu_o) &= \frac{e^{-t/\lambda_1\mu}}{\lambda_o} \int_o^1 \frac{d\mu'}{\mu'} f(\mu'\to\mu) \int_o^t dze^{z/\lambda_1\mu}\, T_o(z,\mu',\mu_o) \\
&= \frac{e^{-t/\lambda_1\mu}}{\lambda_o} \int_o^1 \frac{d\mu'}{\mu'} f(\mu'\to\mu) \int_o^t dze^{z/\lambda_1\mu}\, e^{-z/\lambda_o\mu'}\, \delta(\mu'-\mu_o) \\
&= \frac{e^{-t/\lambda_1\mu}}{\lambda_o\mu_o} f(\mu_o\to\mu) \int_o^t dz\, e^{z\left(\frac{1}{\lambda_1\mu} - \frac{1}{\lambda_o\mu_o}\right)}\,,
\end{aligned}$$

or

$$T_1(t,\mu,\mu_o) = \left\{ \begin{array}{ll} \dfrac{\lambda_1\mu}{\lambda_o\mu_o-\lambda_1\mu} f(\mu_o\to\mu) \left[e^{-t/\lambda_o\mu_o} - e^{-t/\lambda_1\mu}\right] & , \ \mu \neq \mu_o \\[2ex] \dfrac{t}{\lambda_o\mu_o}\, e^{-t/\lambda_o\mu_o} f(\mu_o\to\mu_o)\,, \ \mu = \mu_o & \end{array} \right\}. \tag{54}$$

First order reflection is also obtained using Eq. (53a), so that

$$B_1(t,\mu,\mu_o) = \frac{1}{\lambda_o}\int_o^t dz \int_{-1}^{o} d\mu''\, T_o(z,\mu,\mu'') \int_o^1 \frac{d\mu'}{\mu'} f(\mu'\to\mu'')\, T_o(z,\mu'\mu_o)$$

$$= \frac{1}{\lambda_o}\int_o^t dz \int_{-1}^{o} d\mu''\, e^{-z/\lambda_o|\mu''|}\, \delta(\mu-\mu'') \int_o^1 \frac{d\mu'}{\mu'} f(\mu'\to\mu'')\, e^{-z/\lambda_o\mu'}\, \delta(\mu'\cdot\mu_o)$$

$$= \frac{1}{\lambda_o\mu_o}\int_o^t dz\, e^{-z/\lambda_o\mu_o} \int_{-1}^{o} d\mu''\, e^{-z/\lambda_o|\mu''|}\, \delta(\mu-\mu'')\, f(\mu_o\to\mu'')$$

$$= \frac{1}{\lambda_o\mu_o} f(\mu_o\to\mu) \int_o^t dz\, e^{-z/\lambda_o\left(\frac{1}{|\mu|}+\frac{1}{\mu_o}\right)} ,$$

or

$$B_1(t,\mu,\mu_o) = \frac{|\mu|}{|\mu|+\mu_o} f(\mu_o\to\mu)\left[1 - e^{-t/\lambda_o\left(\frac{1}{\mu_o}+\frac{1}{|\mu|}\right)}\right] . \tag{55}$$

The angular integrals of Eqs. (50) and (51) present a problem which had not occurred previously in the one-dimensional case. It is necessary to cast the equations into a form in which the integrals over angle can be performed both with a sufficient degree of accuracy and within a reasonable amount of computation time. For this reason the method of Gauss quadrature integration was chosen. Briefly stated, given a function g(x) defined on the interval $-1 \le x \le 1$, then a numerical integration of g(x) over this interval can be obtained as follows:[8]

$$\int_{-1}^{1} g(x)\,dx \doteq \sum_{\ell=1}^{L} A_\ell\, g(x_\ell) , \tag{56}$$

where the x_ℓ are the zeros of the Legendre polynomial of order L defined over the interval $-1 \le x \le 1$, and the A_ℓ are the Gaussian weighting coefficients (it can be shown that such a procedure is equivalent to integrating a (2L-1)th order polynomial which agrees with the function g(x) at 2L points). This method of integration can be applied directly in the evaluation of the angular integrals of Eqs. (50) and (51) since the integration intervals are compatible. This approach differs from those that have been widely adopted in the past by others where it has often been the practice in solving transport problems to apply Legendre series expansions directly to functions of the type found in the integrands of Eqs. (50) and (51).[9]

Tables of the Gaussian ordinates and their weighting coefficients are readily available from several sources.[10] When Eqs. (50) and (51) are restated in the discrete ordinate representations of Eq. (56) they appear as

8. Lanczos, C. (1956) Applied Analysis, Prentice Hall, Inc., Englewood Cliffs, N.J.
9. Weinberg, A.M., and Wigner, E.P. (1958) The Physical Theory of Neutron Chain Reactors, Univ. of Chicago Press, Chicago.
10. Stroud, A.H., and Secrest, D. (1966) Gaussian Quadrature Formulas, Prentice Hall, Inc., Englewood Cliffs, N.J.

$$T_n(t, \mu_\ell, \mu_j) \doteq$$

$$e^{-t/\lambda_n\mu_\ell}\left[\int_o^t \frac{dz}{\lambda_{n-1}} e^{z/\lambda_n\mu_\ell} \sum_k A_k f(\mu_k, \mu_\ell) \frac{T_{n-1}(z, \mu_k, \mu_j)}{\mu_k}\right.$$

$$+\sum_{m=1}^{n-1} \int_o^t \frac{dz}{\lambda_{n-m-1}} e^{z/\lambda_n\mu_\ell} \sum_k A_k \frac{T_{n-m-1}(z, \mu_k, \mu_j)}{\mu_k}$$

$$\left.\cdot \sum_p A_p f(\mu_k, \mu_p) B_m(z, \mu_\ell, \mu_p)\right] , \tag{57}$$

and

$$B_m(t, \mu_\ell, \mu_j) \doteq \sum_{m=0}^{n-1} \int_o^t \frac{dz}{\lambda_{n-m-1}}$$

$$\times \sum_p A_p T_m(z, \mu_\ell, \mu_p) \sum_k A_k f(\mu_k, \mu_p) \frac{T_{n-m-1}(z, \mu_k, \mu_j)}{\mu_k} . \tag{58}$$

The remaining problem of integration over the slab thickness z is handled in exact analogy to that of the one-dimensional case. It is assumed that over a sufficiently small interval, $t_1 \le z \le t$, the functions $T_n(z, \mu_j, \mu_k)$ and $B_n(z, \mu_j, \mu_k)$ can be considered linear in the variable z so that they may be written as

$$T_n(z, \mu_j, \mu_k) = m_T^n(\mu_j, \mu_k)z + b_T^n(\mu_j, \mu_k) , \tag{59a}$$

$$B_n(z, \mu_j, \mu_k) = m_B^n(\mu_j, \mu_k)z + b_B^n(\mu_j, \mu_k) , \tag{59b}$$

where the $m_T^n(\mu_j, \mu_k)$ and the $m_B^n(\mu_j, \mu_k)$ are the slopes, and the $b_T^n(\mu_j, \mu_k)$ and $b_B^n(\mu_j, \mu_k)$ are the intercepts of the T_n and B_n, respectively. It is convenient for the expressions for T_n and B_n to be divided into six terms. That is:

$$T_n = T_n^{(1)} + T_n^{(2)} + T_n^{(3)} , \tag{60a}$$

$$B_n = B_n^{(1)} + B_n^{(2)} + B_n^{(3)} , \tag{60b}$$

where

$$T_n^{(1)}(t, \mu_\ell, \mu_j) =$$

$$e^{-t/\lambda_n\mu_\ell} \int_0^t \frac{dz}{\lambda_{n-1}} e^{z/\lambda_n\mu_\ell} \sum_k A_k f(\mu_k, \mu_\ell) \frac{T_{n-1}(z, \mu_k, \mu_j)}{\mu_k}, \tag{61a}$$

$$T_n^{(2)}(t, \mu_\ell, \mu_j) = \sum_{m=1}^{n-2} \int_0^t \frac{dz}{\lambda_{n-m-1}} e^{z/\lambda_n\mu_\ell} \sum_k A_k \frac{T_{n-m-1}(z, \mu_k, \mu_j)}{\mu_k}$$

$$\times \sum_p A_p f(\mu_k, \mu_p) B_m(z, \mu_\ell, \mu_p), \tag{61b}$$

$$T_n^{(3)}(t, \mu_\ell, \mu_j) = \int_0^t \frac{dz}{\lambda o} e^{z\left(\frac{1}{\lambda_n\mu_\ell} - \frac{1}{\lambda\mu_j}\right)}$$

$$\times \sum_p A_p \frac{f(\mu_j, \mu_p)}{\mu_j} B_{n-1}(z, \mu_\ell, \mu_p), \tag{61c}$$

$$B_n^{(1)}(t, \mu_\ell, \mu_j) = \int_0^t \frac{dz}{\lambda_{n-1}} e^{-z/\lambda_o\mu_\ell}$$

$$\times \sum_k A_k f(\mu_k, \mu_\ell) \frac{T_{n-1}(z, \mu_k, \mu_j)}{\mu_k}, \tag{62a}$$

$$B_n^{(2)}(t, \mu_\ell, \mu_j) = \sum_{m=1}^{n-2} \int_0^t \frac{dz}{\lambda_{n-m-1}} \sum_p A_p T_m(z, \mu_\ell, \mu_p)$$

$$\times \sum_k A_k f(\mu_k, \mu_p) \frac{T_{n-m-1}(z, \mu_k, \mu_j)}{\mu_k}, \tag{62b}$$

$$B_n^{(3)}(t, \mu_\ell, \mu_j) = \int_0^t \frac{dz}{\lambda_o\mu_j} e^{-z/\lambda_o\mu_j} \sum_p A_p f(\mu_j, \mu_p) T_{n-1}(z, \mu_\ell, \mu_p). \tag{62c}$$

The above expressions, Eqs. (61a, b, c, 62a, b, c), result from the expansion of the summation terms over orders of scattering present in Eqs. (57) and (58) into terms involving first order transmission and those which do not. In this way direct use of the exact expression, Eq. (54), for $T_1(t, \mu_i, \mu_j)$ could be made by means of explicit substitution. It is expected that this procedure should lead to a more accurate determination of the T_n and B_n than would have been the case if the piecewise linearity assumption had been applied uniformly to all scattering orders. If the piecewise linear assumption is applied to the expressions given in Eqs. (61a, b, c) and (62a, b, c), and if the integrals over z are then performed on the interval $t_1 \le z \le t$, the following expressions result for the six terms:

$$T_n^{(1)}(t, \mu_\ell, \mu_j) = \frac{1}{\lambda_{n-1}} \sum_k A_k \frac{f(\mu_k, \mu_\ell)}{\mu_k} \cdot$$

$$\left\{ \begin{array}{l} m_T^{n-1}(\mu_k, \mu_j)\left[(\lambda_n\mu_\ell t - \lambda_n^2\mu_\ell^2)\, e^{t/\lambda_n\mu_\ell} - (\lambda_n\mu_\ell t_1 - \lambda_n^2\mu_\ell^2)\, e^{t/\lambda_n\mu_\ell}\right] \\ + b_T^{n-1}(\mu_k, \mu_j)\left[\lambda_n\mu_\ell\left(e^{t/\lambda_n\mu_\ell} - e^{t_1/\lambda_n\mu_\ell}\right)\right] \end{array} \right\}, \qquad (63a)$$

$$T_n^{(2)}(t, \mu_\ell, \mu_J) = \sum_{m=1}^{n-2} \frac{1}{\lambda_{n-m-1}} \sum_k \frac{A_k}{\mu_k} \sum_p A_p f(\mu_k, \mu_p) \cdot$$

$$\left(\begin{array}{l} \left[m_T^{n-m-1}(\mu_k, \mu_j)\, m_B^m(\mu_\ell, \mu_p)\right] \cdot \left[(\lambda_n\mu_\ell t^2 - 2\lambda_n^2\mu_\ell^2 t + 2\lambda_n^3\mu_\ell^3)\, e^{t/\lambda_n\mu_\ell} \right. \\ \qquad \left. - (\lambda_n\mu_\ell t_1^2 - 2\lambda_n^2\mu_\ell t_1 + 2\lambda_n^3\mu_\ell^3)\, e^{t_1/\lambda_n\mu_\ell}\right] \\ + \left[b_T^{n-m-1}(\mu_k, \mu_j)\, m_B^m(\mu_\ell, \mu_p) + b_B^m(\mu_\ell, \mu_p)\, m_T^{n-m-1}(\mu_k, \mu_j)\right] \\ \qquad \times \left[(\lambda_n\mu_\ell t - \lambda_n^2\mu_\ell^2)\, e^{t/\lambda_n\mu_\ell} - (\lambda_n\mu_\ell t_1 - \lambda_n^2\mu_\ell^2)\, e^{t_1/\lambda_n\mu_\ell}\right] \\ + \left[b_T^{n-m-1}(\mu_k, \mu_j)\, b_B^m(\mu_\ell, \mu_p)\, \lambda_n\mu_\ell\right] \cdot \left[e^{t/\lambda_n\mu_\ell} - e^{t_1/\lambda_n\mu_\ell}\right] \end{array} \right) \qquad (63b)$$

$$T_n^{(3)}(t, \mu_\ell, \mu_j) = \frac{1}{\lambda_o} \sum_p \frac{f(\mu_j, \mu_p)}{\mu_j}$$

$$\times\ m_B^{n-1}(\mu_\ell, \mu_p) \left\{ \left[\left(\frac{\lambda_o\lambda_n\mu_j\mu_\ell}{\lambda_o\mu_j - \lambda_n\mu_\ell}\right) t - \left(\frac{\lambda_o\lambda_n\mu_j\mu_\ell}{\lambda_o\mu_j - \lambda_n\mu_\ell}\right)^2\right] e^{\left(\frac{1}{\lambda_n\mu_\ell} - \frac{1}{\lambda_o\mu_j}\right)t} \right.$$

$$\left. - \left[\left(\frac{\lambda_o\lambda_n\mu_j\mu_\ell}{\lambda_o\mu_j - \lambda_n\mu_\ell}\right) t_1 - \left(\frac{\lambda_o\lambda_n\mu_j\mu_\ell}{\lambda_o\mu_j - \lambda_n\mu_\ell}\right)^2\right] e^{\left(\frac{1}{\lambda_n\mu_\ell} - \frac{1}{\lambda_o\mu_o}\right)t_1} \right\}$$

$$+\ b_B^{n-1}(\mu_\ell, \mu_p) \left\{ \left(\frac{\lambda_o\lambda_n\mu_j\mu_\ell}{\lambda_o\mu_j - \lambda_n\mu_\ell}\right) \left(e^{\left(\frac{1}{\lambda_n\mu_\ell} - \frac{1}{\lambda_o\mu_j}\right)t} - e^{\left(\frac{1}{\lambda_n\mu_\ell} - \frac{1}{\lambda_o\mu_j}\right)t_1}\right) \right\}, \qquad (63c)$$

$$B_n^{(1)} = \frac{1}{\lambda_{n-1}} \sum_k A_k \frac{f(\mu_k, \mu_\ell)}{\mu_k} \cdot$$

$$\left\{\begin{array}{l} m_T^{n-1}(\mu_k, \mu_j) \left[(\lambda_o \mu_\ell t_1 + \lambda_o^2 \mu_\ell^2) e^{-t_1/\lambda_o \mu_\ell} \right. \\ \qquad \left. - (\lambda_o \mu_\ell t + \lambda_o^2 \mu_\ell^2) e^{-t/\lambda_o \mu_\ell} \right] \\ + b_T^{n-1}(\mu_k, \mu_j) \lambda_o \mu_\ell \left[e^{-t_1/\lambda_o \mu_\ell} - e^{-t/\lambda_o \mu_\ell} \right] \end{array}\right\}, \tag{64a}$$

$$B_n^{(2)} = \sum_{m=1}^{n-2} \frac{1}{\lambda_{n-m-1}} \sum_p A_p \sum_k A_k \frac{f(\mu_k, \mu_p)}{\mu_k} \cdot$$

$$\left\{\begin{array}{l} \left[m_T^m(\mu_\ell, \mu_p)\, m_T^{n-m-1}(\mu_k, \mu_j) \right] \left[\frac{t^3}{3} - \frac{t_1^3}{3} \right] \\ + \left[b_T^m(\mu_\ell, \mu_p)\, m_T^{n-m-1}(\mu_k, \mu_j) \right. \\ \left. + b_T^{n-m-1}(\mu_k, \mu_j)\, m_T^m(\mu_\ell, \mu_p) \right] \left[\frac{t^2}{2} - \frac{t_1^2}{2} \right] \\ + \left[b_T^m(\mu_\ell, \mu_p)\, b_T^{n-m-1}(\mu_k, \mu_j) \right] \left[t - t_1 \right] \end{array}\right\}, \tag{64b}$$

$$B_n^{(3)} = \frac{1}{\lambda_o} \sum_p A_p \frac{f(\mu_j, \mu_p)}{\mu_j} \cdot$$

$$\left\{\begin{array}{l} m_T^{n-1}(\mu_\ell, \mu_p) \left[(\lambda_o \mu_j t_1 + \lambda_o^2 \mu_j^2) e^{-t_1/\lambda_o \mu_j} \right. \\ \qquad \left. - (\lambda_o \mu_j t + \lambda_o^2 \mu_j^2) e^{-t/\lambda_o \mu_j} \right] \\ + b_T^{n-1}(\mu_\ell, \mu_p) \lambda_o \mu_j \left[e^{-t_1/\lambda_o \mu_j} - e^{-t/\lambda_o \mu_j} \right] \end{array}\right\}. \tag{64c}$$

The above relations, Eqs. (63a, b, c) and (64a, b, c), form the basis of a computer program which was written to obtain numerical solutions to the coupled integral recursion relations of Eqs. (50) and (51). The remaining requirement is the specification of the scattering matrix $f(\mu, \mu')$, the mathematical description of the physics of the scattering process. In the sections that follow, the results of four OOSII calculations, corresponding to four forms for $f(\mu, \mu')$, are reported.

4. ISOTROPIC SCATTERING IN THE LABORATORY SYSTEM — OOSII TREATMENT

The simplest form of the scattering matrix $f(\mu, \mu')$ occurs when all of the elements are constant and equal. This situation corresponds to isotropic scattering in the laboratory system. As has been stated previously, regardless of the nature of the scattering interaction $f(\vec{\Omega}\rightarrow\vec{\Omega}')\,d\Omega'$ is the probability of scattering from the initial direction $\vec{\Omega}$ into the solid angle $d\Omega'$ about the direction $\vec{\Omega}'$. For any conservative scattering interaction (no absorption)

$$\int_0^{4\pi} d\Omega'\, f(\vec{\Omega}\rightarrow\vec{\Omega}') = 1 \; . \tag{65}$$

If the scattering is isotropic in the laboratory system (the directions $\vec{\Omega}$ and $\vec{\Omega}'$ are specified with respect to the laboratory frame), then from Eq. (65) it is seen that

$$f(\vec{\Omega}'\rightarrow\vec{\Omega}) = \frac{1}{4\pi} \; .$$

Furthermore, since azimuthal invariance applies, as in Eq. (49)

$$\begin{aligned} f(\mu, \mu') \equiv f_o &= \int_0^{2\pi} d\phi\, f(\vec{\Omega}\rightarrow\vec{\Omega}') \\ &= \frac{1}{4\pi}\int_0^{2\pi} d\phi \\ &= \frac{1}{2} \; . \end{aligned} \tag{66}$$

The above value of f_o was substituted for the $f(\mu_i, \mu_j)$ in Eqs. (63a, b, c) and (64a, b, c), and computer runs were made to determine the values of $T_n(t, \mu_i, \mu_j)$ and $B_n(t, \mu_i, \mu_j)$ where the μ_i and μ_j are Gaussian discrete ordinates corresponding to cosines of the incident and exit polar angles, respectively, for 41 values of t ranging from 0.0 to 8.0 mfp in steps of 0.2 mfp. A constant value was assumed for λ_n. This assumption, while not a necessary restriction of the method, serves to simplify the computation. Current values $T_n(t)$ and $B_n(t)$ were then obtained by integrating the directional currents $T_n(t, \mu, \mu')$ and $B_n(t, \mu, \mu')$ over the incident and exit cosines μ and μ'. That is

$$T_n(t) = \int_0^1 d\mu\, w(\mu) \int_0^1 d\mu'\, T_n(t, \mu, \mu') \Big/ \int_0^1 d\mu\, w(\mu) \; , \tag{67}$$

and

$$B_n(t) = \int_0^1 d\mu\, w(\mu) \int_{-1}^{0} d\mu'\, B_n(t, \mu, \mu') \Big/ \int_0^1 d\mu\, w(\mu) . \tag{68}$$

where $w(\mu)$ is the source angular distribution function at the left face of the slab. Results were obtained for two source configurations:

(1) cosine current (isotropic particle density) distribution

$$w(\mu) = \mu,$$

(2) isotropic current distribution

$$w(\mu) = 1 .$$

The second of these configurations is not physically realizable, since this would correspond to an infinite particle density value along the direction parallel to the slab surface. In other words, if $\phi(\mu)$ is the angular density, or the number of particles per unit volume moving in the direction μ, at the slab surface, then the angular current $J(\mu)$, the number of particles crossing unit area perpendicular to the direction of μ, is given by $J(\mu) = \mu\phi(\mu)$. Therefore, if $J(\mu)$ is to be isotropic and non-zero, it must have a constant finite non-zero value at $\mu = 0$.

The numerator integrals of Eqs. (67) and (68) were evaluated using Gauss quadrature, since the functions $T_n(t, \mu, \mu')$ and $B_n(t, \mu, \mu')$ were already evaluated at the Gaussian ordinates. The denominator integrals were evaluated exactly. For the cosine current source, the value of the denominator is 1/2, and for the isotropic current source it has a value of 1. The working expressions for the transmitted and reflected currents then become

$$T_n(t) = 2\sum_j A_j\mu_j \sum_k A_k\, T_n(t, \mu_j, \mu_k) , \tag{69}$$

$$B_n(t) = 2\sum_j A_j\mu_j \sum A_k\, B_n(t, \mu_j, \mu_k) , \tag{70}$$

for the cosine source and

$$T_n(t) = \sum_j A_j \sum_k A_k\, T_n(t, \mu_j, \mu_k) , \tag{71}$$

$$B_n(t) = \sum_j A_j \sum_k A_k\, B_n(t, \mu_j, \mu_k) . \tag{72}$$

for the isotropic source.

It was found that good comparisons with other calculations were obtained if six discrete ordinates per quadrant were used for all scatterings up to order ten for slab thicknesses up to one mfp. In this way an artificially low transmitted current at the higher orders could be avoided. The use of only two discrete ordinates per quadrant for the thin slab cases exaggerates the transmission at the lower scattering orders because of the high degree of granularity in angle. The Gaussian discrete ordinate values are given in Table 3 for 2, 4, and 6 angles per quadrant. A comparison of the currents obtained using 2 and 6 ordinates with the cosine source configuration is given in Table 4 for ten orders of scattering in thin slabs.

Table 3. Gaussian Discrete Ordinates[10]

Number of Ordinates	6	4	2
Gaussian Ordinate, μ_i	.98156 .90412 .76990 .58732 .36783 .12523	.96029 .70667 .52553 .18343	.86114 .33998

For slab thicknesses greater than one mfp, six discrete ordinates were used for the first three scattering orders, four were used for orders four through six, and two for orders seven through ten. The reasoning leading to this arrangement is that as the number of scatters becomes sufficiently high, and if the slab is sufficiently thick, the granularity inherent in the choice of a low number of discrete ordinates becomes less important. The particle has changed direction several times at this stage, so that for isotropic and nearly isotropic scattering, the angular distribution has grown diffuse, and an adequate description can be achieved with the equivalent of a Legendre expansion of two or three terms.

Curves of $T_n(t)$ and $B_n(t)$ plotted vs t for both source configurations are given in Figures 14, 15, 16, and 17. Twelve curves, representing values of n ranging from 0 to 10 and a total curve, are presented in each graph. A more detailed presentation of the numerical results is given in Table 8 where comparisons with results obtained from Boltzmann equation and Monte Carlo calculations are shown.

Table 4a. Comparison of Particle Currents Obtained with 6 and 2 Discrete Ordinates per Quadrant for 10 Orders of Scattering; Cosine Current Source Configuration; Isotropic Scattering:

Transmission

Slab Width (mfp)	Number of Discrete Ordinates			
	6	2	6	2
	n=1		n=2	
.2	.5580E-01	.6347E-01	.1384E-01	.1266E-01
.4	.7021E-01	.8223E-01	.2823E-01	.2916E-01
.6	.7072E-01	.8160E-01	.3633E-01	.3940E-01
.8	.6566E-01	.7351E-01	.3960E-01	.4349E-01
1.0	.5844E-01	.6334E-01	.3969E-01	.4336E-01
	n=3		n=4	
.2	.3396E-02	.2495E-02	.8315E-03	.4917E-03
.4	.1111E-01	.9997E-02	.4339E-02	.3403E-02
.6	.1814E-01	.1801E-01	.8928E-02	.8095E-02
.8	.2304E-01	.2396E-01	.1314E-01	.1286E-01
1.0	.2581E-01	.2737E-01	.1637E-01	.1666E-01
	n=5		n=6	
.2	.2036E-03	.9694E-04	.4988E-04	.1912E-04
.4	.1689E-02	.1157E-02	.6573E-03	.3933E-03
.6	.4368E-02	.3623E-02	.2132E-02	.1619E-02
.8	.7427E-02	.6833E-02	.4178E-02	.3619E-02
1.0	.1025E-01	.9988E-02	.6374E-02	.5950E-02
	n=7		n=8	
.2	.1223E-04	.3774E-05	.2998E-05	.7455E-06
.4	.2557E-03	.1337E-03	.9946E-04	.4547E-04
.6	.1040E-02	.7236E-03	.5069E-03	.3233E-03
.8	.2346E-02	.1915E-02	.1316E-02	.1013E-02
1.0	.3949E-02	.3536E-02	.2443E-02	.2099E-02
	n=9		n=10	
.2	.7355E-06	.1473E-06	.1805E-06	.2913E-07
.4	.3869E-04	.1546E-04	.1595E-04	.5258E-05
.6	.2471E-03	.1445E-03	.1204E-03	.6456E-04
.8	.7377E-03	.5357E-03	.4136E-03	.2833E-03
1.0	.1510E-02	.1246E-02	.9330E-03	.7390E-03

Table 4b. Comparison of Particle Currents Obtained with 6 and 2 Discrete Ordinates per Quadrant for 10 Orders of Scattering; Cosine Current Source Configuration; Isotropic Scattering:

Reflection

Slab Width (mfp)	Number of Discrete Ordinates 6	2	6	2
	n=1		n=2	
.2	.5864E-01	.6563E-01	.1396E-01	.1270E-01
.4	.8129E-01	.9305E-01	.2945E-01	.2984E-01
.6	.9207E-01	.1053E+00	.3999E-01	.4212E-01
.8	.9767E-01	.1110E+00	.4675E-01	.4980E-01
1.0	.1007E+00	.1139E+00	.5102E-01	.5442E-01
	n=3		n=4	
.2	.3402E-02	.2496E-02	.8319E-03	.4917E-03
.4	.1126E-01	.1004E-01	.4356E-02	.3406E-02
.6	.1881E-01	.1833E-01	.9052E-02	.8135E-02
.8	.2476E-01	.2508E-01	.1357E-01	.1306E-01
1.0	.2911E-01	.2994E-01	.1736E-01	.1727E-01
	n=5		n=6	
.2	.2036E-03	.9694E-04	.4988E-04	.1912E-04
.4	.1691E-02	.1157E-02	.6575E-03	.3934E-03
.6	.4392E-02	.3628E-02	.2137E-02	.1620E-02
.8	.7532E-02	.6869E-02	.4204E-02	.3626E-02
1.0	.1055E-01	.1013E-01	.6463E-02	.5984E-02
	n=7		n=8	
.2	.1923E-04	.3774E-05	.2998E-05	.7454E-06
.4	.2557E-03	.1337E-03	.9946E-04	.4547E-04
.6	.1041E-02	.7237E-03	.5671E-03	.3233E-03
.8	.2352E-02	.1916E-02	.1317E-02	.1013E-02
1.0	.3977E-02	.3544E-02	.2451E-02	.2101E-02
	n=9		n=10	
.2	.7354E-06	.1473E-06	.1805E-06	.2913E-07
.4	.3969E-04	.1546E-04	.1505E-04	.5258E-05
.6	.2471E-03	.1445E-03	.1204E-03	.6455E-04
.8	.7382E-03	.5358E-03	.4137E-03	.2833E-03
1.0	.1513E-02	.1246E-02	.9337E-03	.7391E-03

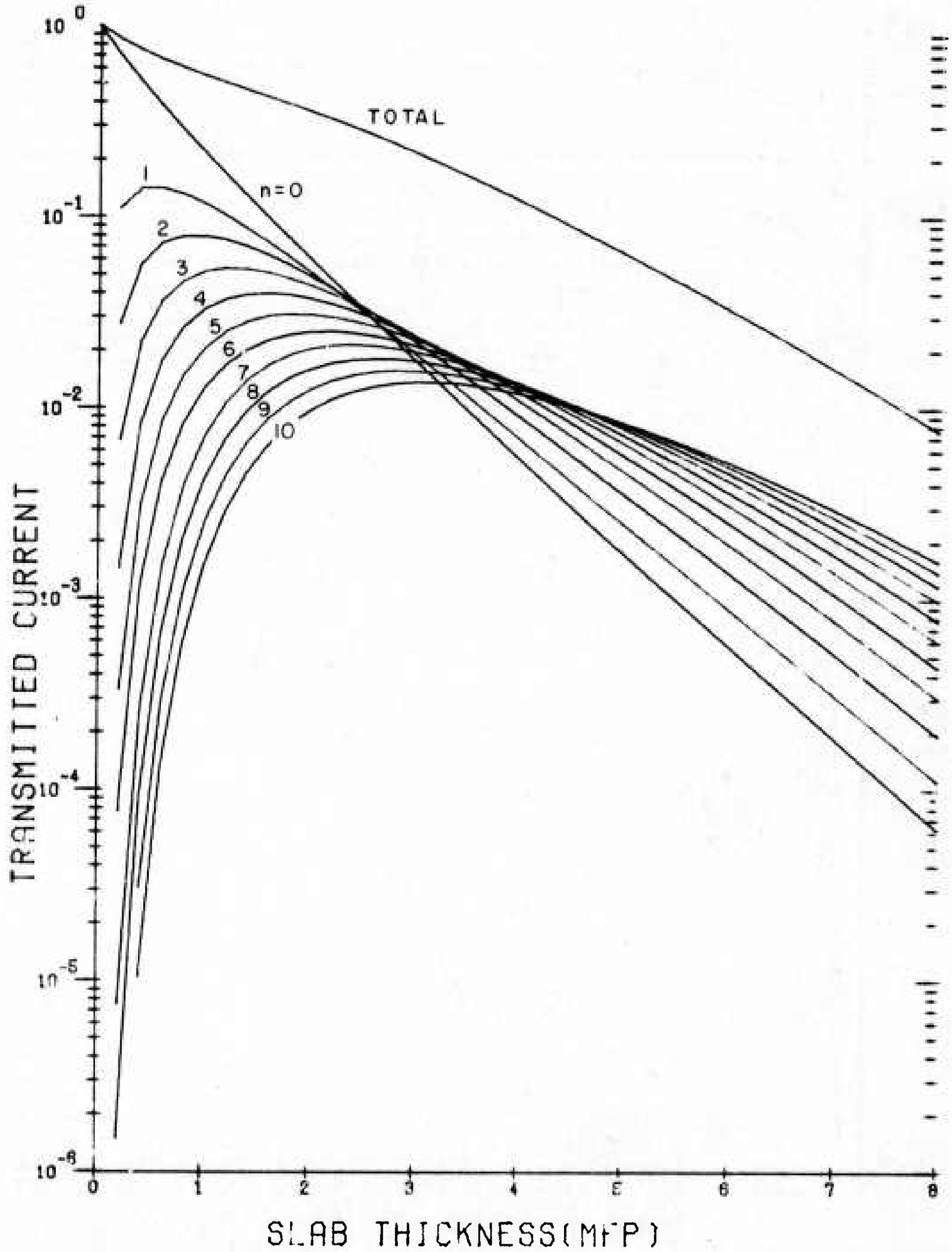

Figure 14. Transmitted Current, $T_n(t)$, vs Slab Thickness, t, for nth Order Isotropic Scattering ($0 \leq n \leq 10$); Cosine Current Source Configuration

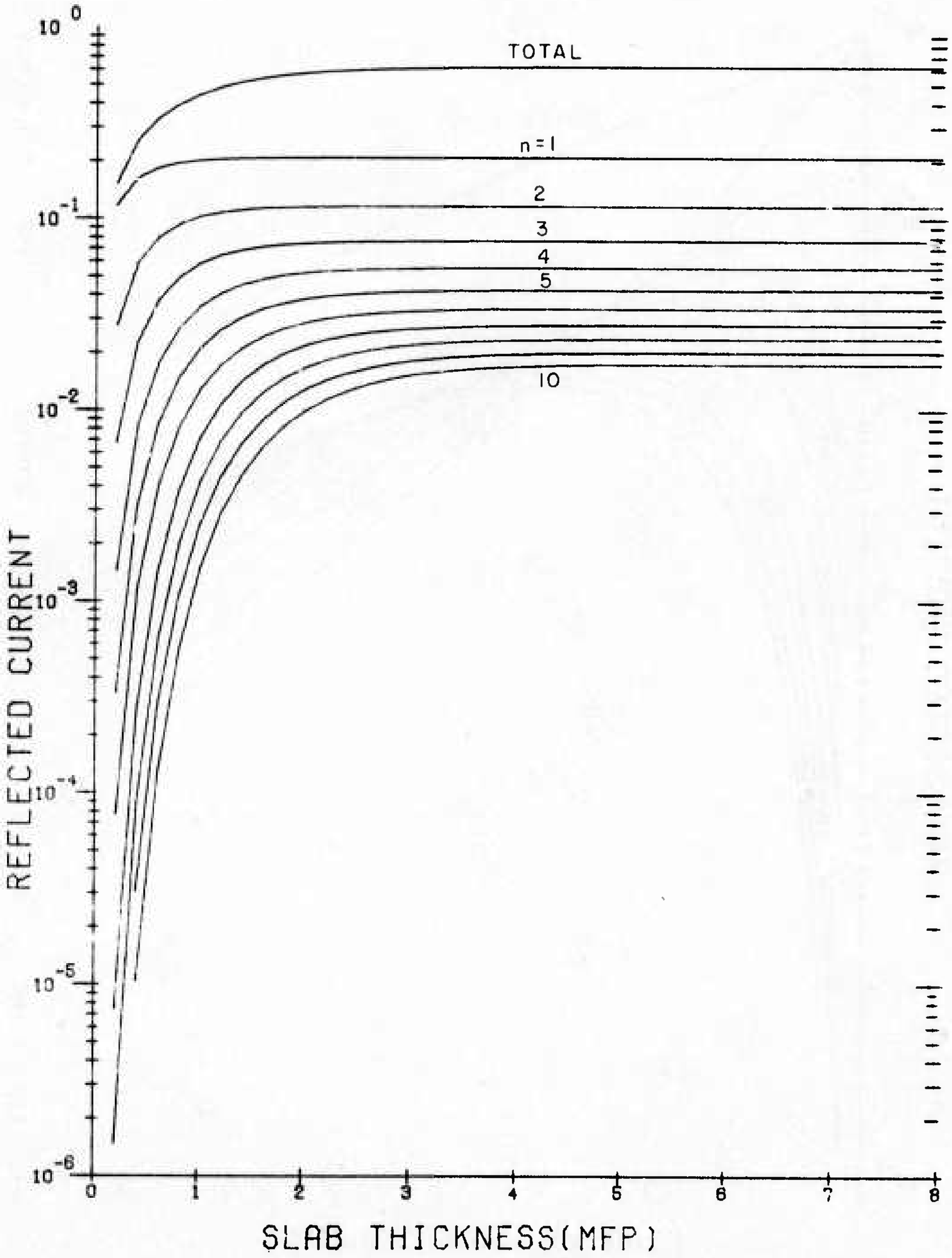

Figure 15. Reflected Current, $B_n(t)$, vs Slab Thickness, t, for nth Order Isotropic Scattering ($1 \leq n \leq 10$); Cosine Current Source Configuration

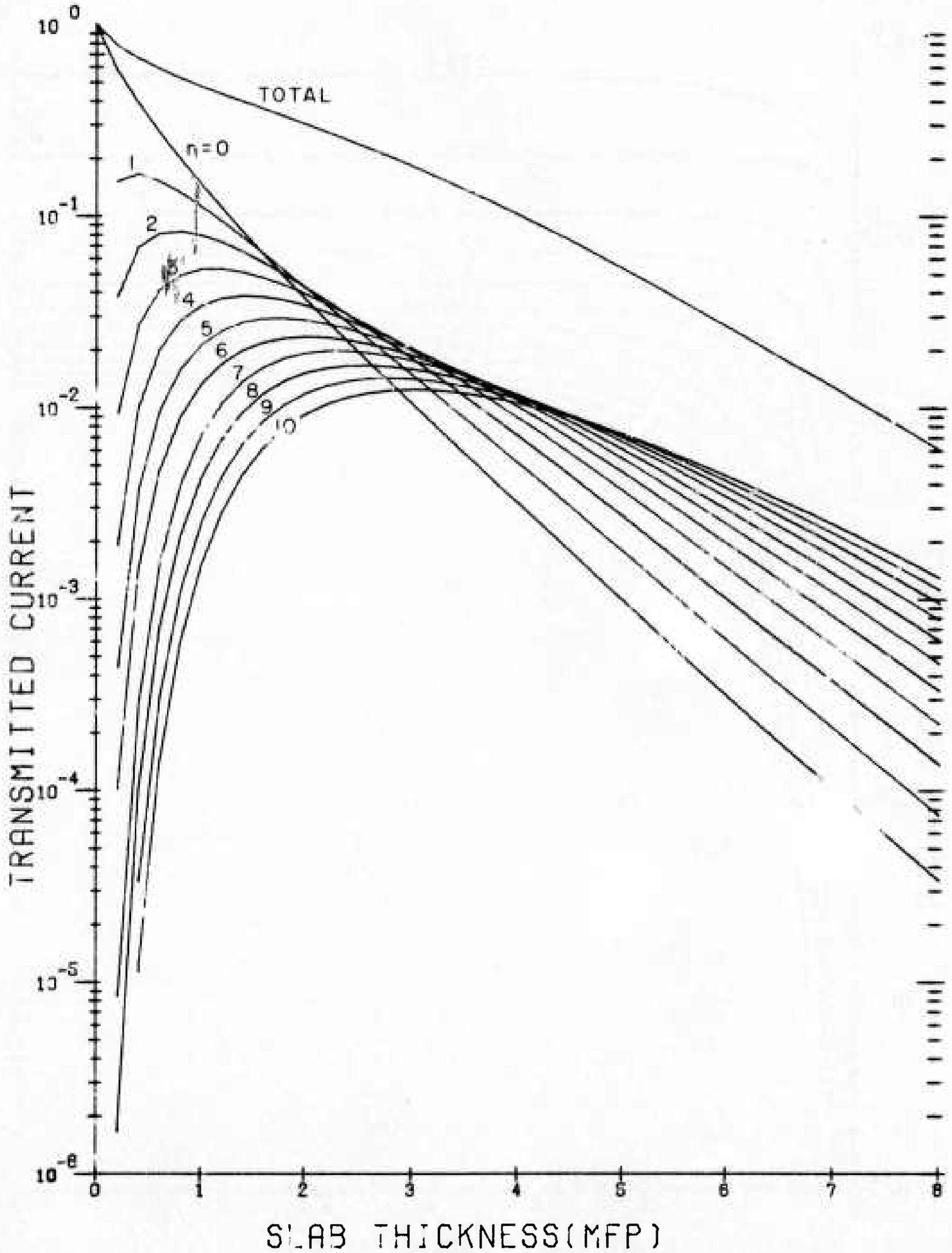

Figure 16. Transmitted Current, $T_n(t)$, vs Slab Thickness, t, for nth Order Isotropic Scattering ($0 \leq n \leq 10$); Isotropic Current Source Configuration

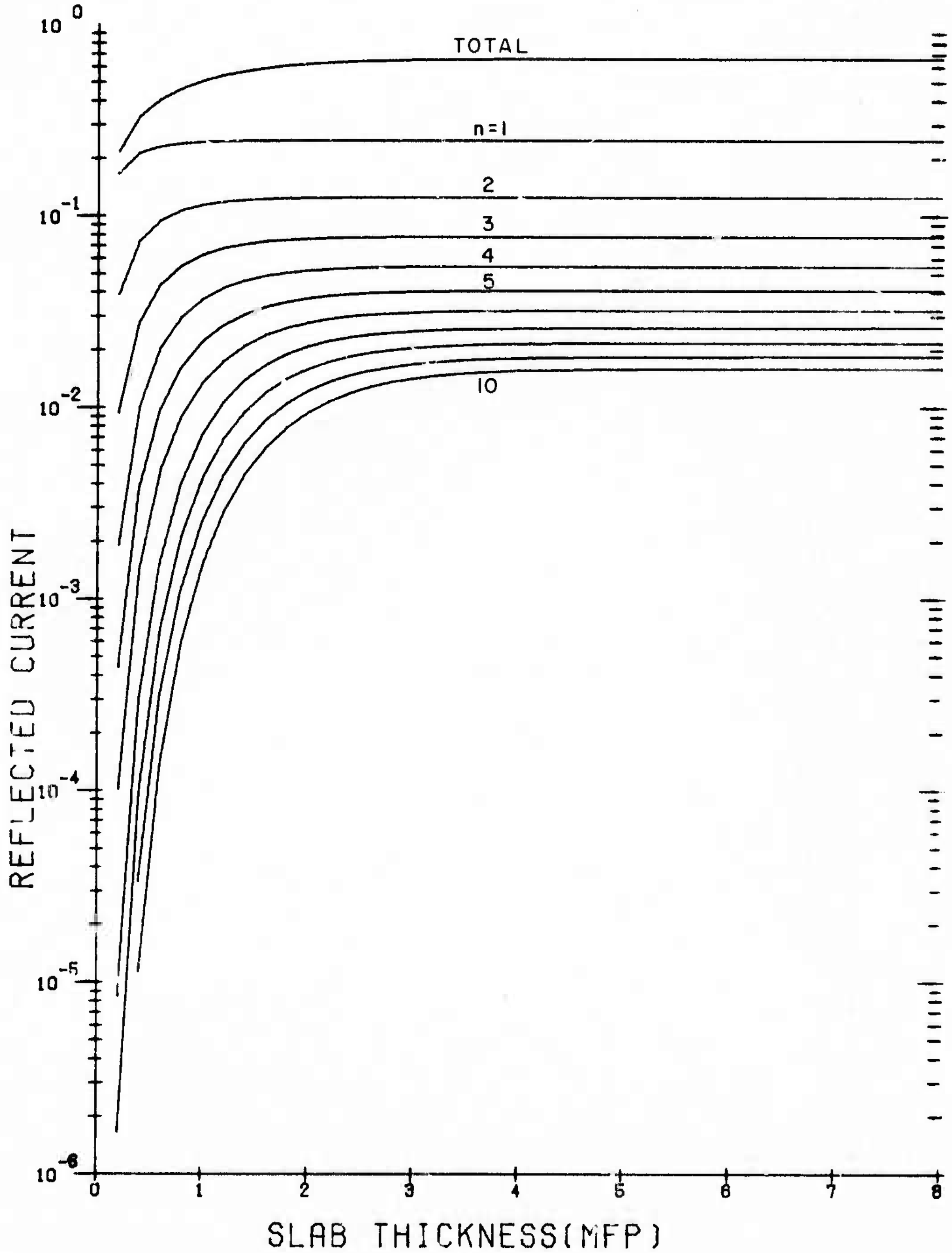

Figure 17. Reflected Current $B_n(t)$, vs Slab Thickness, t, for nth Order Isotropic Scattering ($1 \leq n \leq 10$); Isotropic Current Source Configuration

5. THE ONE-DIMENSIONAL BOLTZMANN EQUATION FOR ISOTROPIC SCATTERING

5.1 Derivation of the One-Dimensional Boltzmann Equation for Scattering in Slabs

The process of scattering in a slab geometry can be described by the one-dimensional Boltzmann equation.[11] A demonstration of this is afforded by considering the contribution to the particle density $d\phi(z)$ at a point a distance z into the slab (Figure 18) due to particles emanating from an element of volume dV, either due to scattering within dV or from an internal source distribution. If λ is the scattering mean-free-path, constant for isotropic scattering, and the probability of a particle surviving a collision is denoted by c, then

$$d\phi_s(z) = \frac{e^{-r/\lambda}}{4\pi r^2}\left[\frac{c}{\lambda}\,\phi(z') + s(z')\right] dV, \tag{73}$$

where s(z) is the internal source distribution, if one exists, and

$$r = \sqrt{x^2 + (z-z')^2} \quad . \tag{74}$$

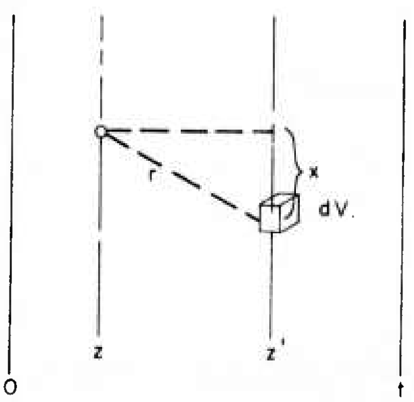

Figure 18. Slab Coordinate System Showing Particle Density Contribution at z from Volume Element dV

Then the total particle density at z due to scatterings or internal sources at every value of z' within the slab is

$$\phi_s(z) = \int_0^t dz' \int_{|z-z'|}^{\infty} dr\, \frac{e^{-\frac{r}{\lambda}}}{4\pi r^2}\left[\frac{c}{\lambda}\,\phi(z') + s(z')\right] 2\pi r\, dr, \tag{75}$$

11. Forbes, I.A. (1973) Private communication.

since $dV = 2\pi x(dx)\,(dz')$ and $r(dr) = x(dx)$.
Integration over r results in

$$\phi_s(z) = 1/2 \int_0^t dz'\, E_1\left(\frac{|z-z'|}{\lambda}\right) \left[\frac{c}{\lambda}\, \phi(z') + s(z')\right] , \tag{76}$$

where $E_1(x) = \int_x^\infty \exp(-u)/u\, du$ is the exponential integral function of order one. In the absence of internal sources, the scattered particle density at any point z within the slab then becomes

$$\phi_s(z) = \frac{c}{2\lambda} \int_0^t dz'\, E_1\left(\frac{|z-z'|}{\lambda}\right) \phi(z') . \tag{77}$$

In order to obtain the total particle density, the unscattered density $\phi_u(z)$ due to the presence of a surface source must also be obtained. The differential form of the Boltzmann equation in the absence of scattering and internal source is

$$\mu \frac{\partial \phi_u}{\partial z} + \frac{1}{\lambda}\, \phi_u = 0 , \tag{78}$$

which has the simple solution

$$\phi_u(z, \mu) = \phi(0, \mu)\, e^{-z/\lambda\mu} , \tag{79}$$

where μ is the cosine of the angle of incidence (Figure 19).

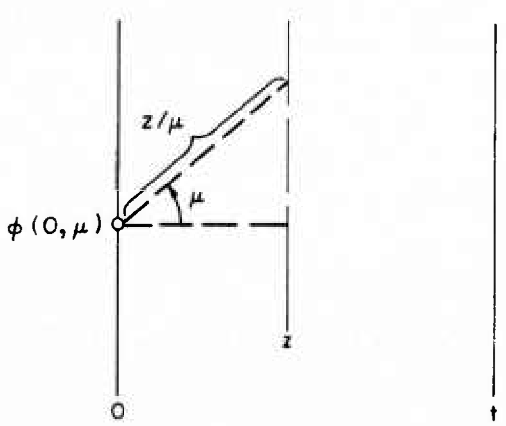

Figure 19. Source of Particles at z = 0

If there is an isotropic density of particles at z = 0,

$$\phi_u(0, \mu) \equiv \phi_o , \tag{80}$$

so that

$$\phi_u(z, \mu) = \phi_o \, e^{-z/\lambda\mu} . \tag{81}$$

Integrating out the angular dependence yields

$$\phi_u(z) = \phi_o \int_o^1 d\mu \, e^{-z/\lambda\mu}$$

$$= \phi_o \, E_2 \, (z/\lambda) , \tag{82}$$

where $E_2(x) = \int_o^1 du \exp(-x/u)$ is the exponential integral function of order two. The total density at z is then

$$\phi(z) = \phi_u(z) + \phi_s(z)$$

$$= \phi_o E_2(\frac{z}{\lambda}) + \frac{c}{2\lambda} \int_o^t dz' \, E_1\left(\frac{|z-z'|}{\lambda}\right) \phi(z') . \tag{83}$$

If a unit incident particle density is assumed, the constant ϕ_o has a value of unity $[E_2(0) = 1]$. Also, the scattering is assumed to be conservative as well as isotropic so that c = 1.

If the distance variable is expressed in units of λ, that is $z/\lambda \to z$, $t/\lambda \to t$, the final form of the one-dimensional Boltzmann equation for the particle density within the slab is

$$\phi(z) = E_2(z) + 1/2 \int_o^t dz' \, E_1(|z-z'|) \, \phi(z') . \tag{84}$$

5.2 Iterative Solution Method and Expressions for Transmitted and Reflected Currents

The integral equation (Eq. 84) is of the Fredholm type and may be solved by means of an iterative procedure.[12] Let $\phi_n(z)$ be the nth approximation to the solution of Eq. (84), and let $\phi_o(z) = E_2(z)$. Then $\phi_n(z)$ is given iteratively by

---

12. Lovitt, W.V. (1950) Linear Integral Equations, Dover Publications, Inc., New York.

$$\phi_n(z) = \phi_o(z) + 1/2 \int_o^t dz' \, E_1\left(|z-z'|\right) \phi_{n-1}(z') . \tag{85}$$

A physical significance can be attributed to these iterations. If the quantity S_n is defined as

$$S_n(z) \equiv \phi_n(z) - \phi_{n-1}(z) , \; n \geq 1 \tag{86a}$$

and

$$S_o(z) \equiv \phi_o(z) , \tag{86b}$$

then $S_n(z)$ satisfies the equation

$$S_n(z) = 1/2 \int_o^t E_1 \left(|z-z'|\right) S_{n-1}(z') \, dz' . \tag{87}$$

Physically, since $E_1\left(|z-z'|\right)$ is the single collision kernel, $S_n(z)$ represents the collision or source density of particles that have collided isotropically n times.[13] In other words, each iteration of Eq. (85) adds another generation of scattering order to the particle density. The logical extension of this argument is that $\phi(z) = \phi_\infty(z)$.

Finally, the transmitted and reflected currents at z = t and z = 0, respectively, can be obtained for each order of scattering. If $S_{n-1}(z)$ is the density of particles scattered n-1 times at z (Figure 20), then the transmitted current of order n at z = t is given by

$$T_n^B(t) = \int_o^1 d\mu \int_o^t \frac{dz}{\mu} e^{-\frac{(t-z)}{\mu}} \mu \, S_{n-1}(z) ,$$

where, as before, z is given in units of mean-free-path, so that the probability of a scatter occurring in the distance interval dz/μ is simply dz/μ. When the angular dependence is integrated out, the result is

$$T_n^B(t) = \int_o^t dz \, E_2(t-z) \, S_{n-1}(z) . \tag{88}$$

---

13. Sobolev, V.V. (1963) A Treatise on Radiative Transfer, D. Van Nostrand Co., Inc., Princeton, N.J.

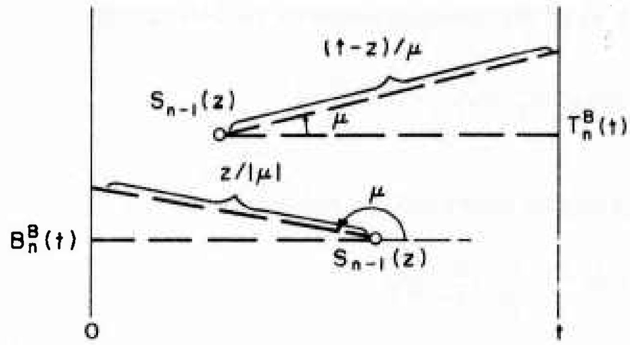

Figure 20. Transmitted and Reflected Currents, $T_n^B(t)$ and $B_n^B(t)$, from Distributed Sources of Scattered Particles $S_{n-1}(z)$

Similarly, for the reflected current

$$B_n^B(t) = \int_{-1}^{0} d\mu \int_{0}^{t} \frac{dz}{|\mu|} e^{-z/\mu} |\mu| S_{n-1}(z)$$

$$= \int_{0}^{t} dz\, E_2(z)\, S_{n-1}(z) . \tag{89}$$

The currents $T_n^B(t)$ and $B_n^B(t)$ (the superscripts denote results obtained from the Boltzmann equation method) should be directly comparable to those obtained by the OOSII method for the cosine current (isotropic particle density) source. The numerical values obtained by these two methods are in fact very close as is shown in Table 8.

5.3 Numerical Solution of the One-Dimensional Boltzmann Equation for Isotropic Scatter in Slabs

A computer program was written which solves the integral equation

$$\phi_n(z) = \phi_o(z) + 1/2 \int_{0}^{t} E_1(|z-z'|)\, \phi_{n-1}(z')\, dz' . \tag{85}$$

If the substitution $y = z-z'$ is made, Eq. (85) can be rewritten in a form more amenable to computation as follows:

$$\phi_n(z) = \phi_o(z) + 1/2 \int_{0}^{t-z} \phi_{n-1}(z+y)\, E_1(y)dy$$
$$+ 1/2 \int_{0}^{z} \phi_{n-1}(z-y)\, E_1(y)dy . \tag{90}$$

Let the first integral in the above expression be denoted as

$$I = \int_{o}^{t-z} \phi_{n-1}(z+y)\, E_1(y)\, dy \; . \tag{91}$$

The function $E_1(y)$ can be expressed in exact form as

$$E_1(y) = -\gamma - \ln y - \sum_{n=1}^{\infty} \frac{(-1)^n y^n}{n \cdot n!} \; , \tag{92}$$

where γ is Euler's constant. The integral I can be separated into the following two integrals:

$$I = -(I_1 + I_2) \; , \tag{93}$$

where

$$I_1 = \int_{o}^{t-z} \phi_{n-1}(z+y) \cdot \ln y \, dy \; , \tag{94}$$

and

$$I_2 = \int_{o}^{t-z} \left[\gamma + \sum_{n=1}^{\infty} \frac{(-1)^n y^n}{n \cdot n!}\right] \phi_{n-1}(z+y)\, dy \; . \tag{95}$$

The first of these integrals, I_1, can be handled by means of a Gauss quadrature specifically developed for evaluating integrals involving products of logarithms with arbitrary nonsingular functions.[10, 14] If the following substitutions are made

$$\Delta \equiv t - z \text{ and } u_1 \equiv y/\Delta \; ,$$

the logarithmic integral becomes

$$I_1 = \Delta \int_{o}^{1} \phi_{n-1}(z + \Delta u_1) \ln (\Delta u_1)\, du_1 \; , \tag{96a}$$

or

14. Crosbie, A.L., Merriam, R.L., and Viskanta, R. (1968) J. Quant. Spectr. Rad. Transfer, 8:1609.

$$I_1 = \Delta \sum_{k=1}^{M_1} A_k \, \phi_{n-1}(z+\Delta u_{1_k}) + I_{1a} , \tag{96b}$$

with

$$I_{1a} = \Delta \ln \Delta \int_o^1 \phi_{n-1}(z+\Delta w)\, dw . \tag{97}$$

The u_{1_k} are the prescribed quadrature ordinates, and the A_k are their corresponding quadrature coefficients. Since the additional term I_{1a} contains no logarithm in the integrand, it is evaluated by the standard Gauss quadrature procedure as will be outlined in the evaluation of the integral I_2.

The second integral, I_2, can be evaluated by the standard Gauss quadrature technique. When the transformations $\Delta = t-z$ and $u_2 = 2y/\Delta - 1$ are made, the result is

$$I_2 = \frac{\Delta}{2} \int_{-1}^{1} \left\{ \gamma + \sum_{\ell=1}^{\infty} \frac{(-1)^{\ell}}{\ell \cdot \ell!} \left[\frac{\Delta(1+u_2)}{2} \right]^{\ell} \right\} \phi_{n-1}\left(z+\frac{\Delta}{2}(1+u_2)\right) du_2 , \tag{98a}$$

or

$$I_2 = \frac{\Delta}{2} \sum_{k=1}^{M_2} B_k \left\{ \gamma + \sum_{\ell=1}^{60} \frac{(-1)}{\ell \cdot \ell!} \left[\frac{\Delta(1+u_{2_k})}{2} \right]^{\ell} \right\} \phi_{n-1}\left(z+\frac{\Delta}{2}(1+u_{2_k})\right) , \tag{98b}$$

where the u_{2_k} and the B_k are the quadrature ordinates and their corresponding coefficients. In the actual calculations, M_1 and M_2 were chosen to be 16 and 32, respectively. The summation over ℓ was not carried out to 60 terms if sufficient covergence could be achieved with a lower ℓ value.

The integrals involving $\phi_{n-1}(z-y)$ are dealt with in the same manner as those above, so that the resulting computational form for Eq. (85) becomes

$$\phi_n(z) = \phi_o(z) - \frac{1}{2}$$

$$\cdot \Delta \sum_{k=1}^{M_1} A_k \, \phi_{n-1}(z_1 \Delta u_{1_k}) + z \sum_{k=1}^{M_1} A_k \, \phi_{n-1}(z - z u_{1_k})$$

$$+ \frac{\Delta}{2}(\gamma + \ln \Delta) \sum_{k=1}^{M_2} B_k \, \phi_{n-1}\left(z+\frac{\Delta}{2}(1+u_{2_k})\right)$$

$$+ \frac{z}{2}(\gamma + \ln z) \sum_{k=1}^{M_2} B_k \, \phi_{n-1}\left(\frac{z}{2}(1-u_{2_k})\right)$$

$$+\sum_{k=1}^{M_2} B_k \sum_{\ell=1}^{60} \left(\frac{\Delta}{2}\right)^{\ell+1} \frac{(-1)^\ell}{\ell \cdot \ell!} (1+u_{2_k})^\ell \phi_{n-1}\left(z+\frac{\Delta}{2}(1+u_{2_k})\right)$$

$$+\sum_{k=1}^{M_2} B_k \sum_{\ell=1}^{60} \left(\frac{z}{2}\right)^{\ell+1} \frac{(-1)^\ell}{\ell \cdot \ell!} (1-u_{2_k})^\ell \phi_{n-1}\left(\frac{z}{2}(1-u_{2_k})\right) . \qquad (99)$$

The function $\phi_o(z)$ was taken to be $E_2(z)$.

Typical computational results for the cumulative particle density distribution up to 10th order of scattering are given in Tables 5, 6, and 7 for slab thicknesses of 1, 5, and 10 mfp, respectively.

A final computation is that of the transmitted and reflected currents as functions of scattering order. The expressions for these, given by Eqs. (88) and (89), are evaluated using a Simpson's rule integration.

6. MONTE CARLO CALCULATION OF PARTICLE TRANSPORT IN SLABS

6.1 General Discussion

The Monte Carlo method as applied to particle transport consists basically of attempting to describe the behavior of an entire ensemble of particles by tracing the histories of many individual particles as they migrate through the scattering medium. Appropriate summations over a sufficiently large number of these histories are made in order to arrive at a description of the ensemble as a whole. While this method lacks the elegance and computational efficiency associated with some other types of transport calculations, it does provide an extremely high degree of flexibility with regard to the variety of problems that can be handled. Results of Monte Carlo calculations are used here to confirm the results obtained by the OOSII method and the Boltzmann equation solutions. The method is conceptually simple and provides a truly independent means to such a confirmation.

A Monte Carlo program was written to study the transport of particles in scattering slabs. The computation is organized into two main parts. Part I consists of: (1) the generation of a plane isotropic (current) source of particles at the boundary of an infinite slab; (2) the tracing of the particle histories through the medium while keeping account and recording the collision site positions, trajectory orientations, and orders of scattering. Part II superimposes a source distribution function on the plane isotropic source and calculates the transmitted and reflected currents for each order of scattering and for a number of finite slab thicknesses assumed to be imbedded within the infinite slab.

Table 5. Cumulative Particle Density Distribution, $\phi_n(z)$: Slab Width = 1.0 mfp

z (mfp)	n = 0	1	2	3	4	5
0.00	.100000E+01	.124448E+01	.135864E+01	.142147E+01	.145841E+01	.148074E+01
.05	.872835E+00	.112003E+01	.125760E+01	.133290E+01	.137700E+01	.143360E+01
.10	.722545E+00	.102822E+01	.117937E+01	.126305E+01	.131219E+01	.134185E+01
.15	.641039E+00	.949353E+00	.110948E+01	.119959E+01	.125279E+01	.128496E+01
.20	.574201E+00	.879339E+00	.104517E+01	.114020E+01	.119669E+01	.123095E+01
.25	.517730E+00	.816197E+00	.985214E+00	.108386E+01	.114296E+01	.117892E+01
.30	.469115E+00	.758707E+00	.928888E+00	.103001E+01	.109108E+01	.112838E+01
.35	.426713E+00	.706016E+00	.875712E+00	.978277E+00	.104074E+01	.107903E+01
.40	.389368E+00	.657483E+00	.825328E+00	.928411E+00	.991694E+00	.103065E+01
.45	.356229E+00	.612601E+00	.777447E+00	.880202E+00	.943773E+00	.983059E+00
.50	.326644E+00	.570949E+00	.731823E+00	.833473E+00	.896820E+00	.936115E+00
.55	.300099E+00	.532170E+00	.688233E+00	.788063E+00	.850696E+00	.889688E+00
.60	.276184E+00	.495951E+00	.646474E+00	.743816E+00	.805265E+00	.843656E+00
.65	.254560E+00	.462011E+00	.606336E+00	.700565E+00	.760374E+00	.797842E+00
.70	.234947E+00	.430086E+00	.567605E+00	.658126E+00	.715853E+00	.752112E+00
.75	.217111E+00	.399921E+00	.530060E+00	.616284E+00	.671490E+00	.706243E+00
.80	.200852E+00	.371250E+00	.493413E+00	.574758E+00	.627002E+00	.659949E+00
.85	.185999E+00	.343769E+00	.457304E+00	.533150E+00	.581969E+00	.612794E+00
.90	.172404E+00	.317074E+00	.421171E+00	.490806E+00	.535676E+00	.564031E+00
.95	.159940E+00	.290442E+00	.383894E+00	.446345E+00	.486578E+00	.511999E+00
1.00	.148495E+00	.260733E+00	.340168E+00	.392972E+00	.426895E+00	.448030E+00

Table 5. Cumulative Particle Density Distribution, $\phi_n(z)$: Slab Width = 1.0 mfp (Cont)

z (mfp)	n = 6	7	8	9	10
0.00	.149440E+01	.150281E+01	.150801E+01	.151122E+01	.151320E+01
.05	.141987E+01	.142988E+01	.143605E+01	.143987E+01	.144223E+01
.10	.135999E+01	.137114E+01	.137803E+01	.138229E+01	.138492E+01
.15	.130466E+01	.131678E+01	.132426E+01	.132888E+01	.133174E+01
.20	.125194E+01	.126487E+01	.127285E+01	.127778E+01	.128084E+01
.25	.120099E+01	.121459E+01	.122298E+01	.122818E+01	.123139E+01
.30	.115131E+01	.116546E+01	.117420E+01	.117959E+01	.118294E+01
.35	.110262E+01	.111718E+01	.112618E+01	.113175E+01	.113519E+01
.40	.105469E+01	.106954E+01	.107872E+01	.108441E+01	.108792E+01
.45	.100735E+01	.102237E+01	.103166E+01	.103741E+01	.104097E+01
.50	.960454E+00	.975523E+00	.984850E+00	.990622E+00	.994196E+00
.55	.913883E+00	.923877E+00	.938161E+00	.943910E+00	.947468E+00
.60	.867503E+00	.882299E+00	.891466E+00	.897144E+00	.900658E+00
.65	.821170E+00	.835649E+00	.844625E+00	.850184E+00	.853626E+00
.70	.774718E+00	.788761E+00	.797468E+00	.802863E+00	.806203E+00
.75	.727937E+00	.741422E+00	.749786E+00	.754968E+00	.758177E+00
.80	.680536E+00	.693389E+00	.701283E+00	.706205E+00	.709254E+00
.85	.632070E+00	.644063E+00	.651504E+00	.656116E+00	.658973E+00
.90	.581766E+00	.592803E+00	.599653E+00	.603899E+00	.606528E+00
.95	.527902E+00	.537798E+00	.543940E+00	.547747E+00	.550105E+00
1.00	.461683E+00	.470007E+00	.475172E+00	.478373E+00	.480356E+00

Table 6. Cumulative Particle Density Distribution, $\phi_n(z)$: Slab Width = 5.0 mfp

z (mfp)	n = 0	1	2	3	4	5
0.0	.100000E+01	.124980E+01	.137554E+01	.145369E+01	.150833E+01	.154930E+01
.2	.574201E+00	.886917E+00	.106884E+01	.118618E+01	.126873E+01	.133057E+01
.4	.389368E+00	.668122E+00	.857669E+00	.990358E+00	.108766E+01	.116218E+01
.6	.276184E+00	.511377E+00	.691354E+00	.827243E+00	.931655E+00	.101396E+01
.8	.200852E+00	.394994E+00	.558181E+00	.689867E+00	.795771E+00	.881880E+00
1.0	.148495E+00	.307013E+00	.450992E+00	.574172E+00	.677571E+00	.764291E+00
1.2	.111104E+00	.239750E+00	.364540E+00	.476972E+00	.575178E+00	.660063E+00
1.4	.838899E-01	.187919E+00	.294741E+00	.395542E+00	.486889E+00	.568155E+00
1.6	.638032E-01	.147741E+00	.238359E+00	.327511E+00	.411099E+00	.487533E+00
1.8	.488153E-01	.116450E+00	.192801E+00	.270813E+00	.346304E+00	.417155E+00
2.0	.375343E-01	.919877E-01	.15597[illegible]E+00	.223661E+00	.291110E+00	.355991E+00
2.2	.289827E-01	.728021E-01	.126207E+00	.184520E+00	.244243E+00	.303048E+00
2.4	.224613E-01	.577142E-01	.102131E+00	.150208E+00	.204559E+00	.257384E+00
2.6	.174630E-01	.458209E-01	.826596E-01	.125228E+00	.171040E+00	.218123E+00
2.8	.136152E-01	.364262E-01	.669055E-01	.103029E+00	.142789E+00	.184462E+00
3.0	.106419E-01	.289914E-01	.541582E-01	.846961E-01	.119021E+00	.155670E+00
3.2	.833663E-02	.230977E-01	.438383E-01	.695629E-01	.990508E-01	.131089E+00
3.4	.654396E-02	.184180E-01	.354789E-01	.570759E-01	.822889E-01	.110131E+00
3.6	.514623E-02	.146965E-01	.287043E-01	.467721E-01	.682253E-01	.922753E-01
3.8	.405383E-02	.117320E-01	.232079E-01	.382653E-01	.564217E-01	.770582E-01
4.0	.319823E-02	.936604E-02	.187409E-01	.312295E-01	.464981E-01	.640678E-01
4.2	.252678E-02	.747272E-02	.150986E-01	.253904E-01	.381242E-01	.529343E-01
4.4	.199890E-02	.595132E-02	.121124E-01	.205135E-01	.310074E-01	.433184E-01
4.6	.158321E-02	.471904E-02	.963655E-02	.163854E-01	.248705E-01	.348848E-01
4.8	.125538E-02	.370169E-02	.752824E-02	.127842E-01	.194047E-01	.272355E-01
5.0	.996469E-03	.277679E-02	.549984E-02	.918923E-02	.137938E-01	.192029E-01

Table 6. Cumulative Particle Density Distribution, $\phi_n(z)$: Slab Width = 5.0 mfp (Cont)

z (mfp)	n = 6	7	8	9	10
0.0	.158148E+01	.160761E+01	.162936E+01	.164783E+01	.166375E+01
.2	.137904E+01	.141832E+01	.145096E+01	.147863E+01	.150244E+01
.4	.122131E+01	.126962E+01	.130995E+01	.134427E+01	.137389E+01
.6	.108051E+01	.113551E+01	.118185E+01	.122152E+01	.125591E+01
.8	.952992E+00	.101266E+01	.106348E+01	.110732E+01	.114556E+01
1.0	.837535E+00	.900015E+00	.953878E+00	.100078E+01	.104199E+01
1.2	.733404E+00	.797056E+00	.852658E+00	.901570E+00	.944893E+00
1.4	.639969E+00	.703397E+00	.759569E+00	.809522E+00	.854149E+00
1.6	.556577E+00	.618636E+00	.674370E+00	.724492E+00	.769680E+00
1.8	.482530E+00	.542318E+00	.596772E+00	.646306E+00	.691381E+00
2.0	.417098E+00	.473935E+00	.526429E+00	.574733E+00	.619108E+00
2.2	.359531E+00	.412939E+00	.462949E+00	.509496E+00	.552665E+00
2.4	.309085E+00	.358758E+00	.405898E+00	.450272E+00	.491816E+00
2.6	.265039E+00	.310811E+00	.354820E+00	.396705E+00	.436286E+00
2.8	.226702E+00	.268522E+00	.309241E+00	.348412E+00	.385767E+00
3.0	.193424E+00	.231331E+00	.268687E+00	.304997E+00	.339928E+00
3.2	.164600E+00	.198697E+00	.232687E+00	.266053E+00	.298422E+00
3.4	.139674E+00	.170111E+00	.200783E+00	.231172E+00	.260890E+00
3.6	.118135E+00	.145090E+00	.172527E+00	.199949E+00	.226966E+00
3.8	.995197E-01	.123182E+00	.147492E+00	.171983E+00	.196278E+00
4.0	.834009E-01	.103963E+00	.125264E+00	.146876E+00	.168448E+00
4.2	.693853E-01	.870271E-01	.105434E+00	.124227E+00	.143083E+00
4.4	.570984E-01	.719750E-01	.875893E-01	.103611E+00	.119756E+00
4.6	.461545E-01	.583812E-01	.712662E-01	.845358E-01	.979500E-01
4.8	.360674E-01	.456693E-01	.558053E-01	.662670E-01	.768553E-01
5.0	.252709E-01	.318432E-01	.387618E-01	.458816E-01	.530754E-01

Table 7. Cumulative Particle Density Distribution, $\phi_n(z)$: Slab Width = 10.0 mfp

z (mfp)	n= 0	1	2	3	4	5
0.0	.100000E+01	.124921E+01	.137646E+01	.145444E+01	.150896E+01	.154986E+01
.5	.326644E+00	.583694E+00	.769793E+00	.990353E+00	.100695E+01	.108593E+01
1.0	.148495E+00	.307014E+00	.450992E+00	.574179E+00	.677598E+00	.764356E+00
1.5	.731008E-01	.166567E+00	.265054E+00	.360008E+00	.447582E+00	.526614E+00
2.0	.375343E-01	.919904E-01	.155991E+00	.223702E+00	.291208E+00	.356191E+00
2.5	.197977E-01	.514211E-01	.919047E-01	.138089E+00	.187259E+00	.237346E+00
3.0	.106419E-01	.290013E-01	.542043E-01	.848290E-01	.119322E+00	.156256E+00
3.5	.580189E-02	.164707E-01	.320023E-01	.519214E-01	.754860E-01	.101863E+00
4.0	.319823E-02	.940672E-02	.189151E-01	.316941E-01	.474811E-01	.658686E-01
4.5	.177869E-02	.539727E-02	.111920E-01	.193072E-01	.297272E-01	.423074E-01
5.0	.996469E-03	.310885E-02	.662673E-02	.117394E-01	.185380E-01	.270175E-01
5.5	.561678E-03	.179664E-02	.392731E-02	.712923E-02	.115228E-01	.171697E-01
6.0	.318258E-03	.104612E-02	.232885E-02	.432345E-02	.714089E-02	.108633E-01
6.5	.181145E-03	.604846E-03	.138220E-02	.262001E-02	.441566E-02	.684927E-02
7.0	.103510E-03	.352007E-03	.820322E-03	.158528E-02	.272290E-02	.430219E-02
7.5	.593527E-04	.205107E-03	.486418E-03	.957325E-03	.167488E-02	.269313E-02
8.0	.341376E-04	.119532E-03	.288088E-03	.577672E-03	.102795E-02	.167982E-02
8.5	.196888E-04	.695397E-04	.170009E-03	.346402E-03	.626535E-03	.104063E-02
9.0	.113836E-04	.402151E-04	.989406E-04	.205334E-03	.378019E-03	.637143E-03
9.5	.659642E-05	.228410E-04	.556177E-04	.118121E-03	.221575E-03	.377954E-03
10.0	.383024E-05	.117937E-04	.275394E-04	.594378E-04	.111066E-03	.189756E-03

Table 7. Cumulative Particle Density Distribution, $\phi_n(z)$: Slab Width = 10.0 mfp (Cont)

z (mfp)	n = 6	7	8	9	10
0.0	.158200E+01	.160811E+01	.162987E+01	.164838E+01	.166435E+01
.5	.114919E+01	.120117E+01	.124480E+01	.128206E+01	.131434E+01
1.0	.837662E+00	.900240E+00	.954244E+00	.100134E+01	.104281E+01
1.5	.597276E+00	.660303E+00	.716596E+00	.767045E+00	.812452E+00
2.0	.417462E+00	.474548E+00	.527395E+00	.576177E+00	.621175E+00
2.5	.286916E+00	.335047E+00	.381198E+00	.425095E+00	.466635E+00
3.0	.194449E+00	.232986E+00	.271201E+00	.308628E+00	.344965E+00
3.5	.132246E+00	.159923E+00	.190299E+00	.220899E+00	.251361E+00
4.0	.863856E-01	.108555E+00	.131933E+00	.156125E+00	.180798E+00
4.5	.568177E-01	.729822E-01	.905099E-01	.109117E+00	.128541E+00
5.0	.371009E-01	.486561E-01	.615182E-01	.755062E-01	.904365E-01
5.5	.240759E-01	.322015E-01	.414712E-01	.517855E-01	.630309E-01
6.0	.155371E-01	.211726E-01	.277517E-01	.352324E-01	.435551E-01
6.5	.997931E-02	.138415E-01	.184494E-01	.237973E-01	.298627E-01
7.0	.638003E-02	.899967E-02	.121897E-01	.159641E-01	.203237E-01
7.5	.406130E-02	.582115E-02	.800557E-02	.106376E-01	.137306E-01
8.0	.257289E-02	.374361E-02	.522302E-02	.703606E-02	.920092E-02
8.5	.161833E-02	.238856E-02	.337700E-02	.460711E-02	.609725E-02
9.0	.100454E-02	.150118E-02	.214756E-02	.296203E-02	.396065E-02
9.5	.601784E-03	.907392E-03	.130894E-02	.181945E-02	.245056E-02
10.0	.301100E-03	.452189E-03	.649736E-03	.900510E-03	.121004E-02

6.2 Generation of Particle Histories (Part I)

The discussion which follows pertains only to conservative scattering, isotropic in the laboratory system. Other Monte Carlo programs were written to handle various types of anisotropic scattering. In later sections these will be discussed only to the extent to which they differ from the present calculation.

When a particle history is originated at the source plane, the initial direction, relative to the laboratory coordinate system, of departure from the source point is determined. The initial polar angle of the trajectory with respect to the z-axis (z is as before perpendicular to the slab surface) is determined by sampling a uniform random number distribution. Let r_1 be a uniformly distributed random number (actually a computer generated pseudo-random number) where $0 < r_1 < 1$. Then the cosine of the initial polar angle is

$$\mu_o = \cos\theta_o = r_1 . \tag{100}$$

The azimuthal direction, ϕ, is chosen to be zero.

The penetration distance between collisions is determined by inversion of the exponential attenuation formula for particle flux in an attenuating medium. The exponential attenuation factor is selected from a set of uniformly distributed random numbers r_2, where $0 < r_2 < 1$, so that

$$r_2 = \exp(-s_n/\lambda) , \tag{101}$$

where λ is the scattering mean-free-path and s_n is the penetration distance after the nth scatter. The inverse of this expression yields the following direct determination of s_n:

$$s_n = -\lambda \cdot \log_e(r_2) . \tag{102}$$

Once the penetration distance is computed, the coordinates of the next point of interaction are determined. Given that the nth interaction occurs at the point (x_n, y_n, z_n) and the direction of the particle trajectory after the interaction is defined by the angles θ^n, ϕ^n, respectively the polar and azimuthal angles in the laboratory frame, then the coordinates of the point of next interaction are given by

$$x_{n+1} = x_n + s_n \sin\theta^n \cos\phi^n , \tag{103a}$$

$$y_{n+1} = y_n + s_n \sin\theta^n \sin\phi^n , \tag{103b}$$

$$z_{n+1} = z_n + s_n \cos\theta^n . \tag{103c}$$

The superscript n denotes orientation after the nth collision. The collision positions and trajectory orientations are recorded in a mass storage file for every collision of every particle. This file is subsequently used for the particle current computations.

Selection of the post-collision orientation for isotropic scattering in the laboratory system consists of making a random choice for the cosine of the polar angle θ^n, as was done for the initial polar angle. Since the scattering is isotropic in azimuth, the azimuthal orientation is obtained by random selection of the angle on the interval (0, 2π). That is, let r_3 be a uniformly distributed random number where $0 < r_3 < 1$, then

$$\phi^n = 2\pi r_3 . \tag{104}$$

The above procedure is repeated until the particle has either undergone a prespecified maximum number of collisions in the slab or has been backscattered out of the slab through the source face.

6.3 Determination of Transmitted and Reflected Currents for Slabs of Various Widths (Part II)

As a result of the operation of Part I of the Monte Carlo program, the pertinent statistics of the scattered particles at every collision site are stored and available for analysis. The program which computes the transmitted and reflected currents consists of a straightforward particle counting procedure. A grid of finite slab boundaries is superimposed within the infinite slab (Figure 21). As was previously stated, particle histories are terminated in one of two ways, either by having undergone a maximum allowed number of collisions within the slab or by backscatter out of the slab. The first situation is depicted by the dashed line trajectory of Figure 21, and the second by the solid line trajectory. The particle counting procedure executed by the program assigns the following interpretation to the dashed line trajectory:

(1) transmission through a slab of thickness t_1 after 0 collisions,

(2) transmission through a slab of thickness t_2 after 1 collision,

(3) transmission through a slab of thickness t_3 after 2 collisions,

(4) transmission through a slab of thickness t_4 after 7 collisions,

and the following interpretation to the solid line trajectory:

(1) transmission through a slab of thickness t_1 after 0 collisions,

(2) transmission through a slab of thickness t_2 after 2 collisions,

(3) transmission through a slab of thickness t_3 after 4 collisions,

(4) transmission through a slab of thickness t_4 after 8 collisions,

(5) backscatter from a slab of thickness t_5 after 11 collisions,

(6) backscatter from a slab of thickness t_6 after 11 collisions,

(7) backscatter from a slab of thickness t_7 after 11 collisions,

.

.

.

backscatter from a slab of thickness t_m after 11 collisions.

The transmission and reflection current bins are filled by the application of this counting procedure to every particle history. As each history is considered, it is assigned a source weighting factor. For the case of the cosine current source, the tallied figure in each bin is simply twice the initial polar angle cosine, μ_o, of each trajectory (the factor of two is required for source normalization). and in the isotropic current source case, the tallied figure in each bin is unity. The final normalized currents are obtained by dividing these sums by the total number of particle histories considered.

The results of these Monte Carlo computations are given in Table 8, where a comparison with the results obtained by the two methods previously discussed is readily available. For the isotropic scattering case, 100, 000 histories were run.

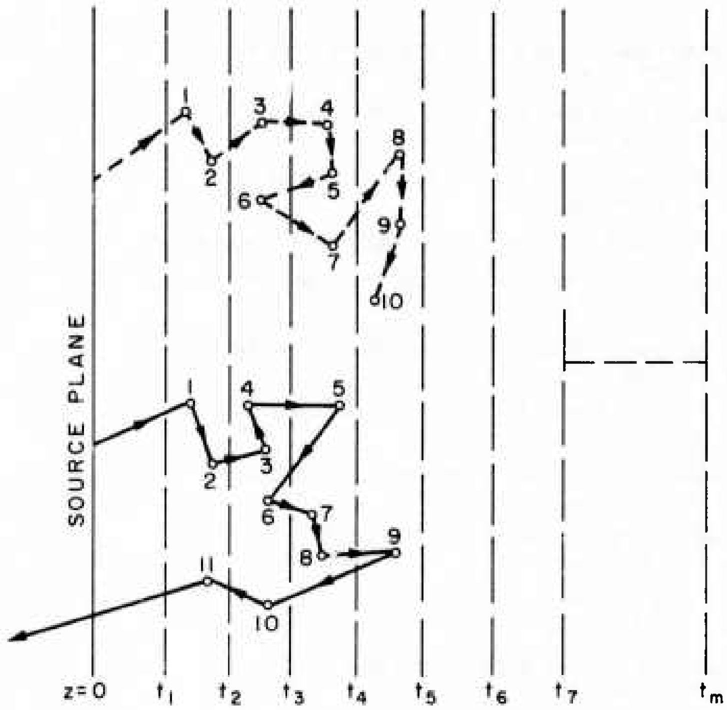

Figure 21. Monte Carlo Slab Configuration

Table 8a. Transmitted Particle Currents, $T_n(t)$ Obtained by Three Methods, Through Slabs of Various Widths, t: Unit Current Cosine Distributed Source; Isotropic Scatter

t	n	Transmitted Current, $T_n(t)$		
		OOSII	Boltzmann	Monte Carlo
	0	.219384E+00	.219384E+00	.217266E+00
	1	.116989E+00	.116293E+00	.116196E+00
	2	.793953E-01	.791163E-01	.795006E-01
	3	.516197E-01	.515542E-01	.519376E-01
	4	.327453E-01	.327732E-01	.335511E-01
1.0	5	.205605E-01	.205669E-01	.208948E-01
	6	.127476E-01	.128200E-01	.128867E-01
	7	.789934E-02	.796341E-02	.804417E-02
	8	.488657E-02	.493785E-02	.533798E-02
	9	.302027E-02	.305902E-02	.319136E-02
	10	.186578E-02	.189426E-02	.190455E-02
	0	.602668E-01	.602667E-01	.608177E-01
	1	.507640E-01	.506139E-01	.499433E-01
	2	.487523E-01	.486028E-01	.484898E-01
	3	.435597E-01	.434810E-01	.429898E-01
	4	.372403E-01	.371008E-01	.369740E-01
2.0	5	.308637E-01	.307182E-01	.308832E-01
	6	.249800E-01	.249417E-01	.246029E-01
	7	.203318E-01	.199941E-01	.204526E-01
	8	.159831E-01	.158952E-01	.157407E-01
	9	.124966E-01	.125687E-01	.127935E-01
	10	.973858E-02	.990299E-02	.103213E-01
	0	.178613E-01	.178613E-01	.174868E-01
	1	.191759E-01	.191271E-01	.193656E-01
	2	.222302E-01	.221743E-01	.217870E-01
	3	.236118E-01	.235604E-01	.232296E-01
	4	.236871E-01	.235764E-01	.240183E-01
3.0	5	.227188E-01	.226268E-01	.225202E-01
	6	.211493E-01	.210775E-01	.204169E-01
	7	.196672E-01	.192161E-01	.195733E-01
	8	.176079E-01	.172466E-01	.172665E-01
	9	.155689E-01	.153026E-01	.152780E-01
	10	.136432E-01	.134642E-01	.134051E-01
	0	.552272E-02	.552272E-02	.533401E-02
	1	.696350E-02	.694996E-02	.680952E-02
	2	.916667E-02	.914695E-02	.878921E-02
	3	.109595E-01	.109391E-01	.107912E-01
	4	.122903E-01	.122224E-01	.123640E-01
4.0	5	.130579E-01	.130005E-01	.132089E-01
	6	.133826E-01	.133291E-01	.129778E-01
	7	.135706E-01	.132888E-01	.131539E-01
	8	.131926E-01	.129663E-01	.133520E-01
	9	.126570E-01	.124419E-01	.124103E-01
	10	.119770E-01	.117839E-01	.119171E-01

Table 8a. Transmitted Particle Currents, $T_n(t)$, Obtained by Three Methods, Through Slabs of Various Widths, t: Unit Current Cosine Distributed Source; Isotropic Scatter (Cont)

t	n	Transmitted Current, $T_n(t)$		
		OOSII	Boltzmann	Monte Carlo
5.0	0	.175560E-02	.175560E-02	.152346E-02
	1	.249086E-02	.248708E-02	.247894E-02
	2	.360551E-02	.359853E-02	.372383E-02
	3	.471388E-02	.470691E-02	.444367E-02
	4	.574610E-02	.572134E-02	.549586E-02
	5	.661721E-02	.658910E-02	.648722E-02
	6	.731006E-02	.728030E-02	.738797E-02
	7	.788730E-02	.778684E-02	.804580E-02
	8	.822948E-02	.811643E-02	.825830E-02
	9	.840564E-02	.828623E-02	.796229E-02
	10	.844041E-02	.831949E-02	.854578E-02
6.0	0	.569208E-03	.569207E-03	.614914E-03
	1	.885422E-03	.883926E-03	.697931E-03
	2	.138164E-02	.137894E-02	.139510E-02
	3	.194011E-02	.193624E-02	.191324E-02
	4	.253101E-02	.252001E-02	.255155E-02
	5	.311022E-02	.309672E-02	.294659E-02
	6	.365447E-02	.363888E-02	.358198E-02
	7	.418247E-02	.412604E-02	.415100E-02
	8	.460644E-02	.454494E-02	.466406E-02
	9	.495542E-02	.488880E-02	.470109E-02
	10	.522713E-02	.515612E-02	.524053E-02
7.0	0	.187313E-03	.187313E-03	.177930E-03
	1	.313978E-03	.313515E-03	.227486E-03
	2	.521129E-03	.520006E-03	.540133E-03
	3	.776366E-03	.774554E-03	.656990E-03
	4	.107192E-02	.106739E-02	.118984E-02
	5	.139112E-02	.138532E-02	.140656E-02
	6	.172232E-02	.171521E-02	.166816E-02
	7	.207847E-02	.204441E-02	.213144E-02
	8	.239820E-02	.236179E-02	.235004E-02
	9	.269736E-02	.265834E-02	.252694E-02
	10	.296904E-02	.292731E-02	.285283E-02
8.0	0	.623614E-04	.623615E-04	.532775E-04
	1	.111272E-03	.111127E-03	.652521E-04
	2	.194559E-03	.193929E-03	.162697E-03
	3	.304786E-03	.303618E-03	.273590E-03
	4	.441752E-03	.439752E-03	.523437E-03
	5	.600873E-03	.598[illegible]89E-03	.608133E-03
	6	.778417E-03	.775282E-03	.624697E-03
	7	.984810E-03	.965275E-03	.975051E-03
	8	.118410E-02	.116280E-02	.115256E-02
	9	.138543E-02	.136239E-02	.124661E-02
	10	.158378E-02	.155896E-02	.147020E-02

Table 8b. Reflected Particle Currents, $B_n(t)$ Obtained by Three Methods, from Slabs of Various Widths, t: Unit Current Cosine Distributed Source; Isotropic Scatter

t	n	Reflected Current, $B_n(t)$		
		OOSII	Boltzmann	Monte Carlo
1.0	0	0.	0.	0.
	1	.201373E+00	.197120E+00	.197135E+00
	2	.102034E+00	.101542E+00	.102447E+00
	3	.582115E-01	.582546E-01	.583891E-01
	4	.347117E-01	.348082E-01	.345327E-01
	5	.210924E-01	.2119[illegible]3E-01	.206014E-01
	6	.129264E-01	.1301[illegible]0E-01	.126899E-01
	7	.795344E-02	.802259E-02	.810657E-02
	8	.490296E-02	.495610E-02	.464572E-02
	9	.302525E-02	.306467E-02	.298956E-02
	10	.186749E-02	.189599E-02	.194834E-02
2.0	0	0.	0.	0.
	1	.208695E+00	.205742E+00	.204594E+00
	2	.114906E+00	.114141E+00	.114853E+00
	3	.744208E-01	.744603E-01	.739735E-01
	4	.521856E-01	.521647E-01	.516625E-01
	5	.381429E-01	.381710E-01	.378436E-01
	6	.286122E-01	.286579E-01	.283033E-01
	7	.217976E-01	.218547E-01	.218936E-01
	8	.166679E-01	.168286E-01	.167427E-01
	9	.128166E-01	.130372E-01	.135114E-01
	10	.988818E-02	.101386E-01	.990597E-02
3.0	0	0.	0.	0.
	1	.209203E+00	.205126E+00	.204999E+00
	2	.116146E+00	.115565E+00	.116038E+00
	3	.765225E-01	.764940E-01	.761445E-01
	4	.551727E-01	.551077E-01	.546451E-01
	5	.419132E-01	.419022E-01	.416410E-01
	6	.330143E-01	.330209E-01	.326485E-01
	7	.267962E-01	.266704E-01	.271258E-01
	8	.219706E-01	.219179E-01	.218503E-01
	9	.182424E-01	.182365E-01	.186176E-01
	10	.152827E-01	.153092E-01	.152552E-01
4.0	0	0.	0.	0.
	1	.209246E+00	.205656E+00	.205047E+00
	2	.116271E+00	.115607E+00	.116124E+00
	3	.767750E-01	.767737E-01	.763996E-01
	4	.559050E-01	.555358E-01	.551250E-01
	5	.425361E-01	.425235E-01	.421764E-01
	6	.338573E-01	.338583E-01	.335986E-01
	7	.278797E-01	.277318E-01	.281716E-01
	8	.232831E-01	.231987E-01	.231327E-01
	9	.197691E-01	.197219E-01	.200510E-01
	10	.170005E-01	.169768E-01	.168694E-01

Table 8b. Reflected Particle Currents, $B_n(t)$, Obtained by Three Methods, from Slabs of Various Widths, t: Unit Current Cosine Distributed Source; Isotropic Scatter (Cont)

t	n	Reflected Current, $B_n(t)$		
		OOSII	Boltzmann	Monte Carlo
5.0	0	0.	0.	0.
	1	.209250E+00	.206296E+00	.205047E+00
	2	.116284E+00	.115511E+00	.116140E+00
	3	.768050E-01	.768363E-01	.764577E-01
	4	.556512E-01	.556022E-01	.551794E-01
	5	.426286E-01	.426197E-01	.422247E-01
	6	.339965E-01	.339983E-01	.337570E-01
	7	.280795E-01	.279267E-01	.283678E-01
	8	.235487E-01	.234572E-01	.233697E-01
	9	.201074E-01	.200509E-01	.203978E-01
	10	.174162E-01	.173808E-01	.173130E-01
6.0	0	0.	0.	0.
	1	.209250E+00	.205173E+00	.205047E+00
	2	.116286E+00	.115700E+00	.116140E+00
	3	.768086E-01	.767840E-01	.764577E-01
	4	.556585E-01	.555903E-01	.551794E-01
	5	.426417E-01	.426248E-01	.422391E-01
	6	.340179E-01	.340160E-01	.337772E-01
	7	.281131E-01	.279574E-01	.284103E-01
	8	.235969E-01	.235031E-01	.234125E-01
	9	.201733E-01	.201146E-01	.204572E-01
	10	.175030E-01	.174651E-01	.174338E-01
7.0	0	0.	0.	0.
	1	.209250E+00	.205398E+00	.205047E+00
	2	.116286E+00	.115660E+00	.116140E+00
	3	.768090E-01	.768008E-01	.764577E-01
	4	.556594E-01	.555957E-01	.551794E-01
	5	.426435E-01	.426284E-01	.422573E-01
	6	.340210E-01	.340199E-01	.337772E-01
	7	.281184E-01	.279628E-01	.284199E-01
	8	.236050E-01	.235109E-01	.234218E-01
	9	.201851E-01	.201258E-01	.204602E-01
	10	.175194E-01	.174808E-01	.174492E-01
8.0	0	0.	0.	0.
	1	.209250E+00	.205660E+00	.205047E+00
	2	.116286E+00	.115611E+00	.116140E+00
	3	.768090E-01	.768195E-01	.764577E-01
	4	.556596E-01	.556007E-01	.551794E-01
	5	.426437E-01	.426306E-01	.422573E-01
	6	.340214E-01	.340212E-01	.337772E-01
	7	.281192E-01	.279639E-01	.284199E-01
	8	.236063E-01	.235123E-01	.234218E-01
	9	.201871E-01	.201277E-01	.204602E-01
	10	.175223E-01	.174835E-01	.174492E-01

Table 8c. Transmitted and Reflected Particle Currents, $T_n(t)$ and $B_n(t)$, Obtained by Two Methods, from Slabs of Various Widths, t: Unit Isotropically Distributed Current Source; Isotropic Scatter

t	n	Transmitted Current, $T_n(t)$		Reflected Current, $B_n(t)$	
		OOSII	Monte Carlo	OOSII	Monte Carlo
1.0	0	.148495E+00	.147040E+00	0.	0.
	1	.112627E+00	.112430E+00	.244480E+00	.245940E+00
	2	.797412E-01	.786850E-01	.113837E+00	.114170E+00
	3	.529593E-01	.530700E-01	.627664E-01	.631200E-01
	4	.339605E-01	.343950E-01	.368739E-01	.366900E-01
	5	.213789E-01	.216600E-01	.222543E-01	.218250E-01
	6	.133308E-01	.133550E-01	.135950E-01	.134500E-01
	7	.827223E-02	.846500E-02	.835216E-02	.850000E-02
	8	.512077E-02	.551000E-02	.514498E-02	.494000E-02
	9	.316611E-02	.333500E-02	.317345E-02	.319000E-02
	10	.195640E-02	.201500E-02	.195863E-02	.205500E-02
2.0	0	.375343E-01	.378100E-01	0.	0.
	1	.424972E-01	.418650E-01	.249648E+00	.251190E+00
	2	.429033E-01	.428650E-01	.123991E+00	.124030E+00
	3	.394960E-01	.389550E-01	.763211E-01	.762700E-01
	4	.344096E-01	.338950E-01	.519736E-01	.518250E-01
	5	.288122E-01	.289850E-01	.374030E-01	.370600E-01
	6	.235500E-01	.230400E-01	.277937E-01	.276950E-01
	7	.193065E-01	.191600E-01	.209224E-01	.210150E-01
	8	.152099E-01	.149500E-01	.159648E-01	.159400E-01
	9	.119075E-01	.122300E-01	.122602E-01	.129050E-01
	10	.928672E-02	.967000E-02	.945162E-02	.955550E-02
3.0	0	.106419E-01	.104600E-01	0.	0.
	1	.149062E-01	.149650E-01	.249972E+00	.251440E+00
	2	.182247E-01	.179300E-01	.124872E+00	.124880E+00
	3	.200259E-01	.198000E-01	.779058E-01	.779250E-01
	4	.205565E-01	.208050E-01	.543191E-01	.541000E-01
	5	.200384E-01	.197100E-01	.404527E-01	.401500E-01
	6	.188723E-01	.180950E-01	.314361E-01	.312650E-01
	7	.177609E-01	.174050E-01	.251382E-01	.252750E-01
	8	.159929E-01	.155350E-01	.205061E-01	.203150E-01
	9	.141983E-01	.139650E-01	.169636E-01	.174100E-01
	10	.124779E-01	.121150E-01	.141736E-01	.142850E-01
4.0	0	.319823E-02	.310500E-02	0.	0.
	1	.515993E-02	.506000E-02	.249997E+00	.251470E+00
	2	.717123E-02	.703000E-02	.124956E+00	.124930E+00
	3	.888635E-02	.871500E-02	.780854E-01	.781100E-01
	4	.102127E-01	.102150E-01	.546323E-01	.544500E-01
	5	.110632E-01	.111950E-01	.409290E-01	.405650E-01
	6	.114983E-01	.111750E-01	.320966E-01	.320100E-01
	7	.117496E-01	.113050E-01	.259979E-01	.261250E-01
	8	.115720E-01	.116350E-01	.215662E-01	.213800E-01
	9	.111755E-01	.108400E-01	.182151E-01	.185750E-01
	10	.106288E-01	.105300E-01	.155991E-01	.156400E-01

Figure 8c. Transmitted and Reflected Particle Currents, $T_n(t)$ and $B_n(t)$, Obtained by Two Methods, from Slabs of Various Widths, t: Unit Isotropically Distributed Current Source; Isotropic Scatter (Cont)

t	n	Transmitted Current, $T_n(t)$		Reflected Current, $B_n(t)$	
		OOSII	Monte Carlo	OOSII	Monte Carlo
5.0	0	.996469E-03	.870000E-03	0.	0.
	1	.178365E-02	.172000E-02	.250000E+00	.251470E+00
	2	.272619E-02	.287000E-02	.124964E+00	.124940E+00
	3	.369712E-02	.353500E-02	.781059E-01	.781450E-01
	4	.462747E-02	.440000E-02	.546723E-01	.544950E-01
	5	.543740E-02	.543500E-02	.409971E-01	.406000E-01
	6	.610041E-02	.621000E-02	.322015E-01	.321400E-01
	7	.666174E-02	.660500E-02	.261508E-01	.262750E-01
	8	.702184E-02	.716000E-02	.217730E-01	.215700E-01
	9	.723269E-02	.692000E-02	.184825E-01	.188550E-01
	10	.731138E-02	.739000E-02	.159320E-01	.160000E-01
6.0	0	.318258E-03	.345000E-03	0.	0.
	1	.617751E-03	.505000E-03	.250000E+00	.251470E+00
	2	.101758E-02	.102500E-02	.124965E+00	.124940E+00
	3	.148256E-02	.149000E-02	.781083E-01	.781450E-01
	4	.198713E-02	.195500E-02	.546774E-01	.544950E-01
	5	.249334E-02	.234500E-02	.410064E-01	.406100E-01
	6	.297844E-02	.301000E-02	.322171E-01	.321600E-01
	7	.345135E-02	.338500E-02	.261758E-01	.263000E-01
	8	.384426E-02	.390500E-02	.218096E-01	.216000E-01
	9	.417427E-02	.399500E-02	.185333E-01	.189000E-01
	10	.443752E-02	.438500E-02	.159998E-01	.160900E-01
7.0	0	.103510E-03	.100000E-03	0.	0.
	1	.214590E-03	.150000E-03	.250000E+00	.251470E+00
	2	.375804E-03	.365000E-03	.124965E+00	.124940E+00
	3	.590874E-03	.515000E-03	.781086E-01	.781450E-01
	4	.824198E-03	.875000E-03	.546780E-01	.544950E-01
	5	.109269E-02	.110000E-02	.410076E-01	.406200E-01
	6	.137620E-02	.132000E-02	.322194E-01	.321600E-01
	7	.168265E-02	.168000E-02	.261797E-01	.263050E-01
	8	.196460E-02	.197500E-02	.218156E-01	.216050E-01
	9	.223185E-02	.214000E-02	.185422E-01	.189100E-01
	10	.247757E-02	.243000E-02	.160123E-01	.161000E-01
8.0	0	.341376E-04	.300000E-04	0.	0.
	1	.747801E-04	.500000E-04	.250000E+00	.251470E+00
	2	.137891E-03	.115000E-03	.124965E+00	.124940E+00
	3	.224060E-03	.195000E-03	.781086E-01	.781450E-01
	4	.333760E-03	.385000E-03	.546781E-01	.544950E-01
	5	.463882E-03	.475000E-03	.410078E-01	.406200E-01
	6	.611551E-03	.495000E-03	.322197E-01	.321600E-01
	7	.784477E-03	.765000E-03	.261803E-01	.263050E-01
	8	.954792E-03	.930000E-03	.218165E-01	.216050E-01
	9	.112882E-02	.980000E-03	.185436E-01	.189100E-01
	10	.130204E-02	.123500E-02	.160145E-01	.161000E-01

7. APPLICATION OF THE OOSH METHOD TO NON-ISOTROPIC SCATTER

7.1 Neutron Slowing-Down in Hydrogen – An Example of Highly Anisotropic Scattering

Thus far the discussion of particle transport has been confined to interactions where the scattering is isotropic in the laboratory system. As has been stated previously, this case was adopted because of its inherent simplicity and the accessibility of at least two other independent calculational methods for verification of the results. However, many important processes can be described adequately only by anisotropic scattering. Such is the case for neutron slowing-down in hydrogen where the scattering is isotropic in the center of mass coordinate system. In the laboratory system this translates into a scattering probability density which is proportional to the cosine of the deflection angle. If $\vec{\Omega}_1$ and $\vec{\Omega}_2$ are defined as the pre- and post-collision directions of motion, respectively, of the scattered particle in the laboratory system (Figure 22) where

$$\vec{\Omega}_1 = \hat{e}_x \sin\theta_1 \cos\phi_1 + \hat{e}_y \sin\theta_1 \sin\phi_1 + \hat{e}_z \cos\theta_1 , \tag{105a}$$

$$\vec{\Omega}_2 = \hat{e}_z \sin\theta_2 \cos\phi_2 + \hat{e}_y \sin\theta_2 \sin\phi_2 + \hat{e}_z \cos\theta_2 , \tag{105b}$$

and if ω_ℓ is defined as the scattering deflection angle in the laboratory system, then

$$\cos\omega_\ell = \vec{\Omega}_1 \cdot \vec{\Omega}_2 . \tag{106}$$

Since the scattering occurs between two particles of equal (or very nearly so) mass, there can be no single collision backscatter in the laboratory reference frame. Therefore

$$\vec{\Omega}_1 \cdot \vec{\Omega}_2 \geq 0 \tag{107}$$

or

$$\sin\theta_1 \sin\theta_2 \cos(\phi_1 - \phi_2) + \cos\theta_1 \cos\theta_2 \geq 0 . \tag{108}$$

Then for a given pair of values θ_1, θ_2, the following constraint holds for the azimuthal deflection:

$$\cos(\phi_1 - \phi_2) \geq - \frac{\cos\theta_1 \cos\theta_2}{\sin\theta_1 \sin\theta_2} , \tag{109}$$

with the maximum allowed deflection, $\Delta\phi_{max} \equiv (\phi_1 - \phi_2)_{max}$, occurring with the equality.

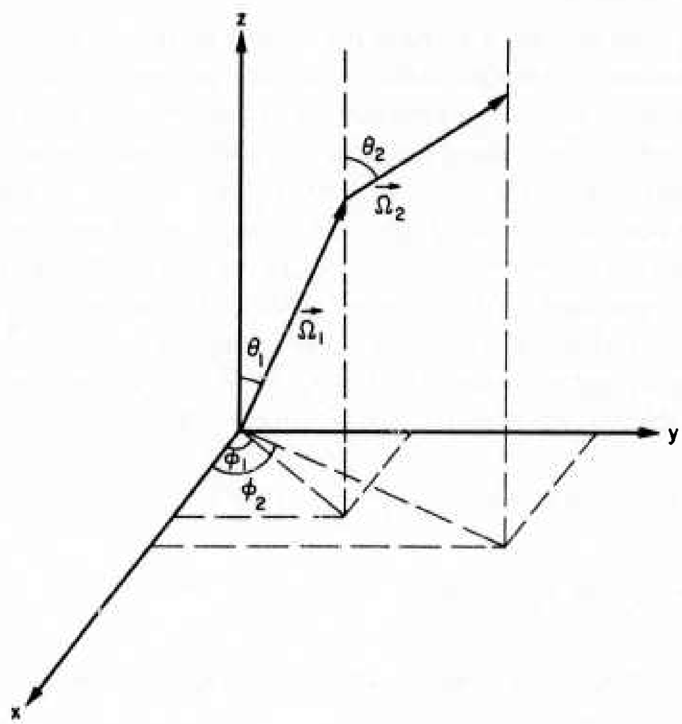

Figure 22. Pre- and Post-Collision Particle Orientations

The scattering probability density in terms of $\vec{\Omega}_1$ and $\vec{\Omega}_2$ is

$$f(\vec{\Omega}_1 \rightarrow \vec{\Omega}_2) = \left\{ \begin{array}{ll} \dfrac{\vec{\Omega}_1 \cdot \vec{\Omega}_2}{\pi} & , \ (\phi_1 - \phi_2) \leq \phi_{max} \\ 0 & , \ (\phi_1 - \phi_2) > \phi_{max} \end{array} \right\} , \tag{110}$$

and, as in the case of isotropic scattering, azimuthal invariance implies

$$\begin{aligned} f(\mu_1, \mu_2) &= \int_0^{2\pi} d\phi_2 \, f(\vec{\Omega}_1 \rightarrow \vec{\Omega}_2) \\ &= \frac{2}{\pi} \left[\sqrt{(1-\mu_1^2)(1-\mu_2^2)} \ \sin \phi_{max} + \mu_1 \mu_2 \, \phi_{max} \right] , \end{aligned} \tag{111}$$

where since the assignment of an initial azimuthal direction is arbitrary, the value of ϕ_1 has been chosen to be zero. The scattering matrix, $f(\mu_1, \mu_2)$ was evaluated at the Gaussian discrete ordinate points corresponding to six angles per quadrant. The elements of f are listed in Tables 9a and 9b. Table 9a contains the submatrix for the case when both angles are in the same quadrant, and Table 9b shows the submatrix when μ_i and μ_j correspond to angles in different quadrants. The scattering matrix is symmetric about both diagonals. This matrix was then substituted into the expressions of Eqs. (63) and (64), and the OOSII computer program was run to provide computations of the transmitted and reflected currents.

The choice of six discrete ordinates per quadrant was made for all orders of scattering up to 10 because it was found that a lesser number was not adequate to provide an accurate description of the forward peaked nature of the scattering angular distribution. The adoption of this number of ordinates was accomplished with virtually no further sacrifice in computational efficiency over that attained for the isotropic scatter case. This was accomplished with a coarsening of the spatial integration step by a factor of four, a modification which produced only third or fourth decimal place changes in the answers. Also a constant mean-free-path was assumed, as is actually the case for neutron scattering in hydrogen at energies ranging from 1 keV down to thermal.[15]

Curves of $T_n(t)$ and $B_n(t)$ are plotted vs t for both the cosine and isotropic source configurations in Figures 23, 24, 25, and 26. As before, twelve curves representing values of n ranging from 0 to 10 plus the total current, are presented in each graph. A more detailed presentation of the numerical results is given in Table 10.

---

15. Lamarsh, J.R. (1967) Nuclear Reactor Theory, Addison Wesley, Reading, Mass.

Table 9a. Upper-Left Submatrix, $f(\mu_i, \mu_j)$, for Both Angles in Same Quadrant; Neutron Scattering in Hydrogen

j \ i	1	2	3	4	5	6
1	1.9629	1.7749	1.5114	1.1530	.72210	.27005
2	1.7749	1.6349	1.3922	1.0620	.68095	.39279
3	1.5114	1.3922	1.1855	.91807	.70488	.50417
4	1.1530	1.0620	.91807	.82125	.71504	.58689
5	.72230	.68095	.70488	.71504	.69254	.63412
6	.27005	.39279	.50417	.58689	.63412	.64240

Table 9b. Lower-Left Submatrix, $f(\mu_i, \mu_j)$, for Angles in Different Quadrants; Neutron Scattering in Hydrogen

j \ i	1	2	3	4	5	6
6	.024198	.16634	.31133	.43979	.54199	.61103
5	0	.015826	.13849	.28297	.42194	.54199
4	0	0	.013711	.13136	.28297	.43979
3	0	0	0	.013711	.13849	.31133
2	0	0	0	0	.015826	.16634
1	0	0	0	0	0	.024198

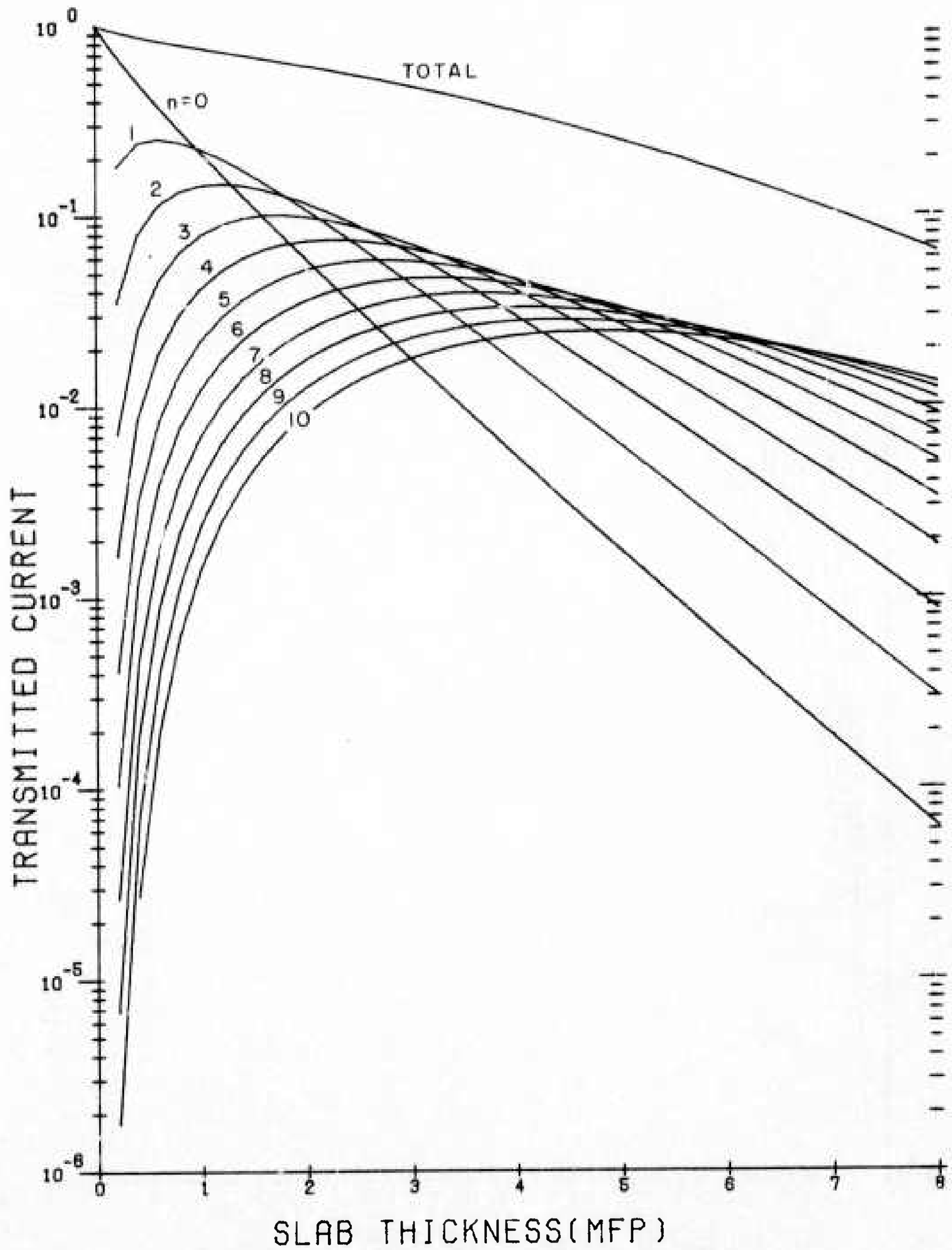

Figure 23. Transmitted Current, $T_n(t)$, vs Slab Thickness, t, for nth Order Neutron Scattering in Hydrogen ($0 \leq n \leq 10$); Cosine Current Source Configuration

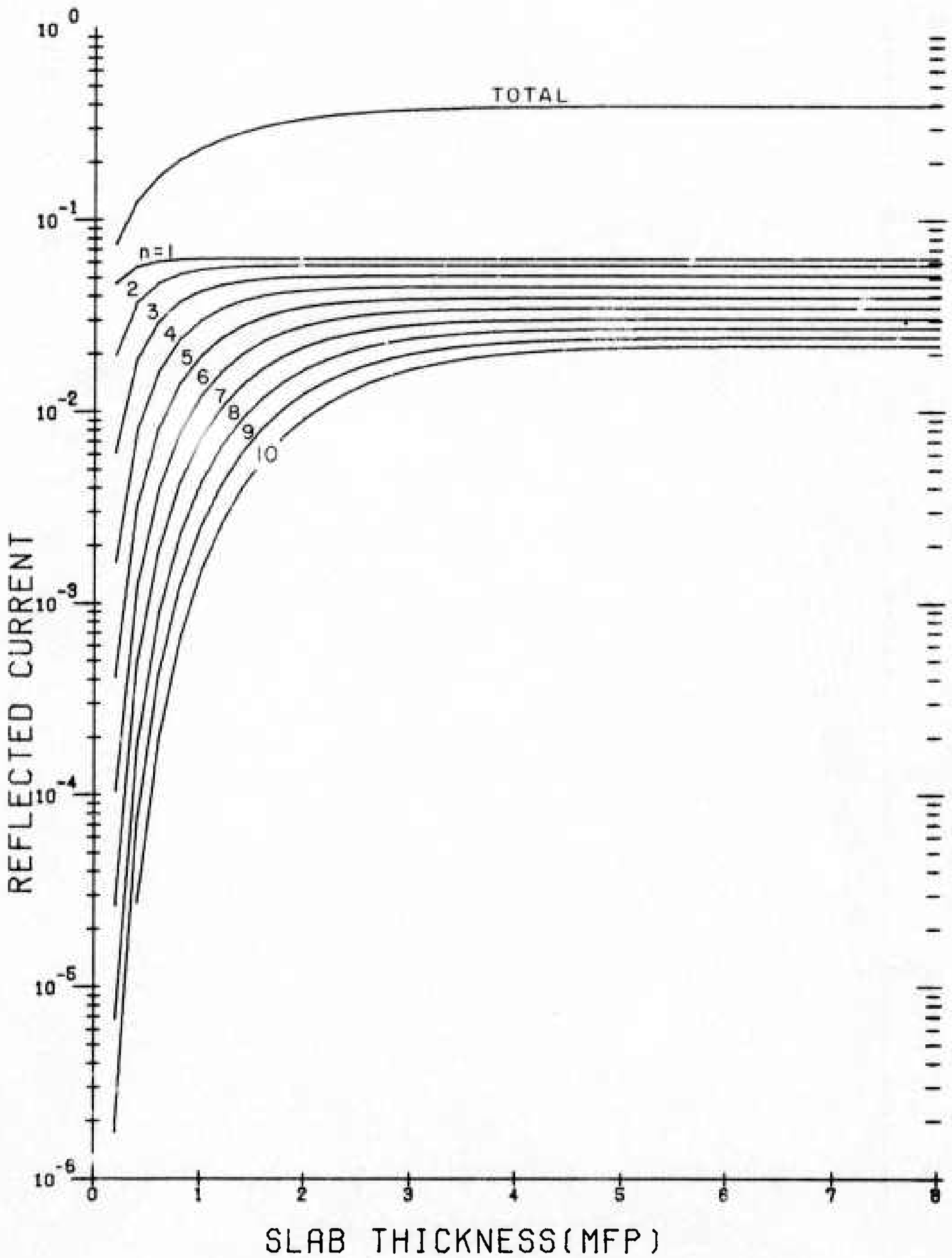

Figure 24. Reflected Current, $B_n(t)$, vs Slab Thickness, t, for nth Order Neutron Scattering in Hydrogen ($1 \leq n \leq 10$); Cosine Current Source Configuration

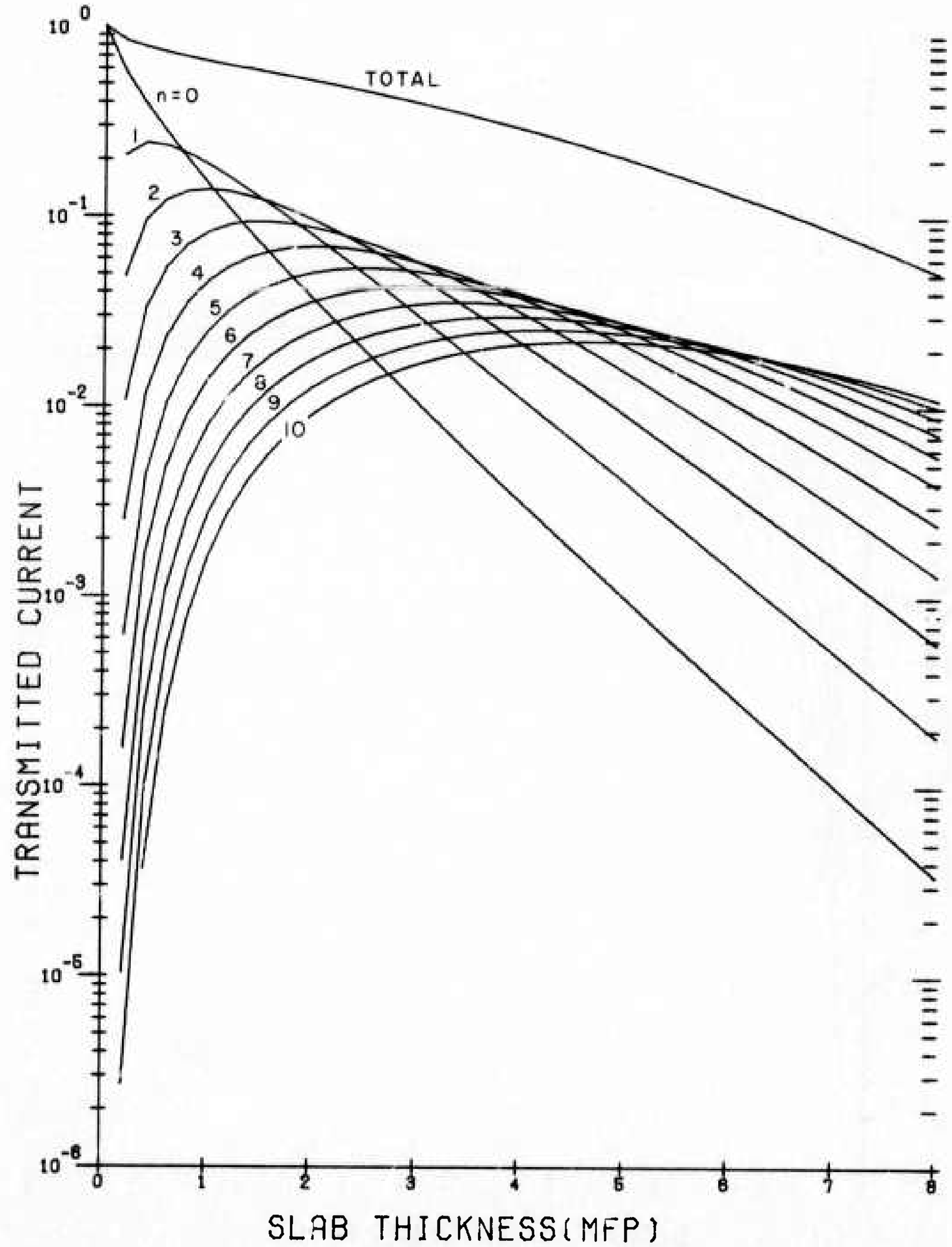

Figure 25. Transmitted Current, $T_n(t)$, vs Slab Thickness, t, for nth Order Neutron Scattering in Hydrogen ($0 \le n \le 10$); Isotropic Current Source Configuration

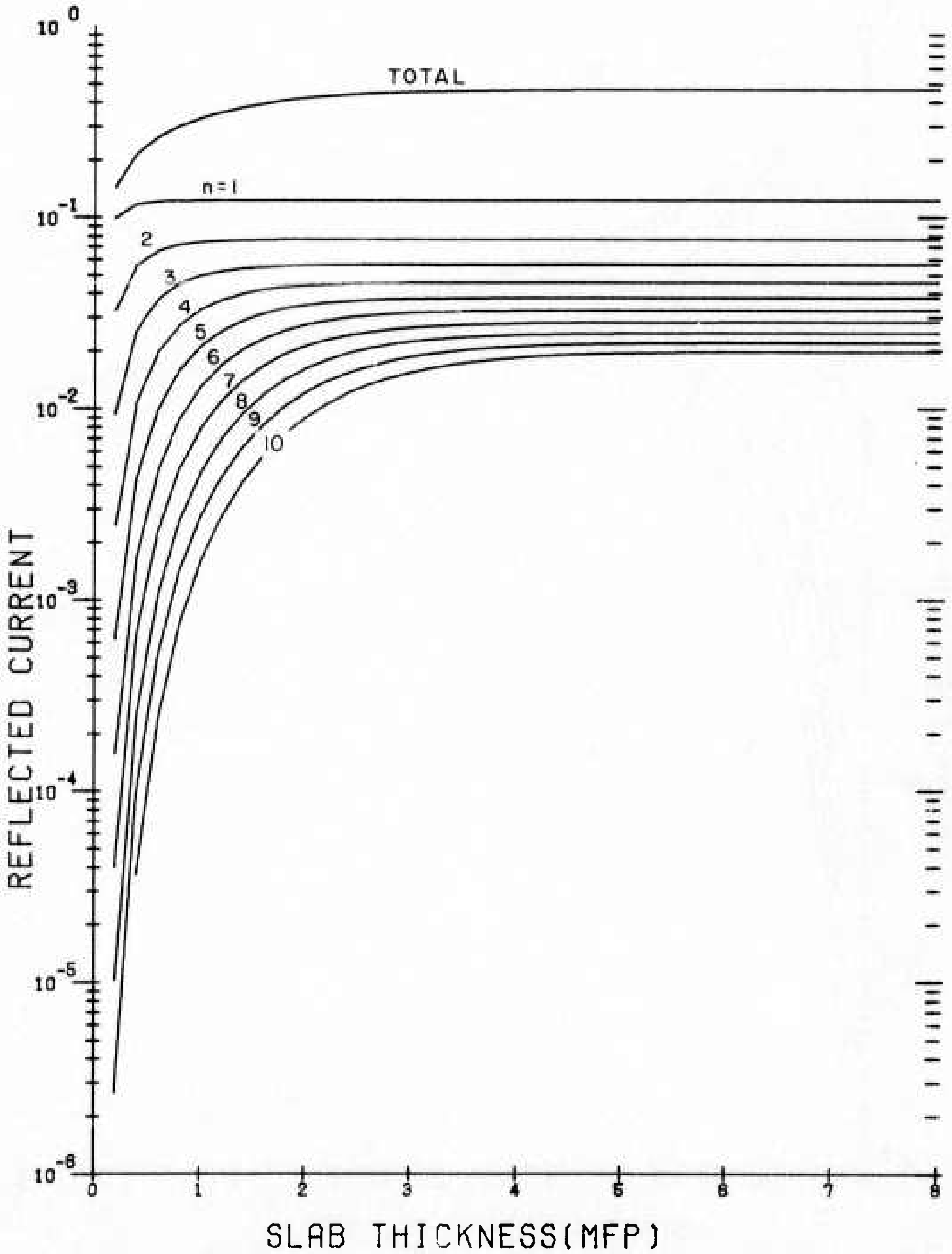

Figure 26. Reflected Current, $B_n(t)$, vs Slab Thickness, t, for nth Order Neutron Scattering in Hydrogen ($1 \leq n \leq 10$); Isotropic Current Source Configuration

Table 10a. Transmitted and Reflected Particle Currents, $T_n(t)$ and $B_n(t)$, Obtained by Two Methods, Resulting from the Scatter of Neutrons by Hydrogen: Unit Current Cosine Distributed Source

t	n	Transmitted Current, $T_n(t)$		Reflected Current, $B_n(t)$	
		OOSII	Monte Carlo	OOSII	Monte Carlo
1.0	0	.219384E+00	.217556E+00	0.	0.
	1	.225017E+00	.226632E+00	.626810E-01	.585498E-01
	2	.145794E+00	.143102E+00	.548762E-01	.548400E-01
	3	.797680E-01	.797376E-01	.425861E-01	.437332E-01
	4	.418482E-01	.426760E-01	.298380E-01	.301978E-01
	5	.223960E-01	.226424E-01	.193945E-01	.196888E-01
	6	.124442E-01	.115718E-01	.119783E-01	.127054E-01
	7	.712811E-02	.701230E-02	.717298E-02	.717474E-02
	8	.415392E-02	.470016E-02	.422721E-02	.454738E-02
	9	.243815E-02	.246576E-02	.247488E-02	.246562E-02
	10	.143365E-02	.129793E-02	.144671E-02	.132911E-02
2.0	0	.602668E-01	.603430E-01	0.	0.
	1	.108299E+00	.107865E+00	.630936E-01	.590488E-01
	2	.116893E+00	.115960E+00	.580285E-01	.579918E-01
	3	.991889E-01	.100539E+00	.507866E-01	.518410E-01
	4	.741942E-01	.746754E-01	.429448E-01	.434990E-01
	5	.522738E-01	.516652E-01	.352708E-01	.355512E-01
	6	.361547E-01	.345814E-01	.281497E-01	.294068E-01
	7	.251255E-01	.244662E-01	.218870E-01	.213594E-01
	8	.177116E-01	.185988E-01	.166535E-01	.169444E-01
	9	.126735E-01	.131761E-01	.124662E-01	.120943E-01
	10	.917394E-02	.937832E-02	.922768E-02	.894896E-02
3.0	0	.178613E-01	.184905E-01	0.	0.
	1	.438078E-01	.440192E-01	.631021E-01	.590576E-01
	2	.636021E-01	.632360E-01	.581955E-01	.581540E-01
	3	.708486E-01	.698018E-01	.515609E-01	.526088E-01
	4	.673154E-01	.671466E-01	.449280E-01	.453542E-01
	5	.579789E-01	.571100E-01	.388881E-01	.393660E-01
	6	.471405E-01	.467314E-01	.334374E-01	.348814E-01
	7	.372140E-01	.362756E-01	.285101E-01	.281626E-01
	8	.290657E-01	.288634E-01	.240722E-01	.243764E-01
	9	.227147E-01	.229126E-01	.201198E-01	.198894E-01
	10	.178592E-01	.177856E-01	.166571E-01	.164842E-01
4.0	0	.552272E-02	.533810E-02	0.	0.
	1	.167247E-01	.167973E-01	.631023E-01	.590576E-01
	2	.298673E-01	.300914E-01	.582060E-01	.581540E-01
	3	.404794E-01	.406784E-01	.516329E-01	.526870E-01
	4	.460718E-01	.473636E-01	.451798E-01	.455788E-01
	5	.466209E-01	.465940E-01	.394939E-01	.399264E-01
	6	.435629E-01	.429772E-01	.345781E-01	.358244E-01
	7	.386264E-01	.379286E-01	.303145E-01	.297556E-01
	8	.331625E-01	.331824E-01	.265779E-01	.269204E-01
	9	.279751E-01	.275762E-01	.232682E-01	.228112E-01
	10	.234227E-01	.233496E-01	.203156E-01	.201930E-01

Table 10a. Transmitted and Reflected Particle Currents, $T_n(t)$ and $B_n(t)$, Obtained by Two Methods, Resulting from the Scatter of Neutrons by Hydrogen: Unit Current Cosine Distributed Source (Cont)

t	n	Transmitted Current, $T_n(t)$		Reflected Current, $B_n(t)$	
		OOSII	Monte Carlo	OOSII	Monte Carlo
5.0	0	.175540E-02	.162074E-02	0.	0.
	1	.622027E-02	.607382E-02	.631024E-01	.590576E-01
	2	.130014E-01	.132612E-01	.582068E-01	.581540E-01
	3	.205195E-01	.201882E-01	.516398E-01	.526870E-01
	4	.269707E-01	.277782E-01	.452102E-01	.456120E-01
	5	.311773E-01	.313024E-01	.395838E-01	.400422E-01
	6	.328510E-01	.327042E-01	.347832E-01	.360120E-01
	7	.323764E-01	.329834E-01	.307027E-01	.301876E-01
	8	.304356E-01	.305472E-01	.272167E-01	.275920E-01
	9	.277062E-01	.276998E-01	.242099E-01	.239690E-01
	10	.247077E-01	.237492E-01	.215865E-01	.214976E-01
6.0	0	.569208E-03	.577124E-03	0.	0.
	1	.228164E-02	.225614E-02	.631024E-01	.590576E-01
	2	.540888E-02	.521482E-02	.582068E-01	.581540E-01
	3	.966089E-02	.103058E-01	.516405E-01	.526870E-01
	4	.143033E-01	.141998E-01	.452138E-01	.456120E-01
	5	.185027E-01	.183908E-01	.395964E-01	.400484E-01
	6	.216416E-01	.223212E-01	.348165E-01	.360744E-01
	7	.234569E-01	.242832E-01	.307758E-01	.302768E-01
	8	.240049E-01	.236130E-01	.273548E-01	.278372E-01
	9	.235382E-01	.236080E-01	.244422E-01	.242754E-01
	10	.223762E-01	.223010E-01	.219423E-01	.218644E-01
7.0	0	.187313E-03	.156239E-03	0.	0.
	1	.830352E-03	.775310E-03	.631024E-01	.590576E-01
	2	.218460E-02	.218868E-02	.582068E-01	.581540E-01
	3	.432804E-02	.406104E-02	.516406E-01	.526870E-01
	4	.708873E-02	.765028E-02	.452143E-01	.456120E-01
	5	.101029E-01	.105515E-01	.395981E-01	.400484E-01
	6	.129508E-01	.133981E-01	.348217E-01	.360744E-01
	7	.152883E-01	.154386E-01	.307884E-01	.302768E-01
	8	.169207E-01	.172782E-01	.273816E-01	.279152E-01
	9	.178083E-01	.178819E-01	.244927E-01	.243218E-01
	10	.180282E-01	.179335E-01	.220285E-01	.219468E-01
8.0	0	.623614E-04	.390856E-04	0.	0.
	1	.300771E-03	.306426E-03	.631024E-01	.590576E-01
	2	.864407E-03	.971476E-03	.582068E-01	.581540E-01
	3	.187149E-02	.153905E-02	.516406E-01	.526870E-01
	4	.334506E-02	.335922E-02	.452143E-01	.456120E-01
	5	.518910E-02	.561360E-02	.395984E-01	.400484E-01
	6	.721467E-02	.735088E-02	.348224E-01	.360744E-01
	7	.919776E-02	.955008E-02	.307905E-01	.302768E-01
	8	.109391E-01	.114759E-01	.273865E-01	.279152E-01
	9	.123036E-01	.120364E-01	.245027E-01	.243218E-01
	10	.132331E-01	.134813E-01	.220473E-01	.219468E-01

Table 10b. Transmitted and Reflected Particle Currents, $T_n(t)$ and $B_n(t)$, Obtained by Two Methods, Resulting from the Scatter of Neutrons by Hydrogen: Unit Isotropically Distributed Current Source

t	n	Transmitted Current, $T_n(t)$		Reflected Current, $B_n(t)$	
		OOSII	Monte Carlo	OOSII	Monte Carlo
1.0	0	.148405E+00	.147480E+00	0.	0.
	1	.188200E+00	.188332E+00	.123114E+00	.125192E+00
	2	.139558E+00	.137138E+00	.742554E-01	.739808E-01
	3	.832227E-01	.830200E-01	.496732E-01	.509800E-01
	4	.458164E-01	.468902E-01	.329962E-01	.334602E-01
	5	.250077E-01	.258800E-01	.211342E-01	.213600E-01
	6	.139351E-01	.133905E-01	.130523E-01	.135705E-01
	7	.795253E-02	.806000E-02	.784963E-02	.813000E-02
	8	.461382E-02	.518002E-02	.464592E-02	.489002E-02
	9	.269962E-02	.270008E-02	.272812E-02	.273008E-02
	10	.158469E-02	.146000E-02	.159731E-02	.140000E-02
2.0	0	.375343E-01	.374302E-01	0.	0.
	1	.801216E-01	.794800E-01	.123535E+00	.125710E+00
	2	.964692E-01	.952505E-01	.769543E-01	.766805E-01
	3	.883089E-01	.892500E-01	.565247E-01	.578800E-01
	4	.696236E-01	.693502E-01	.441137E-01	.446602E-01
	5	.507545E-01	.506208E-01	.349478E-01	.352208E-01
	6	.357789E-01	.347900E-01	.274974E-01	.282900E-01
	7	.250620E-01	.250102E-01	.212995E-01	.214202E-01
	8	.176847E-01	.186800E-01	.162267E-01	.164000E-01
	9	.126256E-01	.131605E-01	.121836E-01	.121805E-01
	10	.911081E-02	.947000E-02	.904742E-02	.875000E-02
3.0	0	.106419E-01	.109902E-01	0.	0.
	1	.304384E-01	.305308E-01	.123543E+00	.125728E+00
	2	.486898E-01	.480400E-01	.770792E-01	.768000E-01
	3	.580842E-01	.572602E-01	.570913E-01	.584302E-01
	4	.580596E-01	.578200E-01	.455944E-01	.460300E-01
	5	.519098E-01	.512105E-01	.377313E-01	.380905E-01
	6	.433300E-01	.433700E-01	.316910E-01	.325300E-01
	7	.347922E-01	.343702E-01	.267084E-01	.268802E-01
	8	.274352E-01	.273308E-01	.224403E-01	.224108E-01
	9	.215294E-01	.214500E-01	.187345E-01	.188000E-01
	10	.169380E-01	.169202E-01	.155233E-01	.152502E-01
4.0	0	.319823E-02	.308000E-02	0.	0.
	1	.111717E-01	.112100E-01	.123543E+00	.125725E+00
	2	.217981E-01	.218400E-01	.770864E-01	.768000E-01
	3	.314728E-01	.315202E-01	.571400E-01	.584902E-01
	4	.375886E-01	.382508E-01	.457691E-01	.461808E-01
	5	.394856E-01	.391500E-01	.381654E-01	.384900E-01
	6	.379715E-01	.377602E-01	.325353E-01	.332302E-01
	7	.343969E-01	.337800E-01	.280843E-01	.281500E-01
	8	.299804E-01	.300605E-01	.244027E-01	.243405E-01
	9	.255409E-01	.255100E-01	.212591E-01	.211600E-01
	10	.215070E-01	.217002E-01	.185179E-01	.182502E-01

Table 10b. Transmitted and Reflected Particle Currents, $T_n(t)$ and $B_n(t)$, Obtained by Two Methods, Resulting From the Scatter of Neutrons by Hydrogen: Unit Isotropically Distributed Current Source (Cont)

t	n	Transmitted Current, $T_n(t)$		Reflected Current, $B_n(t)$	
		OOSII	Monte Carlo	OOSII	Monte Carlo
5.0	0	.996469E-03	.920008E-03	0.	0.
	1	.404090E-02	.395000E-02	.123543E+00	.127720E+00
	2	.917332E-02	.932002E-02	.770869E-01	.768002E-01
	3	.153613E-01	.150500E-01	.571445E-01	.584900E-01
	4	.211364E-01	.217205E-01	.457892E-01	.462005E-01
	5	.253412E-01	.253100E-01	.382270E-01	.385600E-01
	6	.274955E-01	.272402E-01	.326802E-01	.334002E-01
	7	.277365E-01	.284308E-01	.283670E-01	.284908E-01
	8	.265490E-01	.263600E-01	.248804E-01	.248300E-01
	9	.244966E-01	.245502E-01	.219803E-01	.220302E-01
	10	.220564E-01	.214900E-01	.195121E-01	.193100E-01
6.0	0	.318258E-03	.330005E-03	0.	0.
	1	.145147E-02	.146000E-02	.123543E+00	.125720E+00
	2	.371989E-02	.361002E-02	.770869E-01	.768002E-01
	3	.702682E-02	.745008E-02	.571449E-01	.584908E-01
	4	.108677E-01	.107800E-01	.457915E-01	.462000E-01
	5	.145644E-01	.142602E-01	.382353E-01	.385702E-01
	6	.175380E-01	.177500E-01	.327030E-01	.334400E-01
	7	.194698E-01	.202205E-01	.284184E-01	.285505E-01
	8	.203175E-01	.199000E-01	.249802E-01	.250000E-01
	9	.202363E-01	.202502E-01	.221522E-01	.222202E-01
	10	.194731E-01	.193408E-01	.197810E-01	.195808E-01
7.0	0	.103510E-03	.900000E-04	0.	0.
	1	.519579E-03	.490002E-03	.123543E+00	.125722E+00
	2	.147231E-02	.149000E-02	.770869E-01	.768000E-01
	3	.307644E-02	.298005E-02	.571450E-01	.584905E-01
	4	.525423E-02	.555000E-02	.457918E-01	.462000E-01
	5	.774895E-02	.796002E-02	.382364E-01	.385702E-01
	6	.102211E-01	.105508E-01	.327064E-01	.334408E-01
	7	.123595E-01	.122700E-01	.284271E-01	.285500E-01
	8	.139580E-01	.144602E-01	.249991E-01	.250502E-01
	9	.149390E-01	.151200E-01	.221885E-01	.222500E-01
	10	.153313E-01	.150705E-01	.198443E-01	.196505E-01
8.0	0	.341376E-04	.200000E-04	0.	0.
	1	.185693E-03	.200002E-03	.123543E+00	.125722E+00
	2	.573003E-03	.640008E-03	.770869E-01	.768008E-01
	3	.130557E-02	.116000E-02	.571450E-01	.584900E-01
	4	.242923E-02	.247002E-02	.457918E-01	.462002E-01
	5	.399524E-02	.408000E-02	.382365E-01	.385700E-01
	6	.556914E-02	.563005E-02	.327069E-01	.334405E-01
	7	.727114E-02	.735000E-02	.284284E-01	.285500E-01
	8	.882585E-02	.924002E-02	.250024E-01	.250502E-01
	9	.101010E-01	.987008E-02	.221956E-01	.222508E-01
	10	.110253E-01	.112300E-01	.198579E-01	.196500E-01

7.2 Neutron Slowing-Down in Carbon — An Example of Mildly Anisotropic Scattering

If the assumption is made that the scattering of neutrons from the C^{12} nucleus is isotropic[15] in the center of mass coordinate system, the angular scattering probability density in this system is

$$f(\cos \omega_c) = \frac{1}{2}, \tag{112}$$

where ω_c is the deflection angle in the center of mass system. The transformation of this function to the laboratory system is given by

$$f(\cos \omega_\ell) = f(\cos \omega_c) \frac{d(\cos \omega_c)}{d(\cos \omega_\ell)}, \tag{113}$$

where ω_ℓ is the corresponding deflection angle expressed in laboratory coordinates, and where the deflection angles are related by

$$\cos \omega_\ell = \vec{\Omega}_1 \cdot \vec{\Omega}_2 = \frac{1 + A \cos \omega_c}{(1 + 2A \cos \omega_c + A^2)^{1/2}} . \tag{114}$$

Here the directions $\vec{\Omega}_1$ and $\vec{\Omega}_2$ are as defined in Eqs. (105), and A is the mass of the target nucleus. After some algebraic manipulation, the resulting expression for f in the laboratory frame is

$$f(\cos \omega_\ell) = \frac{1}{2A} \left[\frac{\cos^2 \omega_\ell}{\sqrt{A^2 - 1 + \cos^2 \omega_\ell}} + \sqrt{A^2 - 1 + \cos^2 \omega_\ell} + 2 \cos \omega_\ell \right] . \tag{115}$$

As was done for the hydrogen case, an expression for f independent of azimuth is required for implementation of the OOSII algorithm. That is

$$f(\mu_1, \mu_2) = \int_0^{2\pi} d\phi_2 \; f(\vec{\Omega}_1 \rightarrow \vec{\Omega}_2) . \tag{116}$$

When the expression for $\cos \omega_\ell$ given in Eq. (114) is substituted into Eq. (115), it becomes apparent that an exact analytic integration of Eq. (116) is not possible. However, a binomial expansion of the square-root terms in Eq. (115) renders the integration feasible. Letting

$$\alpha \equiv \sqrt{A^2 - 1} , \quad q \equiv \frac{\cos^2 \omega_\ell}{\alpha^2} , \tag{117}$$

leads to

$$\frac{\cos^2\omega_\ell}{\sqrt{A^2 - 1 + \cos\omega_\ell}} \doteq$$

$$\frac{\cos^2\omega_\ell}{\alpha} \left[1 - \frac{q}{2} + \frac{3}{8}q^2 - \frac{5}{16}q^3 + \ldots\right] \quad , \tag{118}$$

for the first term, and

$$\sqrt{A^2 - 1 + \cos^2\omega_\ell} \doteq$$

$$\alpha\left[1 + \frac{q}{2} - \frac{q^2}{8} + \frac{q^3}{16} - \frac{5}{128}q^4 + \ldots\right] \quad , \tag{119}$$

for the second term.
Substitution of the above expressions into the integral of Eq. (116) yields the following result:

$$f(\mu_1, \mu_2) =$$

$$\frac{\alpha}{2A}\left[1 + \frac{2\mu_1\mu_2}{\alpha} + \frac{3}{2}\frac{(\mu_1\mu_2)^2}{\alpha^2} + \frac{3}{4}\frac{\sqrt{(1-\mu_1^2)(1-\mu_2^2)}}{\alpha^2}\right.$$

$$- \frac{5}{8}\frac{(\mu_1\mu_2)^4}{\alpha^4} - \frac{15}{8}\frac{(\mu_1\mu_2)^2(1-\mu_1^2)(1-\mu_2^2)}{\alpha^4} - \frac{15}{64}\frac{[(1-\mu_1^2)(1-\mu_2^2)]^2}{\alpha^4}$$

$$\left. + \ldots\right] \quad . \tag{120}$$

This expression was coded for use in the OOSII computer program. The scattering matrix elements are given in Table 11.

In the computations the spatial integration step was taken to be the same as that for the hydrogen calculations, and six discrete ordinates were employed in the angular integrations. The assumption of a constant mean-free-path was again made. This is valid for neutrons scattering in C^{12} from approximately 10 keV down to the thermal range. Curves of $T_n(t)$ and $B_n(t)$ are plotted vs t for both the cosine and isotropic sources in Figures 27, 28, 29, and 30, and as before, the values of n were chosen to range from 0 to 10. A more extensive presentation of the numerical results is given in Table 12 along with results of a Monte Carlo calculation.

Table 11a. Upper-Left Submatrix, $f(\mu_i, \mu_j)$ for Both Angles in Same Quadrant; Neutron Scattering in Carbon

j \ i	1	2	3	4	5	6
1	.58331	.57627	.56419	.54805	.52909	.50867
2	.57627	.56988	.55893	.54425	.52694	.50823
3	.56419	.55893	.54987	.53670	.52318	.50738
4	.54805	.54425	.53670	.52872	.51797	.50610
5	.52909	.52694	.52318	.51797	.51157	.50433
6	.50867	.50823	.50738	.50610	.50433	.50209

Table 11b. Lower-Left Submatrix, $f(\mu_i, \mu_j)$, for Angles in Different Quadrants; Neutron Scattering in Carbon

j \ i	1	2	3	4	5	6
6	.48820	.48937	.49133	.49385	.49666	.49948
5	.46897	.47156	.47602	.48200	.48904	.49666
4	.45206	.45583	.46238	.47128	.48200	.49385
3	.43836	.44303	.45117	.46238	.47602	.49133
2	.42850	.43377	.44303	.45583	.47156	.48937
1	.42288	.42850	.43836	.45206	.46897	.48820

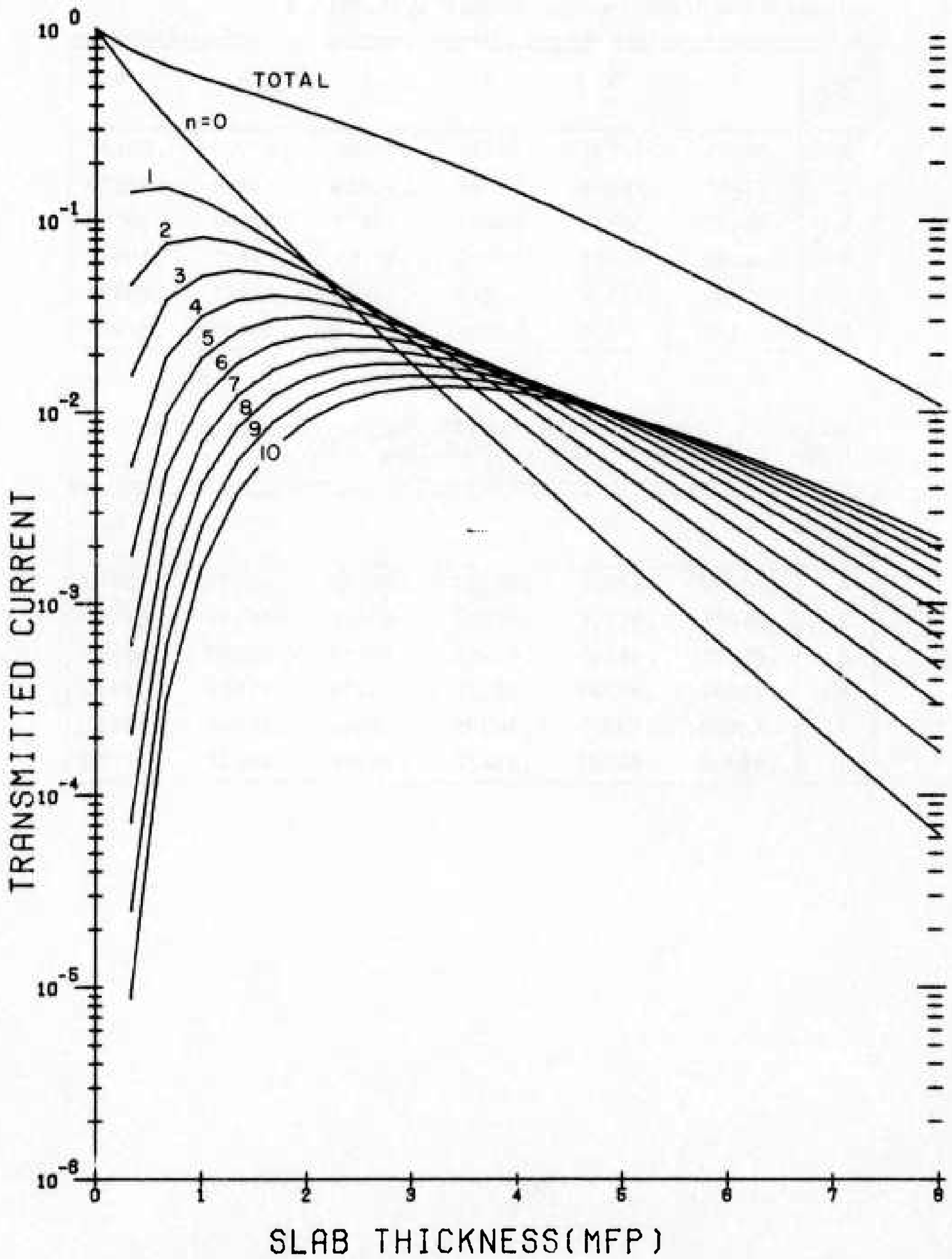

Figure 27. Transmitted Current, $T_n(t)$, vs Slab Thickness, t, for nth Order Neutron Scattering in Carbon ($0 \leq n \leq 10$); Cosine Current Source Configuration

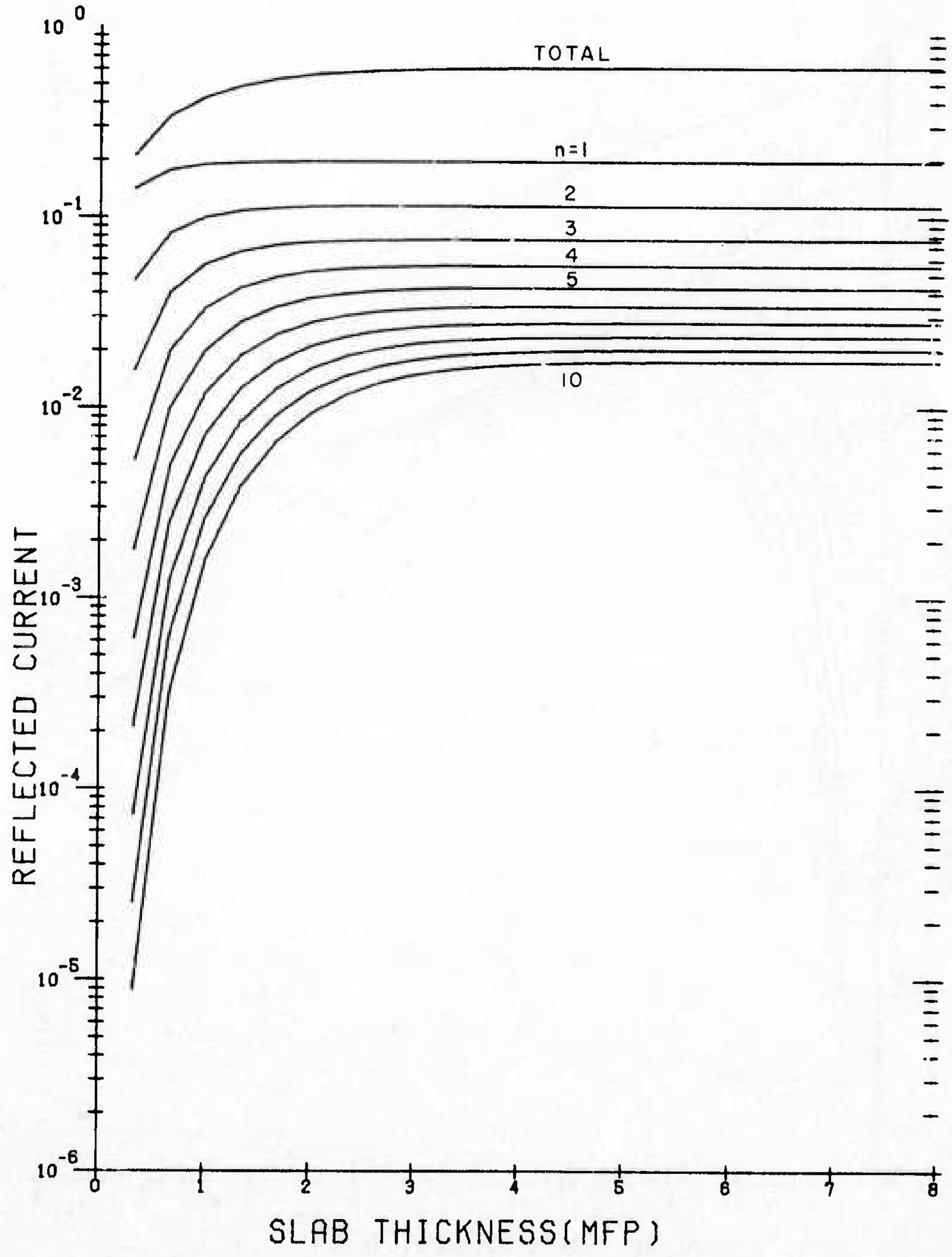

Figure 28. Reflected Current, $B_n(t)$, vs Slab Thickness, t, for nth Order Neutron Scattering in Carbon ($1 \le n \le 10$); Cosine Current Source Configuration

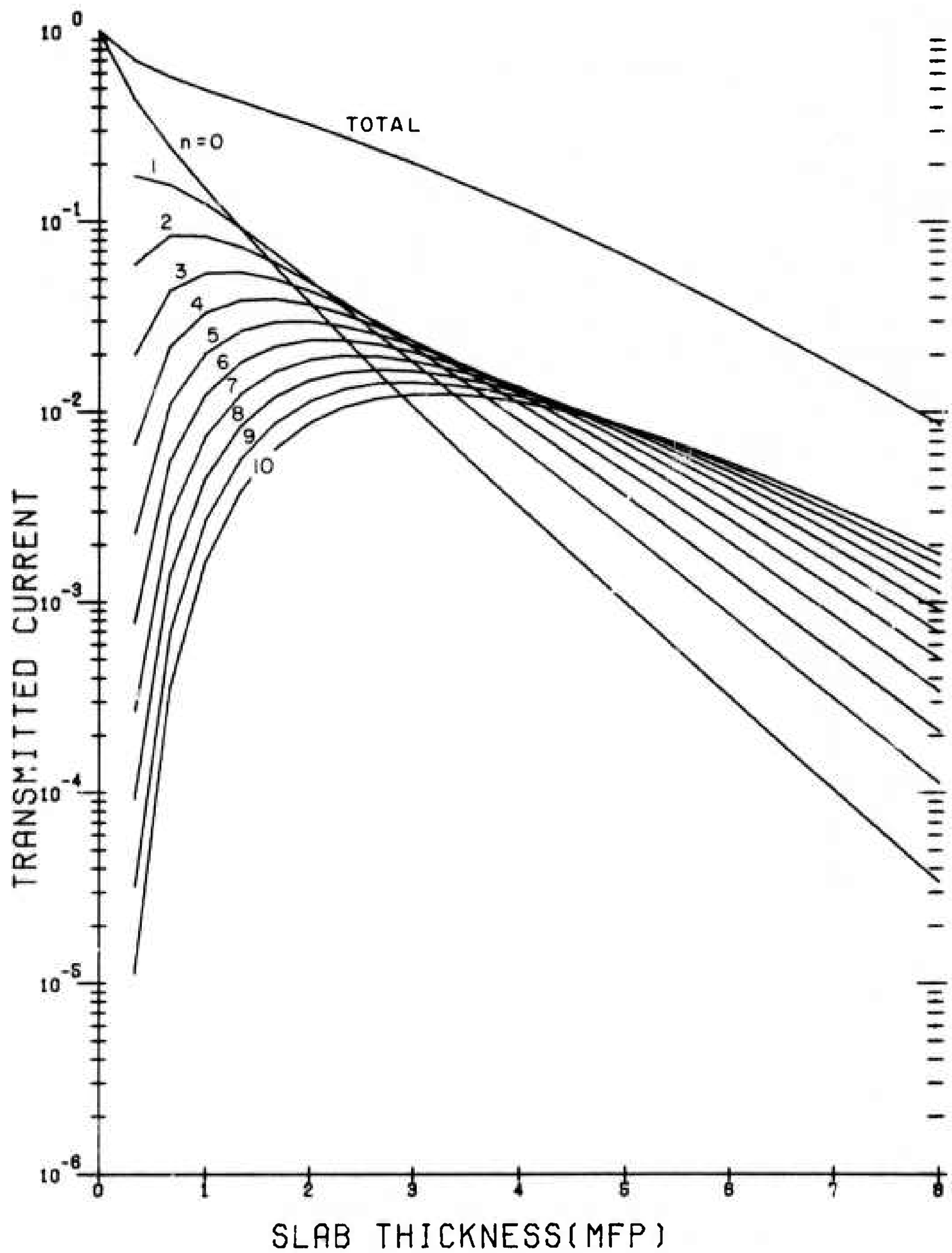

Figure 29. Transmitted Current $T_n(t)$, vs Slab Thickness, t, for nth Order Neutron Scattering in Carbon ($0 \le n \le 10$); Isotropic Current Source Configuration

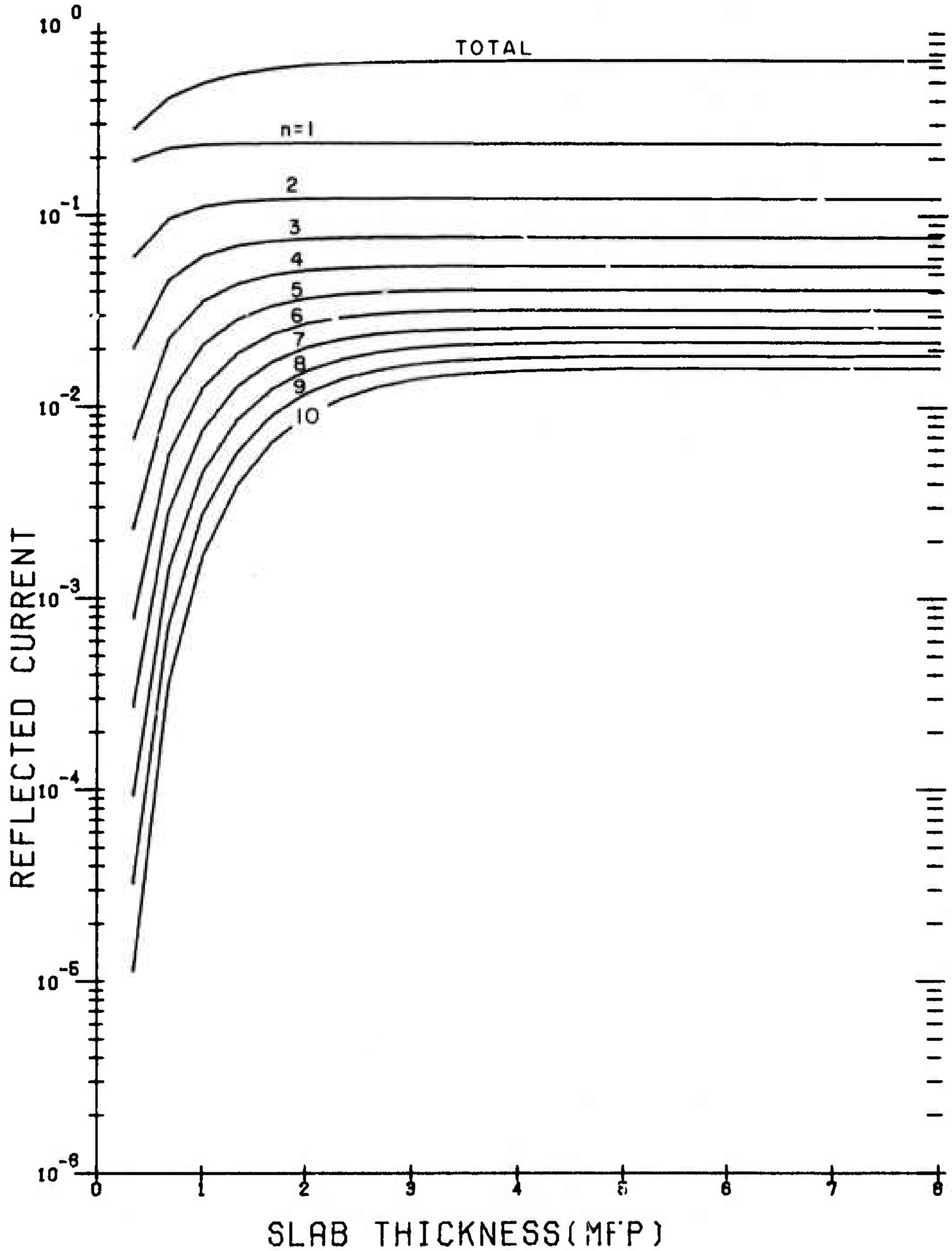

Figure 30. Reflected Current, $B_n(t)$, vs Slab Thickness, t, for nth Order Scattering in Carbon ($1 \leq n \leq 10$); Isotropic Current Source Configuration

Table 12a. Transmitted and Reflected Particle Currents, $T_n(t)$ and $B_n(t)$, Obtained by Two Methods, Resulting from the Scatter of Neutrons by Carbon: Unit Current Cosine Distributed Source

t*	n	Transmitted Current, $T_n(t)$		Reflected Current, $B_n(t)$	
		OOSII	Monte Carlo	OOSII	Monte Carlo
1.0	0	.230836E+00	.230988E+00	0.	0.
	1	.128370E+00	.127981E+00	.188510E+00	.182702E+00
	2	.825249E-01	.816346E-01	.991670E-01	.100127E+00
	3	.517582E-01	.517770E-01	.564029E-01	.555538E-01
	4	.318154E-01	.322348E-01	.331191E-01	.347234E-01
	5	.193578E-01	.200462E-01	.197316E-01	.204006E-01
	6	.117226E-01	.121866E-01	.118328E-01	.117280E-01
	7	.708448E-02	.712438E-02	.711807E-02	.719986E-02
	8	.427825E-02	.455214E-02	.428878E-02	.450690E-02
	9	.258316E-02	.288872E-02	.258645E-02	.253328E-02
	10	.155985E-02	.139027E-02	.156076E-02	.170667E-02
2.0	0	.661818E-01	.669032E-01	0.	0.
	1	.590232E-01	.593600E-01	.195828E+00	.190049E+00
	2	.545255E-01	.547816E-01	.112920E+00	.113492E+00
	3	.473304E-01	.469670E-01	.737885E-01	.724424E-01
	4	.392828E-01	.385448E-01	.515808E-01	.525616E-01
	5	.316885E-01	.321659E-01	.374840E-01	.384174E-01
	6	.251093E-01	.251764E-01	.278605E-01	.277228E-01
	7	.196742E-01	.199569E-01	.209863E-01	.215922E-01
	8	.153078E-01	.154716E-01	.159358E-01	.158127E-01
	9	.118595E-01	.123061E-01	.121602E-01	.123050E-01
	10	.916155E-02	.882766E-02	.930707E-02	.943866E-02
3.0	0	.204292E-01	.203610E-01	0.	0.
	1	.234380E-01	.250278E-01	.196372E+00	.190558E+00
	2	.264336E-01	.258616E-01	.114359E+00	.115006E+00
	3	.274430E-01	.273386E-01	.762697E-01	.747680E-01
	4	.268220E-01	.272210E-01	.550819E-01	.554292E-01
	5	.251461E-01	.248946E-01	.418589E-01	.426848E-01
	6	.229006E-01	.240869E-01	.328953E-01	.328148E-01
	7	.204336E-01	.205112E-01	.264467E-01	.268090E-01
	8	.179698E-01	.180650E-01	.215998E-01	.211564E-01
	9	.156407E-01	.154287E-01	.178367E-01	.183246E-01
	10	.135136E-01	.133371E-01	.148440E-01	.149056E-01
4.0	0	.657264E-01	.625174E-02	0.	0.
	1	.891646E-02	.946770E-02	.196421E+00	.190615E+00
	2	.115193E-01	.114840E-01	.114516E+00	.115122E+00
	3	.135317E-01	.136279E-01	.765956E-01	.751346E-01
	4	.148242E-01	.144587E-01	.556281E-01	.559268E-01
	5	.154445E-01	.162215E-01	.426614E-01	.434688E-01
	6	.155080E-01	.160496E-01	.339716E-01	.338648E-01
	7	.151487E-01	.152799E-01	.277957E-01	.282858E-01
	8	.144928E-01	.148384E-01	.232047E-01	.227554E-01
	9	.136472E-01	.140005E-01	.196688E-01	.200092E-01
	10	.126958E-01	.125712E-01	.168665E-01	.167633E-01

***multiples of 0.96 mfp**

Table 12a. Transmitted and Reflected Particle Currents, $T_n(t)$ and $B_n(t)$, Obtained by Two Methods, Resulting from the Scatter of Neutrons by Carbon: Unit Current Cosine Distributed Source (Cont)

t*	n	Transmitted Current, $T_n(t)$		Reflected Current, $B_n(t)$	
		OOSII	Monte Carlo	OOSII	Monte Carlo
5.0	0	.217278E-02	.214072E-02	0.	0.
	1	.333451E-02	.359160E-02	.196426E+00	.190615E+00
	2	.476975E-02	.479834E-02	.114534E+00	.115154E+00
	3	.615601E-02	.581242E-02	.766378E-01	.751890E-01
	4	.736340E-02	.717528E-02	.557079E-01	.560174E-01
	5	.832812E-02	.836610E-02	.427930E-01	.435138E-01
	6	.902888E-02	.959366E-02	.341687E-01	.340218E-01
	7	.947394E-02	.979992E-02	.280703E-01	.285132E-01
	8	.968966E-02	.904672E-02	.235662E-01	.231266E-01
	9	.971143E-02	.998420E-02	.201234E-01	.205178E-01
	10	.957710E-02	.991430E-02	.174171E-01	.173166E-01
6.0	0	.732330E-03	.779510E-03	0.	0.
	1	.123754E-02	.122875E-02	.196426E+00	.190615E+00
	2	.191969E-02	.208879E-02	.114536E+00	.115154E+00
	3	.267170E-02	.256834E-02	.766433E-01	.751890E-01
	4	.343189E-02	.365522E-02	.557192E-01	.560352E-01
	5	.415187E-02	.405626E-02	.428134E-01	.435140E-01
	6	.479625E-02	.488104E-02	.342020E-01	.341130E-01
	7	.534263E-02	.521708E-02	.281207E-01	.285548E-01
	8	.578018E-02	.585348E-02	.236382E-01	.231966E-01
	9	.610733E-02	.606478E-02	.202212E-01	.206060E-01
	10	.632924E-02	.671384E-02	.175446E-01	.173772E-01
7.0	0	.250462E-03	.287596E-03	0.	0.
	1	.457735E-03	.517984E-03	.196426E+00	.190615E+00
	2	.758951E-03	.767784E-03	.114537E+00	.115154E+00
	3	.112484E-02	.119905E-02	.766440E-01	.751890E-01
	4	.153397E-02	.149776E-02	.557208E-01	.560352E-01
	5	.196460E-02	.199862E-02	.428165E-01	.435140E-01
	6	.239589E-02	.231722E-02	.342074E-01	.341130E-01
	7	.280969E-02	.298506E-02	.281294E-01	.285728E-01
	8	.319166E-02	.366454E-02	.236515E-01	.232282E-01
	9	.353158E-02	.332052E-02	.202404E-01	.206254E-01
	10	.382316E-02	.358698E-02	.175713E-01	.174172E-01
8.0	0	.866456E-04	.114253E-03	0.	0.
	1	.169081E-03	.123444E-03	.196426E+00	.190615E+00
	2	.296621E-03	.270716E-03	.114537E+00	.115154E+00
	3	.463803E-03	.519224E-03	.766441E-01	.751890E-01
	4	.665841E-03	.605546E-03	.557210E-01	.560352E-01
	5	.895846E-03	.112164E-02	.428170E-01	.435140E-01
	6	.114532E-02	.130726E-02	.342082E-01	.341130E-01
	7	.140515E-02	.145860E-02	.281309E-01	.285726E-01
	8	.166644E-02	.157896E-02	.236538E-01	.232282E-01
	9	.192120E-02	.191867E-02	.202439E-01	.206254E-01
	10	.216271E-02	.231446E-02	.175765E-01	.174172E-01

*multiples of 0.96 mfp

Table 12b. Transmitted and Reflected Particle Currents, $T_n(t)$ and $B_n(t)$, Obtained by Two Methods, Resulting from the Scatter of Neutrons by Carbon: Unit Isotropically Distributed Current Source

t*	n	Transmitted Current, $T_n(t)$		Reflected Current, $B_n(t)$	
		OOSII	Monte Carlo	OOSII	Monte Carlo
1.0	0	.156988E+00	.156700E+00	0.	0.
	1	.122893E+00	.122900E+00	.233865E+00	.234520E+00
	2	.835735E-01	.832200E-01	.110432E+00	.111800E+00
	3	.535541E-01	.537200E-01	.608861E-01	.604400E-01
	4	.332498E-01	.331700E-01	.352911E-01	.366500E-01
	5	.203258E-01	.207500E-01	.209065E-01	.217800E-01
	6	.123355E-01	.129500E-01	.125049E-01	.125700E-01
	7	.746212E-02	.777000E-02	.751311E-02	.776000E-02
	8	.450871E-02	.481000E-02	.452396E-02	.459000E-02
	9	.272232E-02	.285000E-02	.272733E-02	.265000E-02
	10	.164390E-02	.149000E-02	.164541E-02	.173000E-02
2.0	0	.413995E-01	.418700E-01	0.	0.
	1	.491398E-01	.489600E-01	.239099E+00	.239810E+00
	2	.483112E-01	.489300E-01	.121303E+00	.122740E+00
	3	.432523E-01	.424700E-01	.754789E-01	.746600E-01
	4	.365675E-01	.361100E-01	.513893E-01	.523400E-01
	5	.298391E-01	.298000E-01	.367889E-01	.379800E-01
	6	.238133E-01	.243200E-01	.271044E-01	.269300E-01
	7	.187428E-01	.186500E-01	.203097E-01	.208000E-01
	8	.146242E-01	.148700E-01	.153732E-01	.152400E-01
	9	.113488E-01	.116300E-01	.117082E-01	.118900E-01
	10	.877736E-02	.871000E-02	.895041E-02	.893000E-02
3.0	0	.122204E-01	.120400E-01	0.	0.
	1	.181266E-01	.191000E-01	.239449E+00	.240140E+00
	2	.217972E-01	.216500E-01	.122326E+00	.123840E+00
	3	.234431E-01	.232600E-01	.773551E-01	.765100E-01
	4	.234496E-01	.235900E-01	.541509E-01	.548000E-01
	5	.223370E-01	.217000E-01	.403471E-01	.415000E-01
	6	.205703E-01	.214500E-01	.312953E-01	.312100E-01
	7	.184997E-01	.188400E-01	.249373E-01	.252600E-01
	8	.163607E-01	.167100E-01	.202419E-01	.200500E-01
	9	.142974E-01	.138600E-01	.166434E-01	.170400E-01
	10	.123885E-01	.121300E-01	.138089E-01	.139200E-01
4.0	0	.382003E-02	.354000E-02	0.	0.
	1	.657457E-02	.702000E-02	.239479E+00	.240170E+00
	2	.905633E-02	.918000E-02	.122431E+00	.123920E+00
	3	.110445E-01	.111300E-01	.775874E-01	.768100E-01
	4	.124144E-01	.122100E-01	.545571E-01	.551800E-01
	5	.131765E-01	.137400E-01	.409634E-01	.421300E-01
	6	.134145E-01	.133600E-01	.321428E-01	.320400E-01
	7	.132406E-01	.133000E-01	.260210E-01	.264100E-01
	8	.127679E-01	.132200E-01	.215523E-01	.212700E-01
	9	.120959E-01	.120600E-01	.181596E-01	.183500E-01
	10	.113052E-01	.112000E-01	.155016E-01	.155100E-01

*multiples of 0.96 mfp

Table 12b. Transmitted and Reflected Particle Currents, $T_n(t)$ and $B_n(t)$, Obtained by Two Methods, Resulting from the Scatter of Neutrons by Carbon: Unit Isotropically Distributed Current Source (Cont)

t*	n	Transmitted Current, $T_n(t)$		Reflected Current, $B_n(t)$	
		OOSII	Monte Carlo	OOSII	Monte Carlo
5.0	0	.123735E-02	.120000E-02	0.	0.
	1	.237623E-02	.254000E-02	.239482E+00	.240170E+00
	2	.362235E-02	.361000E-02	.122443E+00	.123940E+00
	3	.485751E-02	.454000E-02	.776163E-01	.768400E-01
	4	.596966E-02	.587000E-02	.546141E-01	.552400E-01
	5	.688947E-02	.689000E-02	.410606E-01	.421800E-01
	6	.758578E-02	.799000E-02	.322921E-01	.321600E-01
	7	.805660E-02	.786000E-02	.262334E-01	.265700E-01
	8	.831927E-02	.819000E-02	.218368E-01	.215300E-01
	9	.840184E-02	.862000E-02	.185226E-01	.187500E-01
	10	.833652E-02	.851000E-02	.159468E-01	.159700E-01
6.0	0	.410713E-03	.410000E-03	0.	0.
	1	.859289E-03	.880000E-03	.239482E+00	.240170E+00
	2	.141918E-02	.155000E-02	.122444E+00	.123940E+00
	3	.205304E-02	.192000E-02	.776199E-01	.768400E-01
	4	.271155E-02	.273000E-02	.546220E-01	.552500E-01
	5	.335052E-02	.331000E-02	.410753E-01	.421800E-01
	6	.393523E-02	.409000E-02	.323166E-01	.322100E-01
	7	.444201E-02	.415000E-02	.262713E-01	.266100E-01
	8	.485770E-02	.484000E-02	.218919E-01	.215800E-01
	9	.517797E-02	.531000E-02	.185986E-01	.188500E-01
	10	.540514E-02	.569000E-02	.160471E-01	.160200E-01
7.0	0	.138797E-03	.150000E-03	0.	0.
	1	.311349E-03	.320000E-03	.239483E+00	.240170E+00
	2	.549172E-03	.610000E-03	.122444E+00	.123940E+00
	3	.845957E-03	.790000E-03	.776204E-01	.768400E-01
	4	.118660E-02	.117000E-02	.546231E-01	.552500E-01
	5	.155308E-02	.149000E-02	.410774E-01	.421800E-01
	6	.192703E-02	.188000E-02	.323205E-01	.322100E-01
	7	.229180E-02	.241000E-02	.262777E-01	.266200E-01
	8	.263367E-02	.290000E-02	.219018E-01	.216000E-01
	9	.294238E-02	.279000E-02	.186132E-01	.188700E-01
	10	.321121E-02	.314000E-02	.160677E-01	.160400E-01
8.0	0	.475561E-04	.600000E-04	0.	0.
	1	.113088E-03	.700000E-04	.239483E+00	.240170E+00
	2	.210845E-03	.210000E-03	.122445E+00	.123940E+00
	3	.342594E-03	.330000E-03	.776204E-01	.768400E-01
	4	.505947E-03	.420000E-03	.546232E-01	.552500E-01
	5	.695888E-03	.800000E-03	.410777E-01	.421800E-01
	6	.905596E-03	.100000E-02	.323211E-01	.322100E-01
	7	.112735E-02	.112000E-02	.262787E-01	.266200E-01
	8	.135333E-02	.129000E-02	.219035E-01	.216000E-01
	9	.157631E-02	.148000E-02	.186158E-01	.188700E-01
	10	.179003E-02	.185000E-02	.160716E-01	.160400E-01

*multiples of 0.96 mfp

7.3 Monte Carlo Calculations for Neutron Scattering in Hydrogen and Carbon

Monte Carlo computations were made to verify the results obtained for the two anisotropic scattering cases that have been considered. The computer code used was the same as that for the isotropic scattering simulation with the exception of the calculation of the post-collision particle trajectory orientation. This is due to the fact that the scattering must be treated as isotropic in the center of mass rather than the laboratory system.

The cosine of the deflection angle in the laboratory system is given by Eq. (114). The azimuthal deflection, ρ, is determined by a uniform sampling on the interval $(0, 2\pi)$. Then if θ^n and ϕ^n are the polar and azimuthal angles respectively in the laboratory system prior to the nth interaction,[16]

$$\cos\theta^{n+1} = \cos\theta^n \cos\omega_\ell + \sin\theta^n \sin\omega_\ell \cos\rho, \tag{121a}$$

$$\sin\theta^{n+1} = \sqrt{1 - \cos^2\theta^{n+1}}, \tag{121b}$$

$$\cos(\phi^{n+1} - \phi^n) = \frac{\cos\omega_\ell - \cos\theta^n \cos\theta^{n+1}}{\sin\theta^n \sin\theta^{n+1}}, \tag{122a}$$

$$\sin(\phi^{n+1} - \phi^n) = \frac{\sin\rho \sin\omega_\ell}{\sin\theta^{n+1}}. \tag{122b}$$

If $(\sin\theta^n)\cdot(\sin\theta^{n+1}) = 0$, then the last two relations are replaced by

$$\cos\phi^{n+1} = \cos\rho. \tag{123a}$$

$$\sin\phi^{n+1} = \sin\rho. \tag{123b}$$

The Monte Carlo results for both neutron scattering cases, hydrogen and carbon, are given in Tables 10 and 12, respectively, where they may be compared with their corresponding OOSII results.

7.4 The Screened Rutherford Interaction

Another application of the OOSII method can be found in the investigation of the scattering of low energy electrons in thin films. On the basis of empirical studies,[6] it is believed that the contribution due to electron-phonon interactions to

16. Raso, D. J., and Woolf, S. (1965) Ionization Resulting from a Neutron Point Source in an Exponential Atmosphere, Tech. Ops. Res. Rpt. No. TO-B-65-43, Technical Operations, Inc., Burlington, Mass.

the transmitted and reflected electron yields from thin films which have undergone electron beam bombardment may be estimated if the scattering angular distribution of this interaction is characterized by a screened Rutherford cross section. The OOSII formulation is a natural choice for such an analysis since the average energy loss per electron-phonon interaction is known.[17]

As is well known, the Rutherford scattering formula for unscreened coloumb interactions states that in the laboratory system (if the scattering center is massive enough), the probability density of a particle undergoing deflection through an angle ω_ℓ has the form

$$f(\cos \omega_\ell) \propto \frac{1}{(1 - \cos \omega_\ell)^2} . \tag{124}$$

This formula has a singularity in the forward direction ($\cos \omega_\ell = 1$). To overcome this difficulty, a screening factor, $\eta > 0$, can be introduced so that, when normalized, the following modified form of the Rutherford formula results:

$$f(\cos \omega_\ell) = \frac{1}{2\pi} \frac{\eta(1+\eta/2)}{(1+\eta - \cos \omega_\ell)^2} . \tag{125}$$

The degree to which the parameter η influences the anisotropy of f is seen in the expression for $\mu_{1/2}$, the cosine of the deflection angle for which the probability of occurrence is 1/2. It is easily shown that in terms of η,

$$\mu_{1/2} = \frac{1}{1+\eta} . \tag{126}$$

It is apparent that as η tends toward ∞, the scattering tends toward isotropic, and as η tends toward zero, the scattering becomes more forward peaked.

As in the previous scattering cases considered, the form of the scattering probability density function required for use with the OOSII algorithm must be independent of azimuth. This is accomplished in the following way, since:

$$\cos \omega_\ell = \vec{\Omega}_1 \cdot \vec{\Omega}_2 = \sin \theta_1 \sin \theta_2 \cos \phi + \cos \theta_1 \cos \theta_2 , \tag{127}$$

where $\vec{\Omega}_1$ and $\vec{\Omega}_2$ are as defined in Eqs. (105), then

---

17. Stuart, R., Wooten, F., and Spicer, W.E. (1964) Phys. Rev., **135**:A495.

$$f(\mu_1, \mu_2) = \frac{\eta(1+\eta/2)}{2\pi} \int_0^{2\pi} \frac{d\phi}{\left[(1+\eta - \mu_1\mu_2) - (\sqrt{1-\mu_1^2)(1-\mu_2^2)} \cos\phi\right]^2} \quad , (128)$$

or

$$f(\mu_1, \mu_2) = \frac{\eta(1+\eta/2)\,(1+\eta-\mu_1\mu_2)}{\left[\eta^2 + 2\eta\,(1-\mu_1\mu_2) + (\mu_1-\mu_2)^2\right]^{3/2}} \, . \quad (129)$$

The scattering matrix $f(\mu_1, \mu_2)$ of Eq. (129) was evaluated for five values of η corresponding to average deflection angles of 15°, 30°, 45°, 60°, and 75°. Thus a full range of anisotropy was covered. For each of these cases, this matrix was substituted into the expressions of Eqs. (63) and (64), and the OOSII computed program was run to provide computations of transmitted and reflected currents. The results obtained for these cases are plotted in Figures 31 through 40. The transmitted and reflected currents, $T_n(t)$ and $B_n(t)$, are plotted vs slab thickness for the cosine source configuration. The contrast between these curves and those of the isotropic scattering case is quite noticeable if reference is again made to the corresponding plots of Figures 14 and 15.

An independent verification of the screened Rutherford results is made possible by the availability of Monte Carlo calculations made by J.C. Garth in 1974[6] of the transmitted low energy electron current through LiF thin films assuming screened Rutherford scattering to hold. Tables 13 and 14 compare these results for 10 scattering orders. The first table shows the comparison for two slab thicknesses, 1.0 and 3.6 mfp, for an average scattering angle of 15°. The second table compares results for 1.0 and 7.0 mfp thickness given an average scattering angle of 30°. In all cases, six discrete ordinates per quadrant were used in the angular integrations.

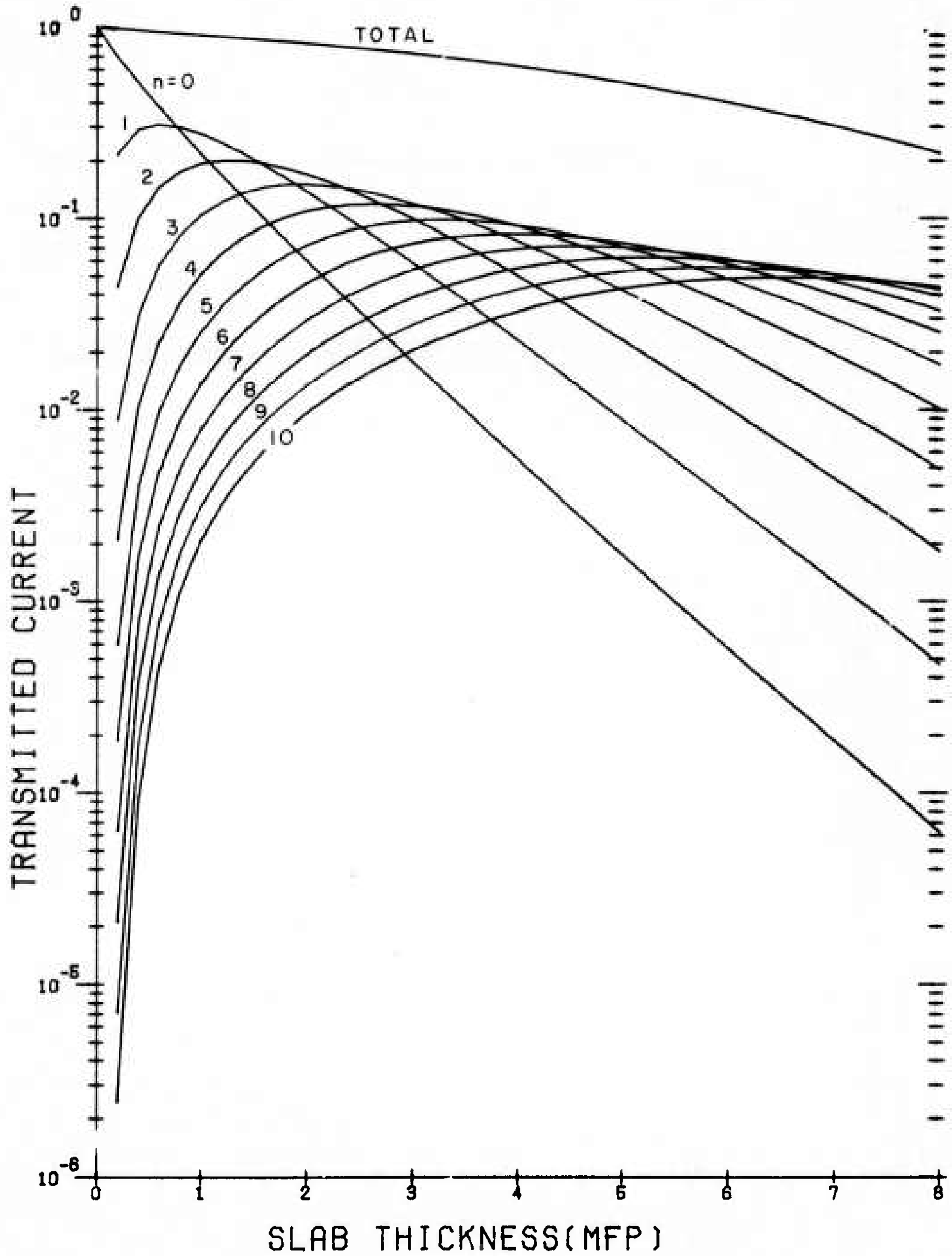

Figure 31. Transmitted Current, $T_n(t)$, vs Slab Thickness, t, for nth Order Screened Rutherford Scattering ($0 \leq n \leq 10$) with 15° Average Scattering Angle; Cosine Current Source Configuration

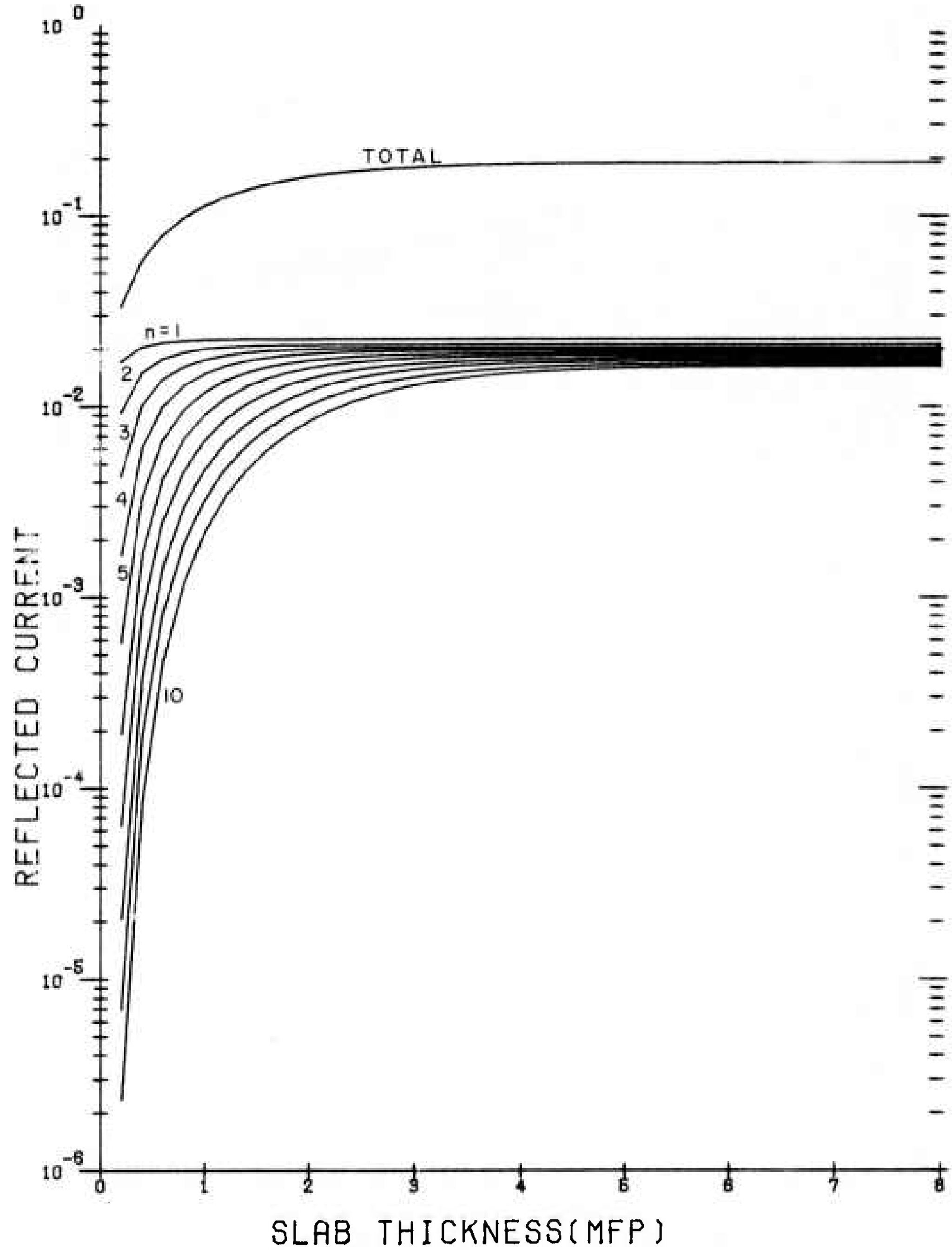

Figure 32. Reflected Current, $B_n(t)$, vs Slab Thickness, t, for nth Order Screened Rutherford Scattering ($1 \leq n \leq 10$) with 15° Average Scattering Angle; Cosine Current Source Configuration

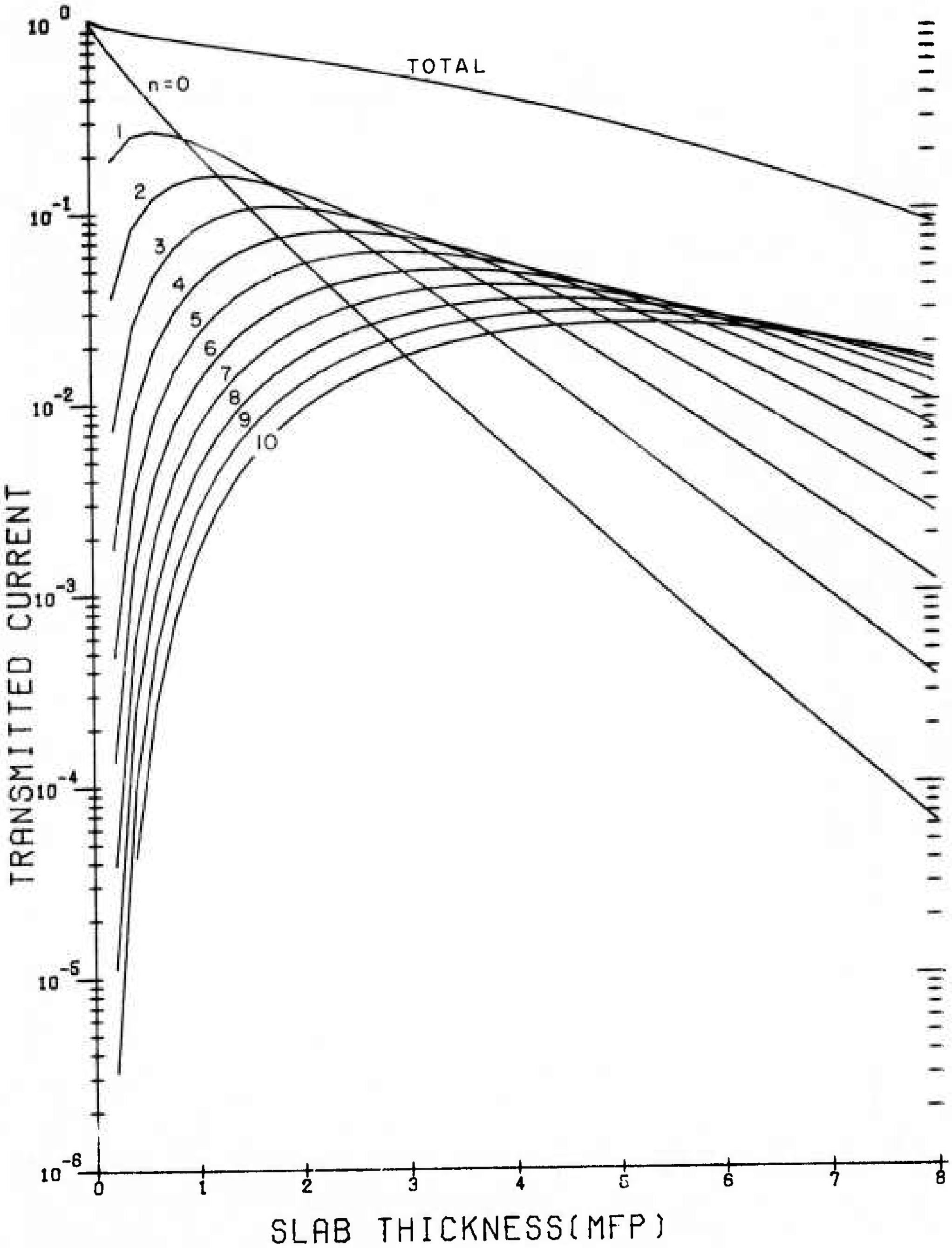

Figure 33. Transmitted Current, $T_n(t)$, vs Slab Thickness, t, for nth Order Screened Rutherford Scattering ($0 \le n \le 10$) with 30° Average Scattering Angle; Cosine Current Source Configuration

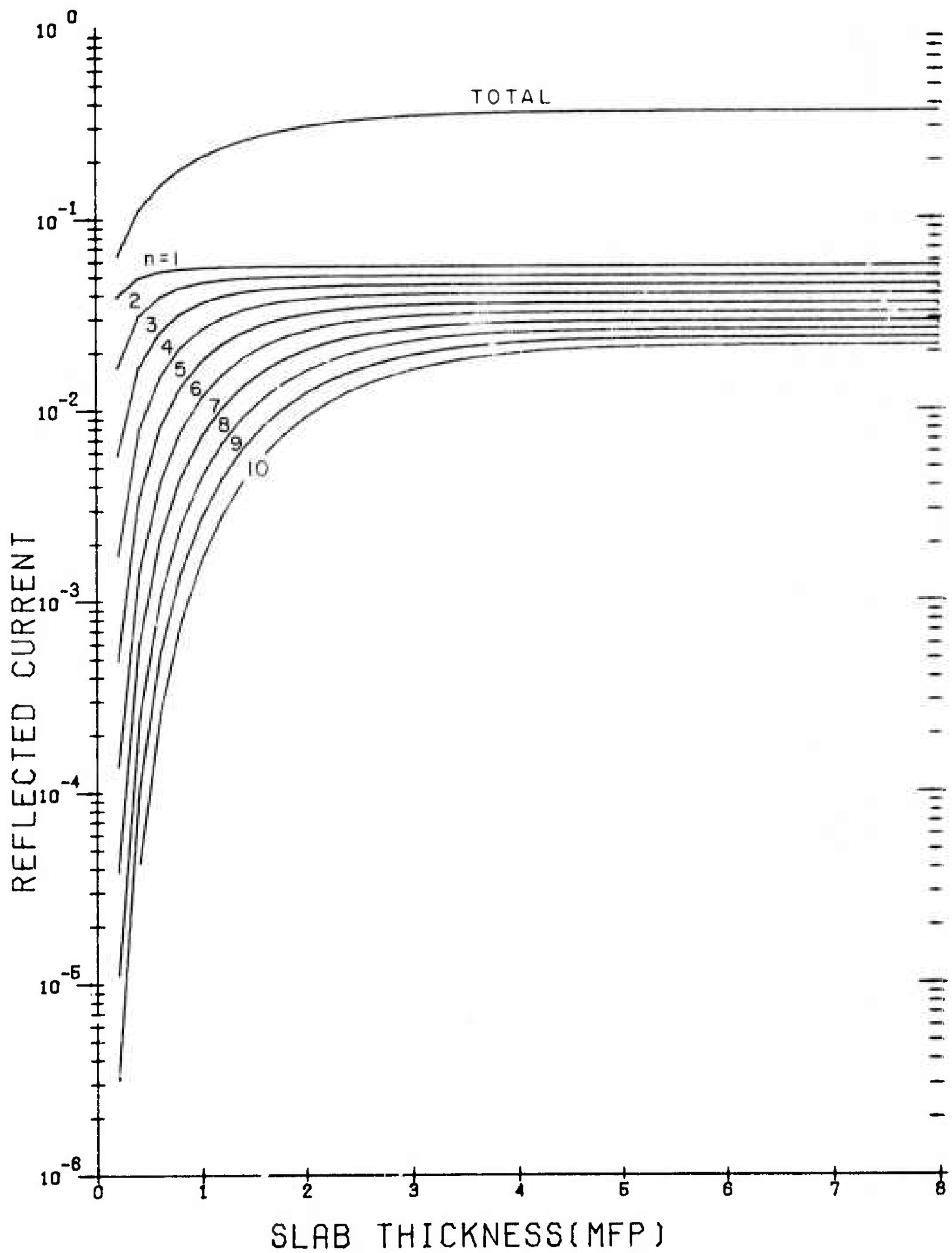

Figure 34. Reflected Current, $B_n(t)$, vs Slab Thickness, t, for nth Order Screened Rutherford Scattering ($1 \leq n \leq 10$) with 30° Average Scattering Angle; Cosine Current Source Configuration

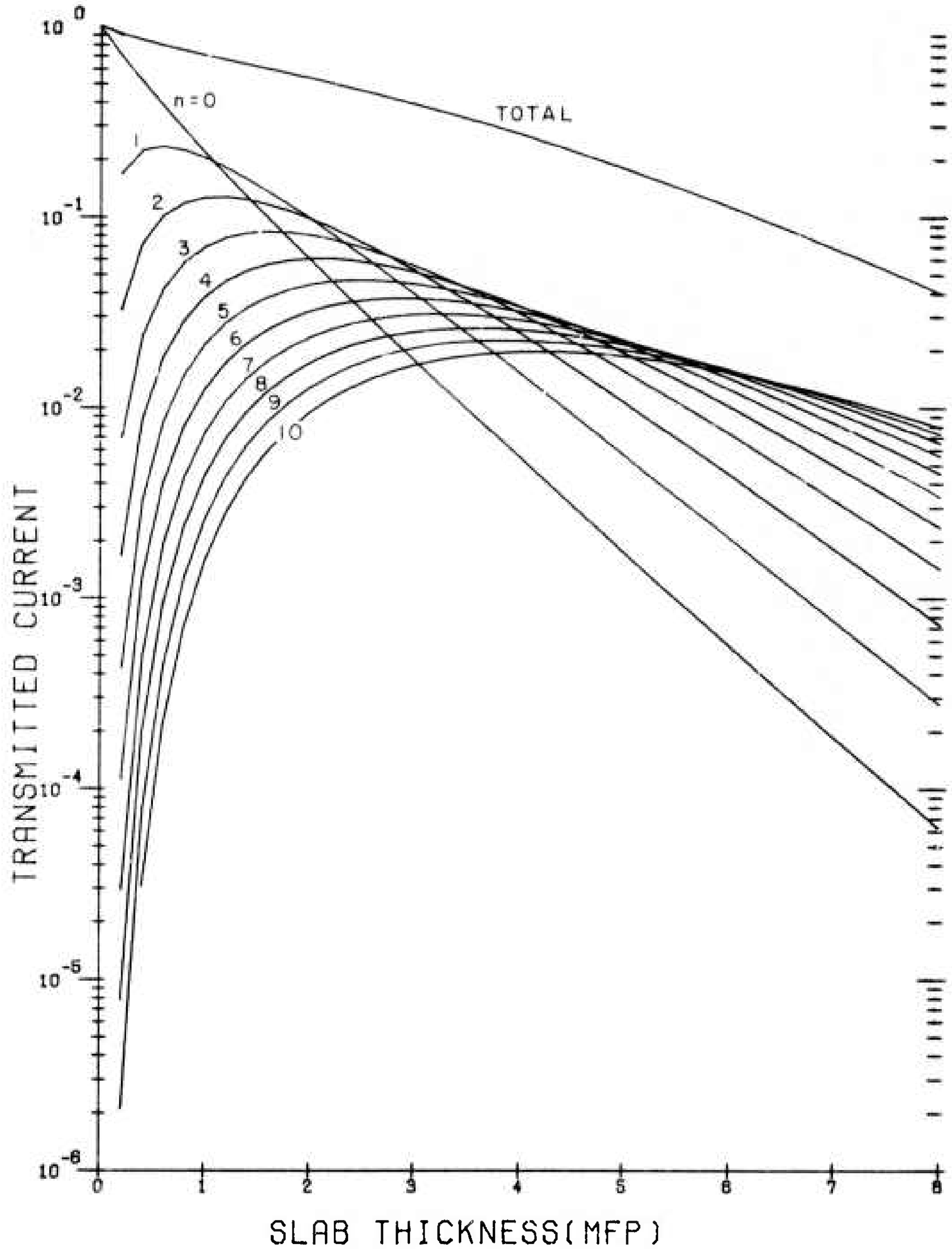

Figure 35. Transmitted Current, $T_n(t)$, vs Slab Thickness, t, for nth Order Screened Rutherford Scattering ($0 \leq n \leq 10$) with 45° Average Scattering Angle; Cosine Current Source Configuration

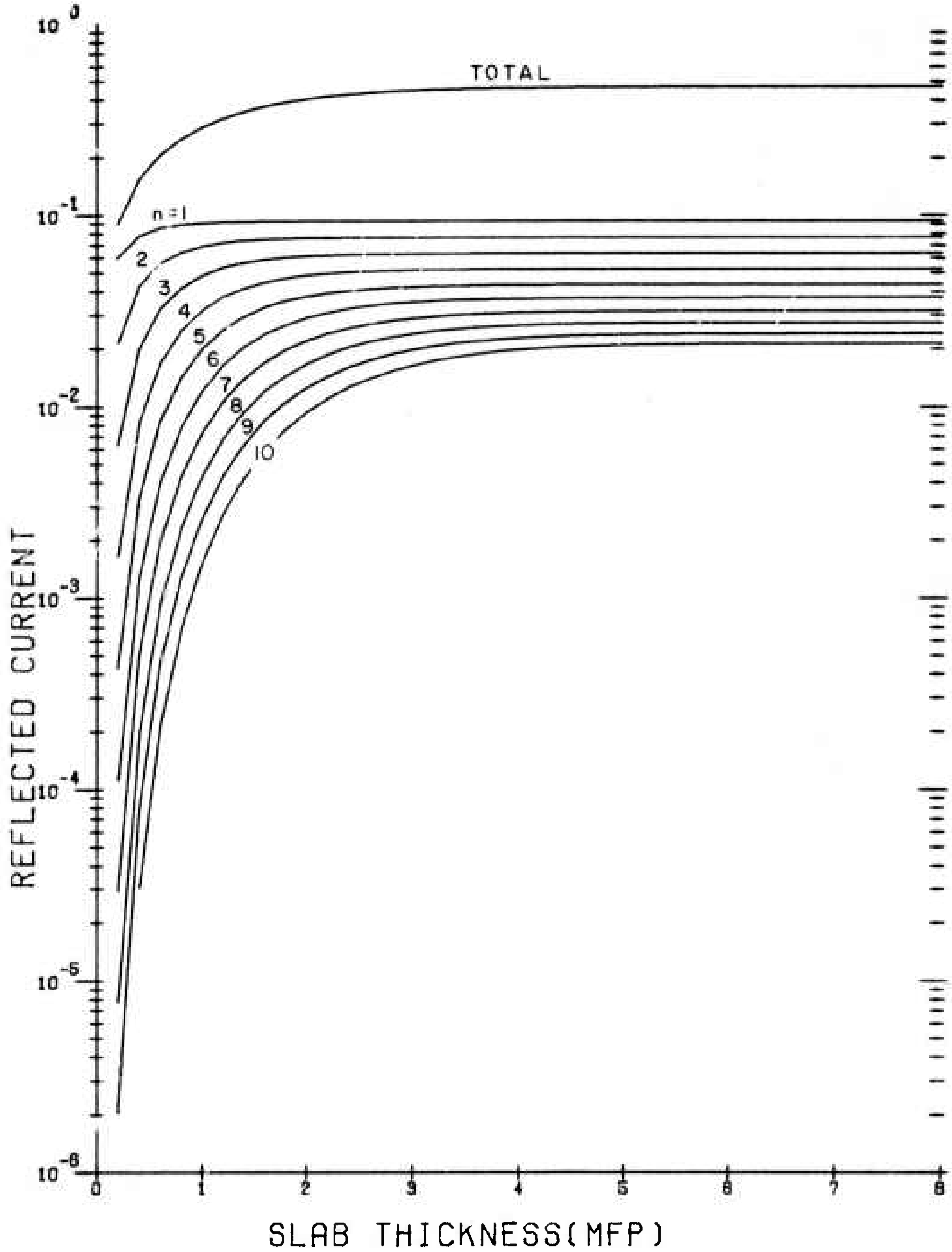

Figure 36. Reflected Current, $B_n(t)$, vs Slab Thickness, t, for nth Order Screened Rutherford Scattering ($1 \leq n \leq 10$) with 45° Average Scattering Angle; Cosine Current Source Configuration

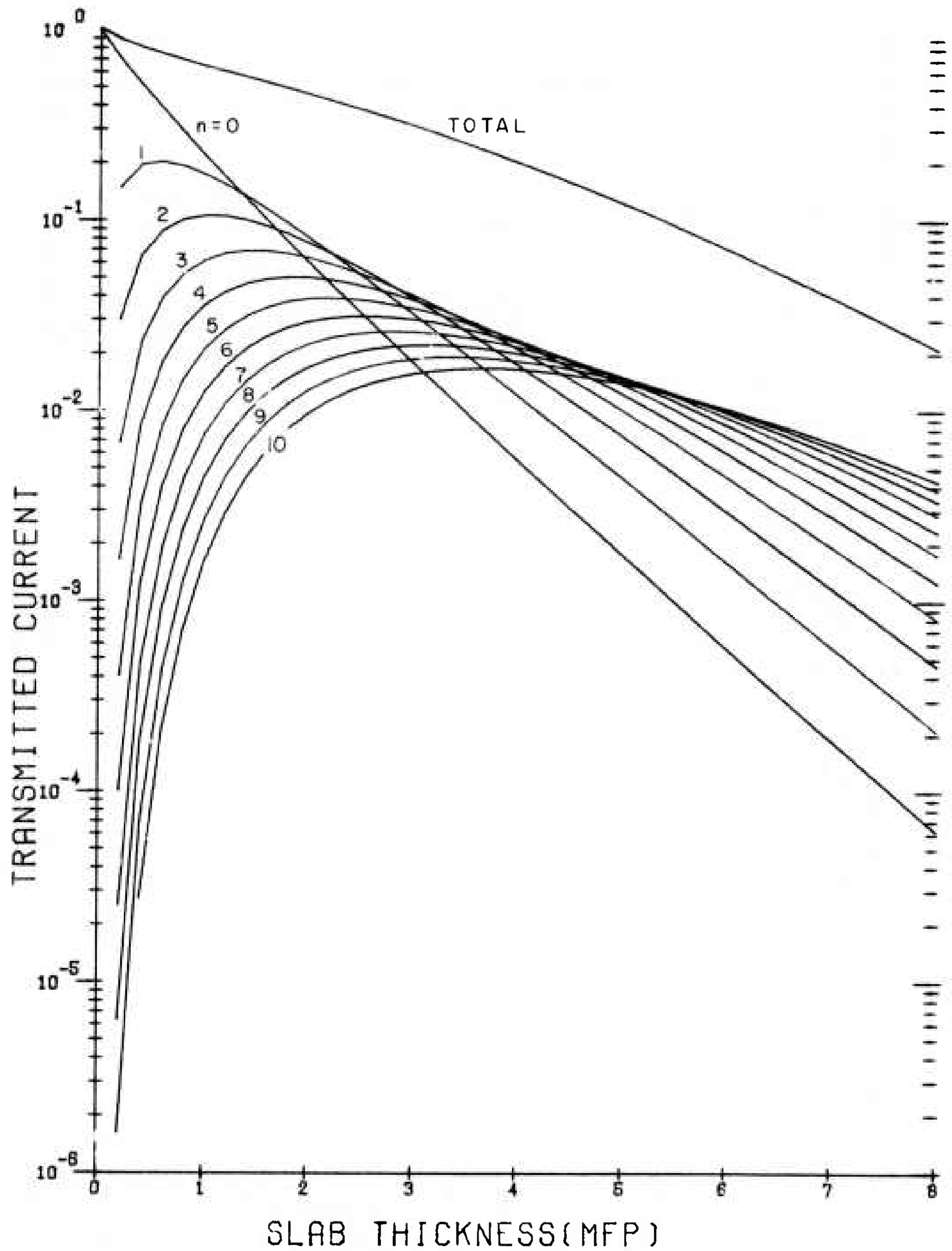

Figure 37. Transmitted Current, $T_n(t)$, vs Slab Thickness, t, for nth Order Screened Rutherford Scattering ($0 \leq n \leq 10$) with 60° Average Scattering Angle; Cosine Current Source Configuration

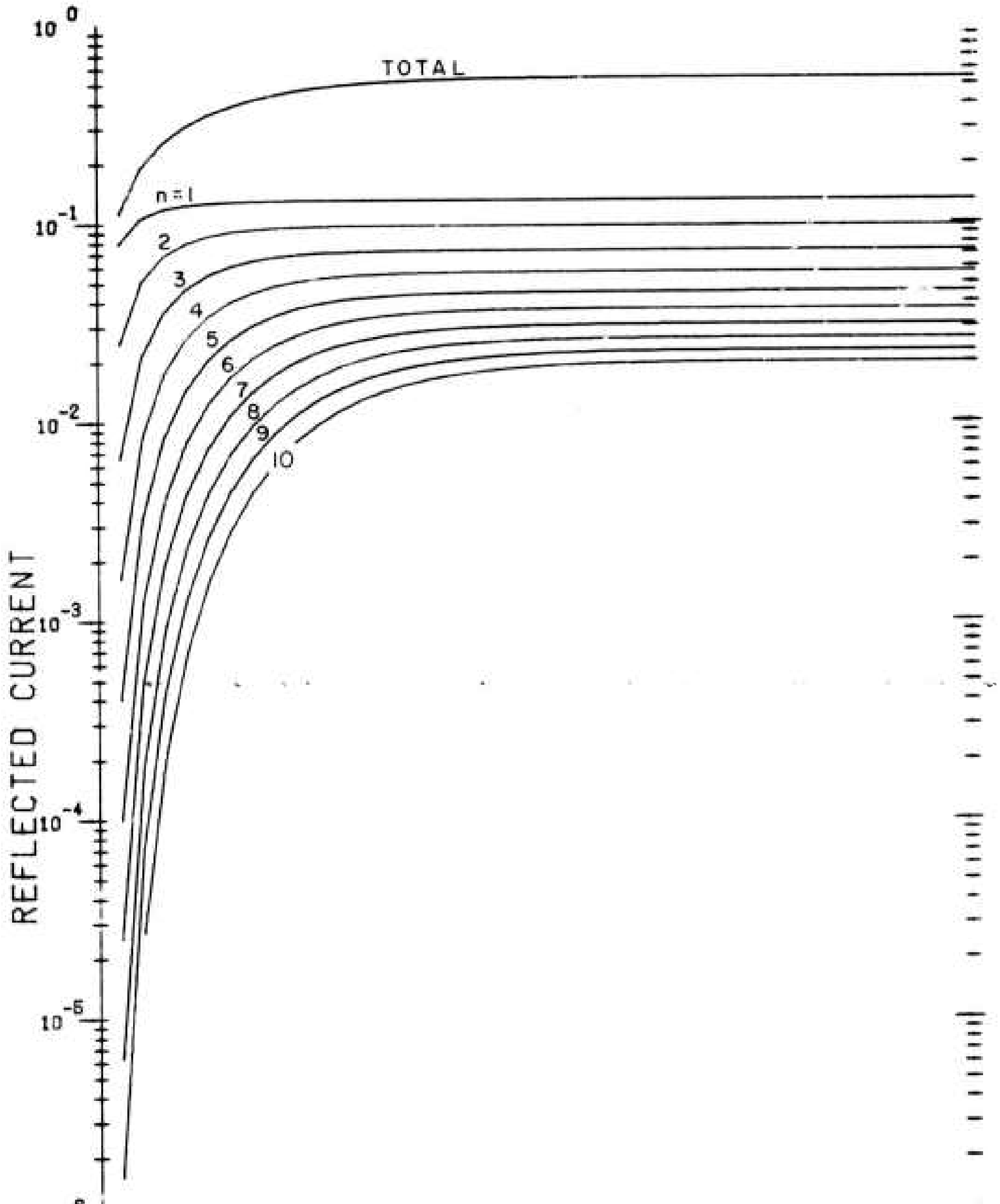

Figure 38. Reflected Current, $B_n(t)$, vs Slab Thickness, t, for nth Order Screened Rutherford Scattering ($1 \le n \le 10$) with 60° Average Scattering Angle; Cosine Current Source Configuration

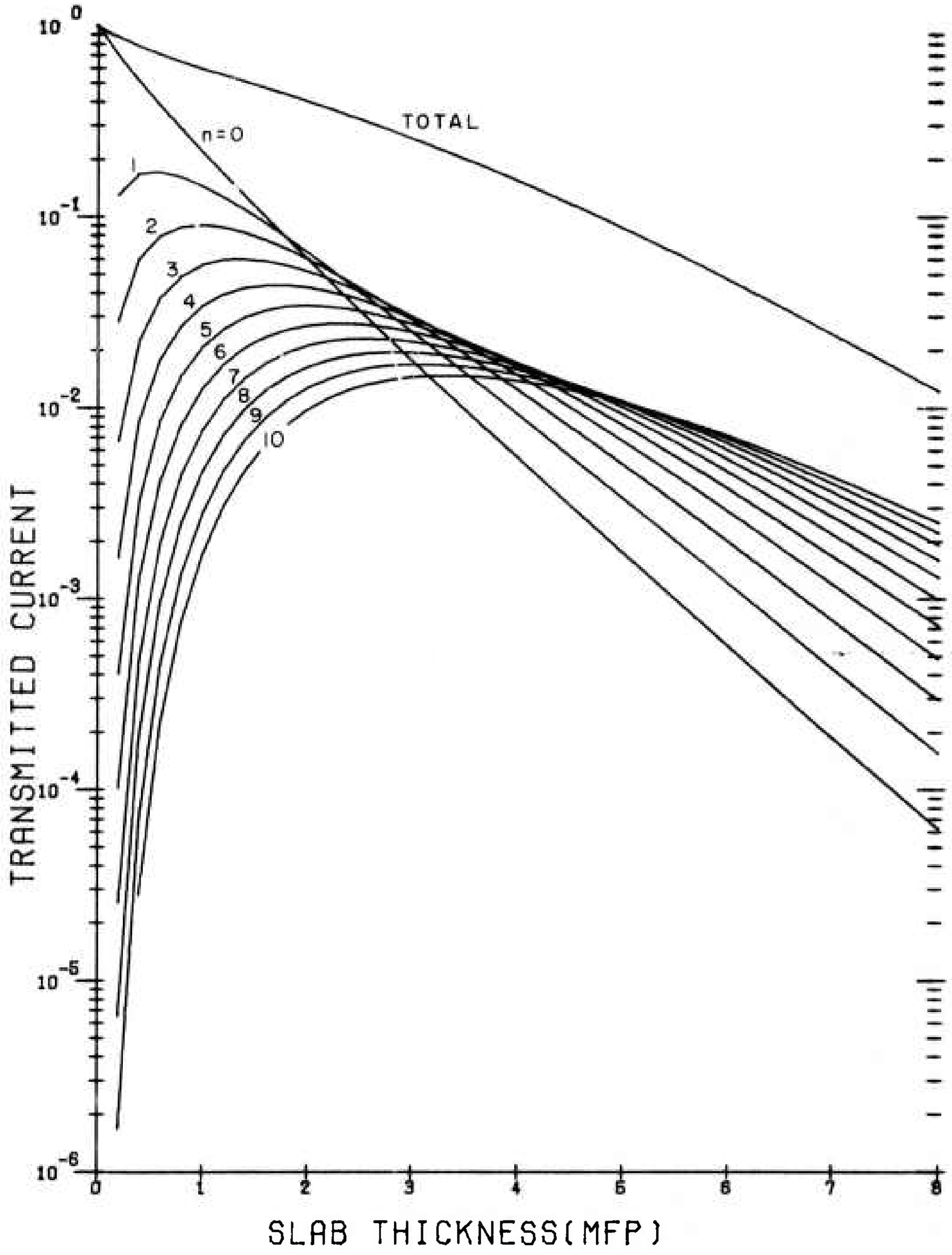

Figure 39. Transmitted Current, $T_n(t)$, vs Slab Thickness, t, for nth Order Screened Rutherford Scattering ($0 \leq n \leq 10$) with 75° Average Scattering Angle; Cosine Current Source Configuration

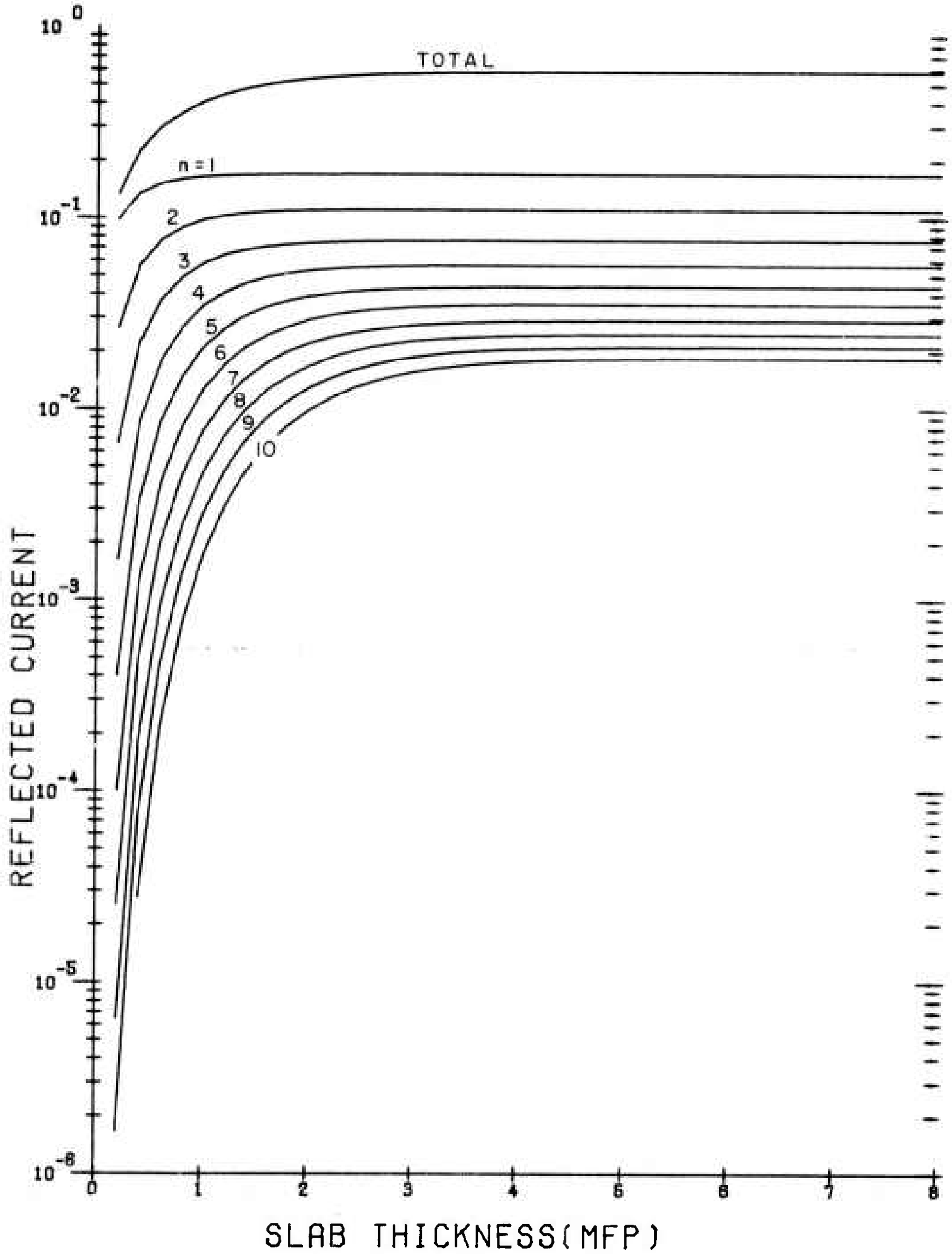

Figure 40. Reflected Current, $B_n(t)$, vs Slab Thickness, t, for nth Order Screened Rutherford Scattering ($1 \le n \le 10$) with 75° Average Scattering Angle; Cosine Current Source Configuration

Table 13. Transmitted Particle Currents, $T_n(t)$, Obtained by Two Methods, Through Two Slabs of Width t=1.0 and t=3.6 mfp: Unit Current Cosine Distributed Source; Screened Rutherford Scattering with an Average Scattering Angle of 15°

t	n	Transmitted Current, $T_n(t)$	
		OOSII	Monte Carlo[6]
1.0	1	.2762 00	.2721 00
	2	.1930 00	.1898 00
	3	.1039 00	.1007 00
	4	.5108-01	.4965-01
	5	.2554-01	.2357-01
	6	.1370-01	.1282-01
	7	.7935-02	.739 -02
	8	.4886-02	.459 -02
	9	.3140-02	.287 -02
	10	.2071-02	.208 -02
3.6	1	.3347-01	.3320-01
	2	.6661-01	.6501-01
	3	.9285-01	.8874-01
	4	.1027 00	.9756-01
	5	.9682-01	.9247-01
	6	.8193-01	.7693-01
	7	.6469-01	.6058-01
	8	.4919-01	.4558-01
	9	.3691-01	.3379-01
	10	.2782-01	.2519-01

Table 14. Transmitted Particle Currents, $T_n(t)$, Obtained by Two Methods, Through Two Slabs of Width t=1.0 and t=7.0 mfp: Unit Current Cosine Distributed Source; Screened Rutherford Scattering with an Average Scattering Angle of 30°

t	n	Transmitted Current, $T_n(t)$	
		OOSII	Monte Carlo[6]
1.0	1	.2388 00	.2382 00
	2	.1542 00	.1551 00
	3	.8205-01	.8109-01
	4	.4196-01	.4276-01
	5	.2224-01	.2208-01
	6	.1246-01	.1272-01
	7	.7299-02	.751 -02
	8	.4385-02	.482 -02
	9	.2665-02	.271 -02
	10	.1626-02	.155 -02
7.0	1	.9883-03	.92 -03
	2	.2824-02	.285 -02
	3	.5788-02	.584 -02
	4	.9540-02	.957 -02
	5	.1346-01	.1333-01
	6	.1691-01	.1721-01
	7	.1946-01	.1956-01
	8	.2095-01	.2051-01
	9	.2144-01	.2069-01
	10	.2115-01	.2086-01

8. CONCLUSIONS

Throughout the preparation of this document, the objective has been that of providing a complete description of the development of a new method for determining emergent nth order scattered particle currents from scattering media. In addition, some applications of the method have been demonstrated.

Areas of further application are suggested in the current invariant imbedding literature. For example, in the field of medical physics, invariant imbedding analyses of finite (nth) order scattered currents have been performed for the problem of the scattering of Co^{60} gammas in skin tissue.[18] The argument is made (op. cit.) that only a few scattering orders are necessary to determine the skin dose because of the large mean-free-path. The analysis presented in Ref. 18 is derived from the equation of radiative transfer and consists of integro-differential recursion relations for the nth order reflection and transmission functions. The energy dependence of the scattering kernel is also retained. As far as can be determined from the available literature, numerical solutions of these equations do not yet exist, most probably because their solution would require a formidable effort. The possibility then arises of the application to this problem of the OOSII method or a modification of it which includes energy dependence in the integral recursion relations.

Another area of possible application occurs in the field of reactor physics. Mingle[5] in his analysis of finite order isotropic scattering of neutrons, showed that for a multiplying medium, the total transmitted and reflected particle currents can be given by the summations over n of terms of the form $c^n T_n$ and $c^n B_n$, where n is the order of scattering, and c is the number of secondary particles produced per collision. Since the OOSII method can be applied to anisotropic scattering, a broader range of utility may be achieved.

With regard to both the efficiency and the accuracy of the calculational method presented here, a most favorable comparison can be made with the equivalent Monte Carlo calculation. An example of this is found in the cosine law scattering situation (neutrons in hydrogen) where the OOSII method consumes 365 seconds of Central Processor time on a CDC(6600) computer for the transmitted and reflected currents to 10th order for 41 slab thicknesses ranging from 0 to 8 mfp. The equivalent Monte Carlo calculation required 508 seconds. Furthermore a degree of accuracy is possible here which cannot be attained feasibly with the Monte Carlo method. For instance, the OOSII method always yields a number for small slab thicknesses (0.2 mfp), even for 10th order scattering, such as 7×10^{-7} for the emergent current, whereas the Monte Carlo calculation of 100,000 particle

18. Bellman, R., Ueno, S., and Vasudevan, R. (1973) Mathematical Biosciences, 17:89.

histories does not. In order to obtain one particle count, approximately 1.5 million histories (or 2 hours of computer time) would be required. A comparable situation applies for very thick slabs, where it is possible to increase the integration step size in the OOSII calculation, assuming near linearity for the reflected current and a decaying exponential approximation for the transmitted current, without a significant increase in error.

References

1. Ambarzumian, V.A. (1942) Soviet Astron. AJ, 19:1.
2. Bellman, R., Kalaba, R., and Wing, G.M. (1960) J. Math. Phys. 1:280.
3. Bellman, R., Kalaba, R., and Prestrud, M.C. (1963) Invariant Imbedding and Radiative Transfer in Slabs of Finite Thickness, American Elsevier, New York.
4. Mingle, J.O. (1967) Nucl. Sci. Eng. 28:177.
5. Mingle, J.O. (1972) J. Math. Anal. Appl. 38:53.
6. Garth, J.C., Parke, N.G., and DeStefano, T.H. (1974) Bull. Am. Phys. Soc., Ser. II, 19No. 3:232.
7. Wing, G.M. (1962) An Introduction to Transport Theory, John Wiley and Sons, Inc., New York.
8. Lanczos, C. (1956) Applied Analysis, Prentice Hall, Inc., Englewood Cliffs, N.J.
9. Weinberg, A.M., and Wigner, E.P. (1958) The Physical Theory of Neutron Chain Reactors, Univ. of Chicago Press, Chicago.
10. Stroud, A.H., and Secrest, D. (1966) Gaussian Quadrature Formulas, Prentice Hall, Inc., Englewood Cliffs, N.J.
11. Forbes, I.A. (1973) Private communication.
12. Lovitt, W.V. (1950) Linear Integral Equations, Dover Publications, Inc., New York.
13. Sobolev, V.V. (1963) A Treatise on Radiative Transfer, D. Van Nostrand Co., Inc., Princeton, N.J.
14. Crosbie, A.L., Merriam, R.L., and Viskanta, R. (1968) J. Quant. Spectr. Rad. Transfer, 8:1609.
15. Lamarsh, J.R. (1967) Nuclear Reactor Theory, Addison Wesley, Reading, Mass.
16. Raso, D.J., and Woolf, S. (1965) Ionization Resulting from a Neutron Point Source in an Exponential Atmosphere, Tech. Ops. Res. Rpt. No. TO-B-65-43, Technical Operations, Inc., Burlington, Mass.

17. Stuart, R., Wooten, F., and Spicer, W.E. (1964) Phys. Rev., **135**:A495.

18. Bellman, R., Ueno, S., and Vasudevan, R. (1973) Mathematical Biosciences, **17**:89.

Appendix A

Computer Code Listing

A1. Orders-of-Scattering Invariant Imbedding Code for the One-Dimensional Geometry

```
      PROGRAM INVIMB(INPUT,OUTPUT,TAPE3)
      CCMMON THK(51),TRAN(41),TRAN1(40),BACK(40),BACK1(40),F,B,K,T,T1,
     1TRAY(51,40),BRAY(51,40),KMAX,TKPLT(10),NCURV
      DIMENSION IDT(51)
      DATA IDT/1,50*40/
      READ 1,NCASE
C     NCASE - NO. OF CASES TO BE RUN
 1    FORMAT(I5)
      DO 500 IJK = 1,NCASE
      THK(1) = 0.0
      READ 9,THICK,F,KMAX
C     THICK - MAXIMUM ROD LENGTH
C     F - FORWARD SCATTERING PROBABILITY
C     KMAX - NO. OF ROD LENGTHS FOR WHICH CURRENTS ARE COMPUTED
    9 FORMAT(2F10.0,I10)
      DT=THICK/FLOAT(KMAX-1)
      DO 11 KT=2,KMAX
      THK(KT)=THK(KT-1)+DT
   11 CONTINUE
      T=0.0
      B=1.-F
      K=1
      KT=1
      KTOT=IDT(KT)
   50 CALL GETFN
      DO 49 N=1,40
      TRAN1(N)=TRAN(N)
      BACK1(N)=BACK(N)
   49 CONTINUE
      IF(K.EQ.KTOT) GO TO 45
      GO TO 48
   45 DO 47 N=1,40
      TRAY(KT,N)=TRAN(N)
      BRAY(KT,N)=BACK(N)
   47 CONTINUE
      KT=KT+1
      IF(KT.GT.KMAX) GO TO 52
      KTOT=KTOT+IDT(KT)
      DTM=(THK(KT)-THK(KT-1))/FLOAT(IDT(KT))
   48 T1=T
      T=T1+DTM
      K=K+1
      IF (T.LE.THK(KMAX)) GO TO 50
   52 CCNTINUE
      PRINT 299
  299 FORMAT(*1*)
      PRINT 300,F,B
      NT=1
      CALL PRNTR(NT)
      PRINT 299
      PRINT 301,F,B
      NT=2
      CALL PRNTR(NT)
  300 FORMAT(1X,*TRANSMISSICN - - - - F=*,F5.3,* B=*,F5.3)
  301 FORMAT(1X,*BACKSCATTER  - - - - F=*,F5.3,* B=*,F5.3)
      WRITE(3)(THK(K),K=1,KMAX)
      WRITE(3)((TRAY(K,N),K=1,KMAX),N=1,40)
      WRITE(3)((BRAY(K,N),K=1,KMAX),N=1,40)
  500 CONTINUE
      STCP
      END
```

```
      SUBROUTINE PRNTR(NT)
      DIMENSION SUM(51),ANSB(51),ANST(51)
      DIMENSION IK(5)
      COMMON THK(51),TRAN(41),TRAN1(40),BACK(40),BACK1(40),F,B,K,T,T1,
     1TRAY(51,40),BRAY(51,40),KMAX,TKPLT(10),NCURV
      K1=-4
      DO 330 I=1,KMAX
      ANSB(I)=(B*THK(I))/(1.+B*THK(I))
      ANST(I)=1.-ANSB(I)-EXP(-THK(I))
      SUM(I)=0.0
      DO 331 NK=1,40
      IF(NT.EQ.1) SUM(I)=SUM(I)+TRAY(I,NK)
      IF(NT.EQ.2) SUM(I)=SUM(I)+BRAY(I,NK)
  331 CONTINUE
  330 CONTINUE
  315 K1=K1+5
      K2=K1+4
      IF(K2.GT.40)GO TO 320
      DO 310 I=1,KMAX
      IK(1)=K1
      DO 360 L=2,5
      IK(L)=IK(L-1)+1
  360 CONTINUE
      IF(I.EQ.1) PRINT 361,(IK(L),L=1,5)
  361 FORMAT(7X,*T*,6X,*N=*,4X,I8,4I16)
      IF(NT.EQ.1) PRINT 321,THK(I),(TRAY(I,NK),NK=K1,K2)
      IF(NT.EQ.2) PRINT 321,THK(I),(BRAY(I,NK),NK=K1,K2)
  321 FORMAT(1X,E12.5,5X,5E16.9)
  310 CONTINUE
      GO TO 315
  320 PRINT 322
      IF(NT.EQ.1)PRINT 362
      IF(NT.EQ.2)PRINT 363
  362 FORMAT(1X,*TRANSMISSION SUM CHECK*)
  363 FORMAT(1X,*BACKSCATTER SUM CHECK*)
      PRINT 364
  364 FORMAT(7X,*T*,14X,*SUMMATION*,4X,*ANALYTIC RESULT*)
      DO 323 I=1,KMAX
      IF(NT.EQ.1) PRINT 324,THK(I),SUM(I),ANST(I)
      IF(NT.EQ.2) PRINT 324,THK(I),SUM(I),ANSB(I)
  323 CONTINUE
  322 FORMAT(*1*)
  324 FORMAT(1X,E12.5,5X,2E16.9)
      RETURN
      END
```

```
      SUBROUTINE GETFN
      COMMON THK(51),TRAN(41),TRAN1(40),BACK(40),BACK1(40),F,B,K,T,T1,
     1TRAY(51,40),BRAY(51,40),KMAX,TKPLT(10),NCURV
      DIMENSION S1(40),S2(40),S3(40),TRINT(40),TRSLP(40),BKINT(40),
     1BKSLP(40)
      IF(K.GT.1) GO TO 11
      DO 80 N=1,40
      TRAN(N)=BACK(N)=0.
   80 CONTINUE
    1 A1=F*B/2.
      A2=A1*B
      A3=A1*F
      A4=0.5*B**2
      A5=B*A4
      A6=0.5*F**2
      A7=F*A6/3.
      RETURN
   11 CONTINUE
      ET=EXP(-T)
      ET2=ET**2
      DT=T-T1
      TRAN(1)=ET*F*T
      BACK(1)=0.5*B*(1.-ET2)
      TRAN(2)=ET*(A6*T**2+A4*T-0.5*A4*(1.-ET2))
      BACK(2)=A1*(1.-ET2*(1.+2.*T))
      TRAN(3)=ET*(A7*T**3+A2*(T**2+0.5*T-1.)+A2*ET2*(1.+1.5*T))
      BACK(3)=A3*(1.-(2.*T**2+2.*T+1.)*ET2)-A5*T*ET2+0.25*A5*(1.-ET2**2)
      DO 49 N=1,3
      TRSLP(N)=(TRAN(N)-TRAN1(N))/DT
      BKSLP(N)=(BACK(N)-BACK1(N))/DT
      TRINT(N)=TRAN(N)-T*TRSLP(N)
      BKINT(N)=BACK(N)-T*BKSLP(N)
   49 CONTINUE
      IF(K.EQ.2) GO TO 50
      ET1=EXP(T1)
      F2=F1
      F4=F3
   50 ET=EXP(T)
      F1=ET*(T**2-2.*T+2.)
      F3=ET*(T-1.)
      F5=ET-1.
      DO 53 N=4,40
      MTOP=N-2
      IF(K.GT.2) GO TO 54
      S2(N)=0.0
      S3(N)=0.0
      TERM1=0.0
      TERM=0.0
      DO 51 M=1,MTOP
      NM=N-M-1
      TERM=TERM+(F1-2.)*TRSLP(NM)*BKSLP(M)+(F3+1.)*(TRINT(NM)*BKSLP(M)+
     1BKINT(M)*TRSLP(NM))+F5*TRINT(NM)*BKINT(M)
      TERM1=TERM1+TRSLP(NM)*TRSLP(M)*(T**3)/3. +
     1      (TRINT(NM)*TRSLP(M)+TRSLP(NM)*TRINT(M))*0.5*T**2   +
     2       TRINT(NM)*TRINT(M)*T
   51 CONTINUE
      S2(N)=S2(N)+TERM+0.5*BKSLP(N-1)*T**2+BKINT(N-1)*T
```

```
      S1(N)=(TRINT(N-1)-TRSLP(N-1)+TRSLP(N-1)*T)*ET-TRINT(N-1)+TRSLP(N-1
     1)
      S3(N)=S3(N)+TERM1+2.*(TRSLP(N-1)+TRINT(N-1)) -
     1           2.*(TRSLP(N-1)*(1.+T)+TRINT(N-1))/ET
      TRAN(N)=(F*S1(N)+B*S2(N))/ET
      BACK(N)=B*S3(N)
      GO TO 55
   54 S1(N)=S1(N)+(TRINT(N-1)-TRSLP(N-1)+T*TRSLP(N-1))*ET
     1           -(TRINT(N-1)-TRSLP(N-1)+T1*TRSLP(N-1))*ET1
      TERM1=0.0
      T33=(T**3-T1**3)/3.
      T22=(T**2-T1**2)/2.
      TERM=0.0
      DO 52 M=1,MTOP
      NM=N-M-1
      TERM=TERM+TRSLP(NM)*BKSLP(M)*(F1-F2)+(TRINT(NM)*BKSLP(M)+
     1BKINT(M)*TRSLP(NM))*(F3-F4)+TRINT(NM)*BKINT(M)*(ET-ET1)
      TERM1=TERM1+TRSLP(NM)*TRSLP(M)*T33+TRINT(NM)*TRINT(M)*DT +
     1      (TRINT(NM)*TRSLP(M)+TRSLP(NM)*TRINT(M))*T22
   52 CONTINUE
      S2(N)=S2(N)+TERM+BKSLP(N-1)*T22+BKINT(N-1)*DT
      S3(N)=S3(N)+TERM1+2.*(TRSLP(N-1)*(1.+T1)+TRINT(N-1))/ET1 -
     1              2.* (TRSLP(N-1)*(1.+T )+TRINT(N-1))/ET
      TRAN(N)=(F*S1(N)+B*S2(N))/ET
      BACK(N)=B*S3(N)
   55 TRSLP(N)=(TRAN(N)-TRAN1(N))/DT
      BKSLP(N)=(BACK(N)-BACK1(N))/DT
      TRINT(N)=TRAN(N)-T*TRSLP(N)
      BKINT(N)=BACK(N)-T*BKSLP(N)
   53 CONTINUE
      RETURN
      END
```

A2. Orders-of-Scattering Invariant Imbedding Code for the Slab Geometry

PRECEDING PAGE BLANK-NOT FILMED

```
      PROGRAM OOSII(INPUT,OUTPUT,TAPE5,TAPE3)
      COMMON THK(51),TRAN(6,6,10),TRAN1(6,6,10),BACK(6,6,10),BACK1(6,6,
     110),F(6,6),PATHO,PATH(10),TRAY(51,10),BRAY(51,10),COEFF(6),
     2ORDNAT(6),K,T,T1,KMAX,MAXORD,NSCATS,TRY(51,10,6),BRY(51,10,6),
     3TROY(51,10,6),BROY(51,10,6),FF(6,6),ADDUP(51)
      DIMENSION IDT(51),ACOF(6,3),ORD(6,3)
      DIMENSION FA(6,6),FB(6,6)
      DATA TWOPI/6.283185307/
      DATA IDT/1,50*4/
      DATA ACOF/0.347854845137,0.652145154863,4*0.,0.101228536290,
     1     0.222381034453,0.313706645878,0.362683783378,2*0.,
     20.047175336387,0.106939325995,0.160078328543,0.203167426723,
     30.233492536538,0.249147045813/
      DATA ORD/0.861136311594,0.339981043585,4*0.,0.960289856498,
     1     0.796666477414,0.525532409916,0.183434642496,2*0.,
     20.981560634247,0.904117256370,0.769902674194,0.587317954287,
     30.367831498998,0.125233408511/
  500 READ 9,THICK,KMAX,MAXORD,NSCATS,KPRNT,IDBG,NVER
C     THICK - MAXIMUM SLAB THICKNESS
C     KMAX - NO. OF SLAB THICKNESSES FOR WHICH CURRENTS ARE COMPUTED
C     MAXORD - NO. OF GAUSS QUADRATURE POINTS TO BE USED
C     NSCATS - MAXIMUM NUMBER OF SCATTERINGS TO BE CONSIDERED
C     KPRNT - CONTROL PARAMETER FOR PRINTING OUT DIRECTIONAL CURRENTS
C              IF EQUAL TO ZERO, PRINTOUT SUPPRESSED
C              IF NOT EQUAL TO ZERO, PRINTOUT ACTIVATED
C     IDBG - CONTROL PARAMETER FOR PRINTING OUT DEBUGGING INFORMATION
C              IF EQUAL TO ZERO, PRINTOUT SUPPRESSED
C              IF NOT EQUAL TO ZERO, PRINTOUT ACTIVATED
C     NVER - CONTROL PARAMETER FOR TYPE OF SCATTERING TO BE CONSIDERED
C            = 1, ISOTROPIC SCATTERING
C            = 2, COSINE LAW SCATTERING
C            = 3, SCREENED RUTHERFORD SCATTERING
C     ETA - RUTHERFORD SCREENING PARAMETER, HAS MEANING ONLY WHEN
C           NVER=3
C     (A BLANK CARD FOR THE ABOVE TERMINATES THE RUN, OTHERWISE THE
C     RUN MAY BE RECYCLED USING VALID PARAMETERS)
      IF(THICK.EQ.0.0) GO TO 501
      REWIND 5
   99 FORMAT(E16.9)
      READ 99,ETA
      IF(NVER.EQ.3)PRINT 991,ETA
  991 FORMAT(1X,*SCREENED RUTHERFORD - - - ETA = *, E16.9)
    9 FORMAT(F10.0,6I10)
      PATHO=1.0
      DO 897 II=1,10
      PATH(II)=PATHO
  897 CONTINUE
      IF(MAXORD-4)31,32,33
   31 DO 34 I=1,MAXORD
      ORDNAT(I)=ORD(I,1)
      COEFF(I)=ACOF(I,1)
   34 CONTINUE
      GO TO 37
   32 DO 35 I=1,MAXORD
      ORDNAT(I)=ORD(I,2)
      COEFF(I)=ACOF(I,2)
   35 CONTINUE
```

```
      GO TO 37
   33 DO 36 I=1,MAXORD
      ORDNAT(I)=ORD(I,3)
      COEFF(I)=ACOF(I,3)
   36 CONTINUE
   37 CONTINUE
      IF(NVER.EQ.1) CALL GF1(MAXORD,ORD,FA,FB)
      IF(NVER.EQ.2) CALL GF2(MAXORD,ORD,FA,FB)
      IF(NVER.EQ.3) CALL GF3(MAXORD,ORD,FA,FB,ETA)
      DO 777 I=1,MAXORD
      DO 777 J=1,MAXORD
      FF(I,J)=FA(I,J)
      F(I,J)=FB(I,J)
  777 CONTINUE
   10 CONTINUE
      DT=THICK/FLOAT(KMAX-1)
      THK(1)=0.0
      DO 13 KT=2,KMAX
      THK(KT)=THK(KT-1)+DT
   13 CONTINUE
      WRITE(5) THICK,KMAX,MAXORD,NSCATS
      WRITE(5) (ORDNAT(I),COEFF(I),I=1,MAXORD)
      WRITE(5) (THK(I),I=1,KMAX)
   74 CONTINUE
      T=0.0
      K=1
      KT=1
      KTOT=IOT(K )
   50 CALL INTGRL
      DO 49 N=1,NSCATS
      DO 49 IK=1,MAXORD
      DO 49 IP=1,MAXORD
      TRAN1(IK,IP,N)=TRAN(IK,IP,N)
      BACK1(IK,IP,N)=BACK(IK,IP,N)
   49 CONTINUE
      IF(K.EQ.KTOT) GO TO 45
      GO TO 48
   45 IF(IOBG.EQ.0) GO TO 398
      DO 47 N=1,NSCATS
      TRAY(KT,N)=0.0
      BRAY(KT,N)=0.0
      DO 46 IP=1,MAXORD
      TRY(KT,N,IP)=0.0
      BRY(KT,N,IP)=0.0
      DO 44 IK=1,MAXORD
      TRY(KT,N,IP)=TRY(KT,N,IP)+TRAN(IK,IP,N)*COEFF(IK)
      BRY(KT,N,IP)=BRY(KT,N,IP)+BACK(IK,IP,N)*COEFF(IK)
      TROY(KT,N,IK)=0.0
      BROY(KT,N,IK)=0.0
   44 CONTINUE
      TRAY(KT,N)=TRAY(KT,N)+TRY(KT,N,IP)*COEFF(IP)
      BRAY(KT,N)=BRAY(KT,N)+BRY(KT,N,IP)*COEFF(IP)
      DO 43 IK=1,MAXORD
      TROY(KT,N,IK)=TROY(KT,N,IK)+TRAN(IK,IP,N)*COEFF(IP)
      BROY(KT,N,IK)=BROY(KT,N,IK)+BACK(IK,IP,N)*COEFF(IP)
   43 CONTINUE
   46 CONTINUE
```

```
 47 CONTINUE
398 WRITE(5) KT
    DO 75 N=1,NSCATS
    WRITE(5)((TRAN(IK,IP,N),IK=1,MAXORD),IP=1,MAXORD)
    WRITE(5)((BACK(IK,IP,N),IK=1,MAXORD),IP=1,MAXORD)
 75 CONTINUE
    IF(KPRNT.EQ.0.AND.IDBG.EQ.0) GO TO 400
    PRINT 299
    PRINT 600,THK(KT)
600 FORMAT(1X,*THICKNESS =*,E12.5)
    DO 601 IP=1,MAXORD
    PRINT 602,IP,ORDNAT(IP)
602 FORMAT(//1X,*INCIDENT DISCRETE ORDINATE NUMBER*,I2,5X,*COSINE OF I
   1NCIDENT ANGLE =*,E16.9/)
    DO 603 N=1,NSCATS
    PRINT 604,N
604 FORMAT(/1X,*ORDER OF SCATTERING =*,I5/1X,*EXIT ORDINATE NO. =*,8H
   1       1,15X,*2*,15X,*3*,15X,*4*,15X,*5*,15X,*6*)
605 FORMAT(1X,*EXIT COSINE =*,7X,6E16.9)
    PRINT 605,(ORDNAT(IK),IK=1,MAXORD)
    PRINT 606,(TRAN(IK,IP,N),IK=1,MAXORD)
    PRINT 607,(BACK(IK,IP,N),IK=1,MAXORD)
606 FORMAT(1X,*TRANSMISSION =*,6X,6E16.9)
607 FORMAT(1X,*BACKSCATTER =*,7X,6E16.9)
603 CONTINUE
601 CONTINUE
400 KT=KT+1
    IF(KT.GT.KMAX) GO TO 52
    KTOT=KTOT+IDT(KT)
    DTM=(THK(KT)-THK(KT-1))/FLOAT(IDT(KT))
 48 T1=T
 51 T=T1+DTM
    K=K+1
    IF(T.LE.THICK) GO TO 50
 52 CONTINUE
    IF(IDBG.EQ.0) GO TO 399
    PRINT 299
299 FORMAT(*1*)
    PRINT 300,MAXORD
    NT=1
    CALL PRNTR(NT)
    PRINT 299
    PRINT 301,MAXORD
    NT=2
    CALL PRNTP(NT)
300 FORMAT(1X,*TRANSMISSION - -  3 DIMENSIONAL CALCULATION WITH*,I3,*
   1DISCRETE ORDINATES*)
301 FORMAT(1X,* BACKSCATTER - -  3 DIMENSIONAL CALCULATION WITH*,I3,*
   1DISCRETE ORDINATES*)
    PRINT 299
    DO 450 IP=1,MAXORD
    DO 440 KK=1,KMAX
    DO 440 NK=1,NSCATS
    TRAY(KK,NK)=TRY(KK,NK,IP)
    BRAY(KK,NK)=BRY(KK,NK,IP)
440 CONTINUE
    PRINT 430,ORDNAT(IP)
```

```
430 FORMAT(/////////1X,*TOTAL TRANSMISSION DUE TO SOURCE WITH INCIDENT
   1COSINE = *,E16.9)
    NT=1
    CALL PRNTR(NT)
    PRINT 431,ORDNAT(IP)
431 FORMAT(/////////1X,*TOTAL BACKSCATTER DUE TO SOURCE WITH INCIDENT C
   1OSINE = *,E16.9)
    NT=2
    CALL PRNTR(NT)
450 CONTINUE
    PRINT 299
    DO 451 IK=1,MAXORD
    DO 441 KK=1,KMAX
    DO 441 NK=1,NSCATS
    TRAY(KK,NK)=TROY(KK,NK,IK)
    BRAY(KK,NK)=BROY(KK,NK,IK)
441 CONTINUE
    PRINT 432,ORDNAT(IK)
432 FORMAT(/////////1X,*TOTAL TRANSMISSION WITH EXIT COSINE =*,E16.9)
    NT=1
    CALL PRNTR(NT)
    PRINT 433,ORDNAT(IK)
433 FORMAT(/////////1X,*TOTAL BACKSCATTER WITH EXIT COSINE =-*,E16.9)
    NT=2
    CALL PRNTR(NT)
451 CONTINUE
399 CALL OSTBN
    GO TO 500
501 CONTINUE
    STOP
    END
```

```
    SUBROUTINE GF1(MAXORD,ORD,FA,FB)
    DIMENSION FA(6,6),FB(6,6) ,CRO(6,3)
    DO 100 I=1,MAXORD
    DO 100 J=1,MAXORD
    FA(I,J)=FB(I,J)=0.5
100 CONTINUE
    RETURN
    END
```

```
      SUBROUTINE GF2(MAXORD,ORD,FA,FB)
      DIMENSION F(12,12),ORD(6,3),ORDNAT(12),MX(3),SRD(12)
      DIMENSION FA(6,6),FB(6,6)
      DATA PI/3.141592653/
      IM=MAXORD/2
      MQ=2*MAXORD
      DO 101 I=1,MAXORD
      ORDNAT(I)=ORD(I,IM)
      J=I-1
      ORDNAT(MQ-J)=-ORDNAT(I)
  101 CONTINUE
      DO 103 I=1,MQ
      SRD(I)=SQRT(1.-ORDNAT(I)**2)
  103 CONTINUE
      DO 102 I=1,MQ
      ARC1=ACOS(ORDNAT(I))
      DO 102 J=I,MQ
      F(I,J)=0.0
      ARC=ACOS(ORDNAT(J))-ARC1
      IF(ABS(ARC).GE.0.5*PI) GO TO 104
      F(I,J)=1./PI
      TF=ORDNAT(I)*ORDNAT(J)/(SRD(I)*SRD(J))
      IF(ABS(TF).LT.1.0) GO TO 114
      F(I,J)=ORDNAT(I)*ORDNAT(J)
      GO TO 104
  114 CONTINUE
      PHI=ACOS(-TF)
      SP=SIN(PHI)
      CP=COS(0.5*PHI)
      F(I,J)=F(I,J)*(SRD(I)*SRD(J)*SP+PHI*ORDNAT(I)*ORDNAT(J))
  104 F(J,I)=F(I,J)
  102 CONTINUE
  106 FORMAT(////////)
  105 FORMAT(1X,6E16.9)
      DO 100 I=1,MAXORD
      DO 100 J=1,MAXORD
      JM=MQ-(J-1)
      FA(I,J)=2.*F(I,J)
      FB(I,J)=2.*F(I,JM)
  100 CONTINUE
      PRINT 107
  107 FORMAT(/1X,*SCATTERING MATRIX - - FIRST QUADRANT TO FIRST QUADRANT
     1*/)
      PRINT 105,((FA(I,J),I=1,MAXORD),J=1,MAXORD)
      PRINT 106
      PRINT 108
  108 FORMAT(/1X,*SCATTERING MATRIX - -FIRST QUADRANT TO SECOND QUADRANT
     1*/)
      PRINT 105,((FB(I,J),I=1,MAXORD),J=1,MAXORD)
      RETURN
      END
```

```
      SUBROUTINE GF3(MAXORD,ORD,FA,FB,ETA)
      DIMENSION F(12,12),ORD(6,3),ORDNAT(12),MX(3),SRD(12)
      DIMENSION FA(6,6),FB(6,6)
      DATA PI/3.141592653/
      IM=MAXORD/2
      MQ=2*MAXORD
      DO 101 I=1,MAXORO
      ORDNAT(I)=ORO(I,IM)
      J=I-1
      ORDNAT(MQ-J)=-ORDNAT(I)
  101 CONTINUE
      AK=ETA*(1.+0.5*ETA)
      DO 102 I=1,MQ
      DO 102 J=I,MQ
      TF=ORDNAT(I)*ORDNAT(J)
      BF=(ORDNAT(I)-ORONAT(J))**2
      F(I,J)=(AK*(1.+ETA-TF))/((ETA**2+2.*ETA*(1.-TF)+BF)**1.5)
  104 F(J,I)=F(I,J)
  102 CONTINUE
  106 FORMAT(////////)
  105 FORMAT(1X,6E16.9)
      DO 100 I=1,MAXORO
      DD 100 J=1,MAXORO
      JM=MQ-(J-1)
      FA(I,J)=F(I,J)
      FB(I,J)=F(I,JM)
  100 CONTINUE
      PRINT 107
  107 FORMAT(/1X,*SCATTERING MATRIX - - FIRST QUADRANT TO FIRST QUADRANT
     1*/)
      PRINT 105,((FA(I,J),I=1,MAXORO),J=1,MAXORD)
      PRINT 106
      PRINT 108
  108 FORMAT(/1X,*SCATTERING MATRIX - -FIRST QUADRANT TO SECCNO QUADRANT
     1*/)
      PRINT 105,((FB(I,J),I=1,MAXORD),J=1,MAXCRD)
      RETURN
      ENO
```

```
      SUBROUTINE DSTBN
      COMMON THK(51),TRAN(6,6,10),TRAN1(6,6,10),BACK(6,6,10),BACK1(6,6,
     110),F(6,6),PATHO,PATH(10),TRAY(51,10),BRAY(51,10),COEFF(6),
     2ORDNAT(6),K,T,T1,KMAX,MAXORD,NSCATS,TRY(51,10,6),BRY(51,10,6),
     3TROY(51,10,6),BROY(51,10,6),FF(6,6),ADDUP(51)
      DIMENSION WT(6,4),TITLE(5,4)
      DATA TITLE/10HCOSINE SOU,10HRCE      ,10H          ,10H
     1,10H          ,10HISOTROPIC ,10HSOURCE    ,10H          ,10H
     2    ,10H          /
      DATA JSOURCE,NSOURCE/0,2/
      DATA TWOPI/6.283185307/
      JSOURCE=0
      NSCURCE=2
    1 REWIND 5
      JSCURCE=JSOURCE+1
    5 REAC(5) THICK,KMAX,MAXORD,NSCATS
      IF(EOF(5))6,4
    4 READ(5) (ORDNAT(I),COEFF(I),I=1,MAXORD)
      READ(5) (THK(I),I=1,KMAX)
      DO 2 K=1,KMAX
      ADDUP(K)=0.0
      READ(5) KT
      DO 10 N=1,NSCATS
      READ(5) ((TRAN(I,J,N),I=1,MAXORD),J=1,MAXORD)
      READ(5) ((BACK(I,J,N),I=1,MAXORD),J=1,MAXORD)
   10 CONTINUE
C
C
C     SOURCE WEIGHT FUNCTION LOOP
      DO 7 J=1,MAXORD
      IF(JSOURCE.EQ.1)WT(J,JSOURCE)=2.*ORDNAT(J)
      IF(JSOURCE.EQ.2) WT(J,JSOURCE)=1.0
    7 CONTINUE
C
C
      DO 15 N=1,NSCATS
      TRAY(KT,N)=0.0
      BRAY(KT,N)=0.0
      DO 16 J=1,MAXORD
      TRY(KT,N,J)=0.0
      BRY(KT,N,J)=0.0
      DO 17 I=1,MAXORD
      TRY(KT,N,J)=TRY(KT,N,J)+TRAN(I,J,N)*COEFF(I)
      BRY(KT,N,J)=BRY(KT,N,J)+BACK(I,J,N)*COEFF(I)
   17 CONTINUE
      TRAY(KT,N)=TRAY(KT,N)+TRY(KT,N,J)*COEFF(J)*WT(J,JSOURCE)
      BRAY(KT,N)=BRAY(KT,N)+BRY(KT,N,J)*COEFF(J)*WT(J,JSOURCE)
   16 CONTINUE
      ADDUP(KT)=ADDUP(KT)+TRAY(KT,N)+BRAY(KT,N)
   15 CONTINUE
      IF(JSOURCE.EQ.1) ADD=E3(THK(KT))*2.
      IF(JSOURCE.EQ.2) ADD=E2(THK(KT))
      ADDUP(KT)=ADDUP(KT)+ADD
    2 CONTINUE
      WRITE(3)KMAX,MAXORD,NSCATS,JSOURCE
      WRITE(3)(THK(KK),KK=1,KMAX)
      WRITE(3)((TRAY(KK,N),KK=1,KMAX),N=1,NSCATS)
```

```
      WRITE(3)((BRAY(KK,N),KK=1,KMAX),N=1,NSCATS)
      PRINT 20,(TITLE(L,JSOURCE),L=1,5)
   20 FORMAT(*1*,1X,5A10)
  299 FORMAT(*1*)
      PRINT 300,MAXORD
      NT=1
      CALL PRNTR(NT)
      PRINT 299
      PRINT 301,MAXORD
      NT=2
      CALL PRNTR(NT)
  300 FORMAT(1X,*TRANSMISSION - -  3 DIMENSIONAL CALCULATION WITH*,I3,*
     1DISCRETE ORDINATES*)
  301 FORMAT(1X,* BACKSCATTER - -  3 DIMENSIONAL CALCULATION WITH*,I3,*
     1DISCRETE ORDINATES*)
      GO TO 5
    6 IF(JSOURCE.LT.NSOURCE) GO TO 1
      RETURN
      END



      FUNCTION E2(Z)
      CALL EXPI(Z,RES)
      E2   =EXP(-Z)-Z*RES
      RETURN
      END



      FUNCTION E3(Z)
      A=E2(Z)
      E3=0.5*(EXP(-Z)-Z*A)
      RETURN
      END
```

```
      SUBROUTINE EXPI(X,RES)
      IF(X-1.)2,1,1
    1 Y=1./X
      AUX=1.-Y*(((Y+3.377358E0)*Y+2.052156E0)*Y+2.709479E-1)/((((Y*      -F
     11.072553E0+5.716943E0)*Y+6.945239E0)*Y+2.593888E0)*Y+2.709496E-1)  -F
      RES=AUX*Y*EXP(-X)
      RETURN
    2 IF(X+3.)6,6,3
    3 AUX=(((((((7.122452E-7*X-1.766345E-6)*X+2.928433E-5)*X-2.335379E-4 -F
     1)*X+1.664156E-3)*X-1.041576E-2)*X+5.555682E-2)*X-2.500001E-1)*X     -F
     2+9.999999E-1
      RES=-1.E75
      IF(X)4,5,4
    4 RES=X*AUX-ALOG(ABS(X))-5.772157E-1
    5 RETURN
    6 IF(X+9.)8,8,7
    7 AUX=1.-((((5.176245E-2*X+3.061037E0)*X+3.243665E1)*X+2.244234E2)*X -F
     1+2.486697E2)/((((X+3.995161E0)*X+3.893944E1)*X+2.263818E1)*X       -F
     2+1.807837E2)
      GOTO 9
    8 Y=9./X
      AUX=1.-Y*(((Y+7.659824E-1)*Y-7.271015E-1)*Y-1.080693E0)/((((Y      -F
     1*2.518750E0+1.122927E1)*Y+5.921405E0)*Y-8.666702E0)*Y-9.724216E0)  -F
    9 RES=AUX*EXP(-X)/X
      RETURN
      END
```

```
      SUBROUTINE INTGRL
      COMMON THK(51),TRAN(6,6,10),TRAN1(6,6,10),BACK(6,6,10),BACK1(6,6,
     110),F(6,6),PATHO,PATH(10),TRAY(51,10),BRAY(51,10),COEFF(6),
     2ORDNAT(6),K,T,T1,KMAX,MAXORD,NSCATS,TRY(51,10,6),BRY(51,10,6),
     3TROY(51,10,6),BROY(51,10,6),FF(6,6),ADDUP(51)
      DIMENSION TRSLP(6,6,10),TRINT(6,6,10),BKSLP(6,6,10),BKINT(6,6,10),
     1TR1(10),TR2(10),TR4(10),TR5(10),BK1(10),BK2(10),SUM(6,6,10)
      DATA TWOPI/6.283185307/
      IF(K.GT.1) GO TO 11
      DO 10 N=1,NSCATS
      DC 10 IK=1,MAXORD
      DO 10 IP=1,MAXORD
      TRAN(IK,IP,N)=BACK(IK,IP,N)=0.0
   10 CONTINUE
      RETURN
   11 DT =T-T1
      T2=T**2
      T21=T1**2
      DT2=(T2-T21)/2.
      OT3=(T**3-T1**3)/3.
      DO 131 IK=1,MAXORO
      ET2=EXP(-T/(PATH(1)*ORDNAT(IK)))
      OO 131 IP=1,MAXORD
      IF(IP.NE.IK.OR.PATHO.NE.PATH(1)) GO TO 132
      TRAN(IK,IP,1)=    T*FF  (IK,IP)*ET2/(PATHO*ORDNAT(IK))
      GO TO 130
  132 ET1=EXP(-T/(PATHO*ORONAT(IP)))
      TRAN(IK,IP,1)=    PATHO*ORONAT(IK)*(ET1-ET2)*FF (IP,IK)/(PATHO*
     1ORDNAT(IP)-PATH(1)*ORDNAT(IK))
  130 CONTINUE
      BACK(IK,IP,1)=    PATHO*F   (IP,IK)*ORDNAT(IK)/
     1          (PATH(1)*(ORDNAT(IK)+ORDNAT(IP)))*
     2          (1.-EXP(-T/PATHO*(1./ORDNAT(IP)+1./ORDNAT(IK))))
      TRSLP(IK,IP,1)=(TRAN(IK,IP,1)-TRAN1(IK,IP,1))/DT
      TRINT(IK,IP,1)=TRAN(IK,IP,1)-T*TRSLP(IK,IP,1)
      BKSLP(IK,IP,1)=(BACK(IK,IP,1)-BACK1(IK,IP,1))/DT
      BKINT(IK,IP,1)=BACK(IK,IP,1)-T*BKSLP(IK,IP,1)
  131 CONTINUE
C
      DO 500 N=2,NSCATS
C
      MTCF=N-2
C
      OO 501 L=1,MAXORD
      PC=PATH(N)*ORONAT(L)
      P2=PATHO*  ORDNAT(L)
      PO2=PO**2
      PO3=2.*PO**3
      P22=P2**2
      ETB=EXP(-T/P2)
      ETB1=EXP(-T1/P2)
      ET=EXP(T/PO)
      ET1=EXP(T1/PO)
      ETM=ET-ET1
      ETMB=ETB1-ETB
      TERM1=(PO*T2-2.*PO2*T+PO3)*ET-(PO*T21-2.*PO2*T1+PO3)*ET1
      TERM2=(PO*T-PO2)*ET-(PO*T1-PO2)*ET1
```

```
      TERM3=PO*ETM
      TERM4=((P2*T1+P22)*ETB1-(P2*T+P22)*ETB)
      TERM5=P2*ETMB
C
C
      DC 501 J=1,MAXORO
      IF(K.EQ.2)SUM(L,J,N)=BACK(L,J,N)=0.0
      P3=PATHO*ORONAT(J)
      P33=P3**2
      ETC=EXP(-T/P3)
      ETC1=EXP(-T1/P3)
      ETMC=ETC1-ETC
      TERM6=((P3*T1+P33)*ETC1-(P3*T+P33)*ETC)
      TERM7=P3*ETMC
      TERM8=DT2
      TERM9=DT
      IF(L.EQ.J) GO TO 499
      P4=FO*ORONAT(J)*PATHO/(PATHO*ORDNAT(J)-PO)
      ETT=EXP(T/P4)
      ETT1=EXP(T1/P4)
      P44=P4**2
      ETTM=ETT-ETT1
      TERM8=((P4*T-P44)*ETT-(P4*T1-P44)*ETT1)
      TERM9=P4*ETTM
C
  499 DO 502 I=1,MAXORO
      TRS=TRSLP(I,J,N-1)
      TRI=TRINT(I,J,N-1)
C
      SUM(L,J,N)=SUM(L,J,N)+
C
C     TYPE1
C
     1(COEFF(I)*FF(I,L)/ORONAT(I)*(TRS*TERM2+TRI*TERM3)/PATH(N-1) +
C
C     TYPE3
C
     2COEFF(I)*F(J,I)/(ORDNAT(J)*PATHO) *
     3              (BKSLP(L,I,N-1)*TERM8+BKINT(L,I,N-1)*TERM9))
C
C
      BACK(I,J,N)=BACK(L,J,N)+
C
C     TYPE 4
C
     1(COEFF(I)*F(I,L)/(ORONAT(I)*PATH(N-1))*(TRS*TERM4+TRI*TERM5) +
C
C     TYPE 6
C
     2COEFF(I)*F(J,I)/(ORDNAT(J)*PATHO) *
     3     (TRSLP(L,I,N-1)*TERM6+TRINT(L,I,N-1)*TERM7))
C
      IF(N.EQ.2) GO TO 502
C
      DO 512 M=1,MTOP
      TR4(M)=TRSLP(I,J,M)
      TR5(M)=TRINT(I,J,M)
```

```
  512 CONTINUE
C
      DO 503 IP=1,MAXORD
C
      DO 513 M=1,MTOP
      BK1(M)=BKSLP(L,IP,M)
      BK2(M)=BKINT(L,IP,M)
      TR1(M)=TRSLP(L,IP,M)
      TR2(M)=TRINT(L,IP,M)
  513 CONTINUE
C
      COF=COEFF(IP)*COEFF(I)*F(I,IP)/ORDNAT(I)/PATH(M)
C
C
      DO 504 M=  ,MTOP
      NM=N-M-1
      T14=TR4(NM)
      T15=TR5(NM)
      T11=TR1(M)
      B11=BK1(M)
      ˋ12=BK2(M)
      1ˎ2=TR2(M)
C
      SUM(L,J,N)=SUM(L,J,N)+COF*
C
C     TYPE 2
C
     1     (T14*B11*TERM1+(T15*B11+B12*T14)*TERM2+T15*B12*TERM3)
C
      BACK(L,J,N)=BACK(L,J,N)+COF *
C
C     TYPE 5
C
     1    (T11*T14*DT3+(T12*T14+T15*T11)*DT2+T12*T15*DT)
  504 CONTINUE
  503 CONTINUE
  502 CONTINUE
      TRAN(L,J,N)=SUM(L,J,N)/ET
  501 CONTINUE
      DO 602 I=1,MAXORD
      DO 602 J=1,MAXORD
      TRSLP(I,J,N)=(TRAN(I,J,N)-TRAN1(I,J,N))/DT
      BKSLP(I,J,N)=(BACK(I,J,N)-BACK1(I,J,N))/DT
      TRINT(I,J,N)=TRAN(I,J,N)-T*TRSLP(I.J,N)
      BKINT(I,J,N)=BACK(I,J,N)-T*BKSLP(I,J,N)
  602 CONTINUE
  500 CONTINUE
      RETURN
      END
```

```
      SUBROUTINE PRNTR(NT)
      DIMENSION IK(5)
      COMMON THK(51),TRAN(6,6,10),TRAN1(6,6,10),BACK(6,6,10),BACK1(6,6,
     110),F(6,6),PATHO,PATH(10),TRAY(51,10),BRAY(51,10),COEFF(6),
     2ORDNAT(6),K,T,T1,KMAX,MAXORD,NSCATS,TRY(51,10,6),BRY(51,10,6),
     3TROY(51,10,6),BROY(51,10,6),FF(6,6),ADDUP(51)
      K1=-4
      K2=0
  315 K1=K1+5
      K2P=K2
      K2=K1+4
      IF(K2P.LT.NSCATS.AND.K2.GT.NSCATS) K2=NSCATS
      IF(K2P.GE.NSCATS) GO TO 316
      DO 310 I=1,KMAX
      IK(1)=K1
      DO 360 L=2,5
      IK(L)=IK(L-1)+1
  360 CONTINUE
      IF(I.EQ.1) PRINT 361,(IK(L),L=1,5)
  361 FORMAT(7X,*T*,6X,*N=*,4X,I8,4I16)
      IF(NT.EQ.1) PRINT 321,THK(I),(TRAY(I,NK),NK=K1,K2)
      IF(NT.EQ.2) PRINT 321,THK(I),(BRAY(I,NK),NK=K1,K2)
  321 FORMAT(1X,E12.5,5X,5E16.9)
  310 CONTINUE
      GO TO 315
  316 IF(NT.EQ.1) RETURN
      PRINT 317
  317 FORMAT(*1*,6X,*T*,16X,*TOTALS*)
      DO 318 I=1,KMAX
      PRINT 319,ADDUP(I)
  318 CONTINUE
  319 FORMAT(1X,E12.5,5X,E16.9)
      RETURN
      END
```

A3. Boltzmann Equation Code for Isctropic Scattering in the Slab Geometry

```
      PRCGRAM FROHLM(INPUT,CUTPUT,TAPE1,TAPE4,TAPE5)
      DIMENSION DT(5),NMAX(5),THKNSS(5)
      OIMENSION ITER(5),E22(101)
      DIMENSION PHP(110)
      COMMON THICK,DELTA,X,CONST1,CONST2,GAMMA,CORINT,IX,MAX,MTH,U1(16),
     1U2(32),PHINP1(110),PHINP2(110),XX(110),P0(110),P1(110),P2(110),
     2P3(110),Q0(110),Q1(110),Q2(110),Q3(110),F1(16),F2(32),G1(16),
     3G2(32),GRAND2(16),XPY1(16),XPY2(32),XMY1(16),XMY2(32),GX1(16),
     4GRAND1(16)
      COMMON/GAUSQ/W1(16),W2(16),AW1(16),AW2(32)
      COMMON/FLX/ETRAN(101),EBACK(101),TFAC(101),BFAC(101)
      GAMMA=0.5772156649
      CALL GCOEFF
      MTH=2
      READ 11,NTHK,(THKNSS(I),I=1,NTHK)
C     NTHK - NO. OF SLAB THICKNESSES TO BE CONSIDERED
C     THKNSS(I) - SLAB THICKNESSES (MFP)
C     NMAX - NO. OF POINTS INSIDE SLAB AT WHICH PARTICLE OENSITY IS
C            TO BE EVALUATEO
C     ITER - NO. OF SCATTERING OROERS TO BE CALCULATED FOR A GIVEN
C            SLAB THICKNESS
C     NSK - OFTION PARAMETER FOR SOKOLOV CONVERGENCE ACCELERATION
      READ 10,(NMAX(NT),ITER(NT),NT=1,NTHK)
      READ 10,NSK,NRUN
      MSK=1
      IF(NSK.NE.0) MSK=2
      IF(NRUN.EQ.0) GO TO 150
  149 READ(4)TKK,NPTS
      IF(EOF(4))150,151
  151 READ(4)(TFAC(K),K=1,NPTS)
      READ(4)(BFAC(K),K=1,NPTS)
      WRITE(5)TKK,NPTS
      WRITE(5)(TFAC(K),K=1,NPTS)
      WRITE(5)(BFAC(K),K=1,NPTS)
      GO TO 149
  150 CONTINUE
   10 FORMAT(16I5)
   11 FORMAT(I5,5F10.0)
      DO 200 NT=1,NTHK
      REWIND 1
      THICK=THKNSS(NT)
      IT=ITER(NT)
      MAX=NMAX(NT)
      XX(1)=0.0
      DT(NT)=THKNSS(NT)/FLOAT(NMAX(NT)-1)
      O=OT(NT)
      DO 101 I=2,MAX
      XX(I)=XX(I-1)+O
  101 CONTINUE
      K=0
      IHIT=0
      PRINT 55,THKNSS(NT),K,IHIT
      OO 102 IX=1,MAX
      X=XX(IX)
      E22(IX)=F2(X)
      TX=THICK-X
      BFAC(IX)=E22(IX)
```

```
      TFAC(IX)=E2(TX)
      PHINP1(IX)=PHINP2(IX)=PHP(IX)=E22(IX)
  102 CONTINUE
      WRITE(1)MAX
      WRITE(1)(XX(I),I=1,MAX)
      WRITE(1)(PHINP1(I),I=1,MAX)
      WRITE(1)(PHINP2(I),I=1,MAX)
      K=1
      PRINT 55,THKNSS(NT),K,IHIT
      IHIT=0
   55 FORMAT(1X,*THICKNESS =*, E12.5,5X,*ITERATION NO.*,I6,5X,*IHIT =*,I
     16)
      DO 1 IX=1,MAX
      X=XX(IX)
      CALL START
      CALL TYPE1(1,QSP1,QSPP1)
      CALL TYPE1(2,QSP2,QSPP2)
      CALL TYPE2(1,QREG1,QREGP1)
      CALL TYPE2(2,QREG2,QREGP2)
      PHINP1(IX)=E22(IX)-0.5*(QREG1+QREG2-QSP1-QSP2)
      IF(NSK.EQ.0) GO TO 1
      CORINT=0.5*(QSPP1+QSPP2-QREGP1-QREGP2)
      CALL SOKOL(K,CORR)
      PHINP2(IX)=PHINP1(IX)+CORR
    1 CONTINUE
      DO 111 I=1,MAX
      IF(PHINP1(I).LT.0.0) GO TO 112
      IF(PHINP1(I).LT.PHP(I)) GO TO 112
  111 CONTINUE
      GO TO 113
  112 IHIT=I
      ISAFE=IHIT-6
      IF(ISAFE.LT.0) CALL CRASH
      IS=ISAFE+1
      RTIO=PHINP1(ISAFE)/PHP(ISAFE)
      DO 114 I=IS,MAX
      PHINP1(I)=RTIO*PHP(I)
  114 CONTINUE
      DO 115 I=1,MAX
      PHP(I)=PHINP1(I)
  115 CONTINUE
  113 CONTINUE
      WRITE(1)(PHINP1(I),I=1,MAX)
      WRITE(1)(PHINP2(I),I=1,MAX)
      DO 50 K=2,IT
      PRINT 55,THKNSS(NT),K,IHIT
      IHIT=0
      CALL INTERP(XX,PHINP1,P0,P1,P2,P3,MAX)
      CALL INTERP(XX,PHINP2,Q0,Q1,Q2,Q3,MAX)
   57 FORMAT(1X,4E16.9)
      DO 12 IX=1,MAX
      DO 40 MTH=1,MSK
      X=XX(IX)
      CALL RESET
      CALL TYPE1(1,QSP1,QSPP1)
      CALL TYPE1(2,QSP2,QSPP2)
      CALL TYPE2(1,QREG1,QREGP1)
```

```
      CALL TYPE2(2,QREG2,QREGP2)
      IF(MTH.EQ.2) GO TO 41
      PHINP1(IX)=E22(IX)-0.5*(QREG1+QREG2-QSP1-QSP2)
      GO TO 40
   41 CORINT=0.5*(QSPP1+QSPP2-QREGP1-QREGP2)
      CALL SOKOL(K,CORR)
      PHINP2(IX)=E22(IX)-0.5*(QREG1+QREG2-QSP1-QSP2)+CORR
   40 CONTINUE
   12 CONTINUE
      DO 211 I=1,MAX
      IF(PHINP1(I).LT.0.0) GO TO 212
      IF(PHINP1(I).LT.PHP(I)) GO TO 212
  211 CONTINUE
      GO TO 213
  212 IHIT=I
      ISAFE=IHIT-6
      IF(ISAFE.LT.0) CALL CRASH
      IS=ISAFE+1
      RTIO=PHINP1(ISAFE)/PHP(ISAFE)
      DO 214 I=IS,MAX
      PHINP1(I)=RTIO*PHP(I)
  214 CONTINUE
      DO 215 I=1,MAX
      PHP(I)=PHINP1(I)
  215 CONTINUE
  213 CONTINUE
      WRITE(1)(PHINP1(I),I=1,MAX)
      WRITE(1)(PHINP2(I),I=1,MAX)
    2 FORMAT(1X,*X = *,E16.8,*  PHI(N)= *,E16.8)
   50 CONTINUE
      REWIND 1
      CALL PRCC(NTHK,NT,THKNSS,ITER,NSK)
  200 CONTINUE
      STOP
      END
```

```
      SUBROUTINE SOKOL(K,CORR)
      COMMON THICK,DELTA,X,CONST1,CONST2,GAMMA,CORINT,IX,MAX,MTH,U1(16),
     1U2(32),PHINP1(110),PHINP2(110),XX(110),P0(110),P1(110),P2(110),
     2P3(110),Q0(110),Q1(110),Q2(110),Q3(110),F1(16),F2(32),G1(16),
     3G2(32),GRAND2(16),XPY1(16),XPY2(32),XMY1(16),XMY2(32),GX1(16),
     4GRAND1(16)
      COMMON/GAUSQ/W1(16),W2(16),AW1(16),AW2(32)
      H=XX(2)-XX(1)
      KODE=1
      IF(K-2)1,2,3
    1 IF(IX.NE.1) GO TO 11
      TK=THICK
      CALL EXPI(TK,RES)
      E3=-0.5*((THICK-1.0)*EXP(-THICK)-(THICK**2)*RES)
      EYE0=THICK-0.5+E3
      AL1=1.0/(1.0-0.5/E3)
   11 CORR=AL1*CORINT
      RETURN
    2 IF(IX.NE.1) GO TO 21
      CALL TYPE3(H,KODE,EYE1)
      EYNM2=EYE0
      EYNM1=EYE1
      AL2=(EYE1-AL1*EYE0)/(THICK-EYE0)
      ALNM1=AL2
   21 CORR=AL2*CORINT
      RETURN
    3 IF(IX.NE.1) GO TO 31
      EYNM2=EYNM1
      CALL TYPE3(H,KODE,EYNM1)
      ALN=(EYNM1-EYNM2-ALNM1*EYE0)/(THICK-EYE0)
      ALNM1=ALN
   31 CORR=ALN*CORINT
      RETURN
      END
```

```
      SUBROUTINE TYPE3(H,KODE,Q)
      COMMON THICK,DELTA,X,CONST1,CONST2,GAMMA,CORINT,IX,MAX,MTH,U1(16),
     1U2(32),PHINP1(110),PHINP2(110),XX(110),P0(110),P1(110),P2(110),
     2P3(110),Q0(110),Q1(110),Q2(110),Q3(110),F1(16),F2(32),G1(16),
     3G2(32),GRAND2(16),XPY1(16),XPY2(32),XMY1(16),XMY2(32),GX1(16),
     4GRAND1(16)
      COMMON/GAUSQ/W1(16),W2(16),AW1(16),AW2(32)
      COMMON/FLX/ETRAN(101),EBACK(101),TFAC(101),BFAC(101)
      DIMENSION TS(101)
      Q=0.0
      H3=H/3.
      M1=MAX-1
      DO 50 I=1,MAX
      TS(I)=1.0
      IF(KODE.EQ.1)  TS(I)=2.-TFAC(I)-BFAC(I)
   50 CONTINUE
      GO TO (10,12,13),KODE
   12 DO 120  I=1,MAX
      PHINP2(I)=ETRAN(I)
  120 CONTINUE
      GO TO 10
   13 DO 130  I=1,MAX
      PHINP2(I)=EBACK(I)
  130 CONTINUE
   10 DO 1  I=2,M1,2
      Q=Q+4.*H3*PHINP2(I)*TS(I)
    1 CONTINUE
      M2=MAX-2
      DO 11 I=3,M2,2
      Q=Q+2.*H3*PHINP2(I)*TS(I)
   11 CONTINUE
      Q=Q+H3*(PHINP2(1)*TS(1)+PHINP2(MAX)*TS(MAX))
      IF(KODE.EQ.1)Q=0.5*Q
      RETURN
      END
```

```
      SUBROUTINE RESET
      COMMON THICK,DELTA,X,CONST1,CONST2,GAMMA,CORINT,IX,MAX,MTH,U1(16),
     1U2(32),PHINP1(110),PHINP2(110),XX(110),P0(110),P1(110),P2(110),
     2P3(110),Q0(110),Q1(110),Q2(110),Q3(110),F1(16),F2(32),G1(16),
     3G2(32),GRAND2(16),XPY1(16),XPY2(32),XMY1(16),XMY2(32),GX1(16),
     4GRAND1(16)
      COMMON/GAUSQ/W1(16),W2(16),AW1(16),AW2(32)
      DIMENSION XRAY(112),FR(112)
      EQUIVALENCE(F1(1),FR(1)),(XPY1(1),XRAY(1))
      DELTA=THICK-X
      U0=CONST1=CONST2=0.0
      IF(DELTA.EQ.0.0) GO TO 3
      CONST1=GAMMA+ALOG(DELTA)
      IF(X.EQ.0.0) GO TO 3
      CONST2=GAMMA+ALOG(X)
      U0=X/DELTA
    3 DO 2 I=1,16
      XPY1(I)=DELTA*(U1(I)+U0)
      XMY1(I)=X*(1.-U1(I))
    2 CONTINUE
      DO 4 I=1,32
      XPY2(I)=DELTA*(0.5*(1.+U2(I))+U0)
      XMY2(I)=X*(1.-0.5*(1.+U2(I)))
    4 CONTINUE
      DO 51 J=1,112
      DO 52 M=1,MAX
      IF(XRAY(J).LT.XX(M)) GO TO 53
   52 CONTINUE
      XRAY(J)=XX(MAX)
      IF(MTH.EQ.1) FR(J)=PHINP1(MAX)
      IF(MTH.EQ.2) FR(J)=PHINP2(MAX)
      MARK=MAX
      GO TO 51
   53 MARK=M-1
      IF(MARK.NE.0) GO TO 54
      XRAY(J)=XX(1)
      IF(MTH.EQ.1) FR(J)=PHINP1(1)
      IF(MTH.EQ.2) FR(J)=PHINP2(1)
      GO TO 51
   54 XDIF=XRAY(J)-XX(MARK)
      GO TO (48,49),MTH
   48 FR(J)=P0(MARK)+P1(MARK)*XDIF+P2(MARK)*XDIF**2+P3(MARK)*XDIF**3
      GO TO 51
   49 FR(J)=Q0(MARK)+Q1(MARK)*XDIF+Q2(MARK)*XDIF**2+Q3(MARK)*XDIF**3
   51 CONTINUE
      RETURN
      END
```

```
      SUBROUTINE TYPE1(N,Q,QP)
      COMMON THICK,DELTA,X,CONST1,CONST2,GAMMA,CORINT,IX,MAX,MTH,U1(16),
     1U2(32),PHINP1(110),PHINP2(110),XX(110),P0(110),P1(110),P2(110),
     2P3(110),Q0(110),Q1(110),Q2(110),Q3(110),F1(16),F2(32),G1(16),
     3G2(32),GRAND2(16),XPY1(16),XPY2(32),XMY1(16),XMY2(32),GX1(16),
     4GRAND1(16)
      COMMON/GAUSQ/W1(16),W2(16),AW1(16),AW2(32)
      Q=0.0
      QP=0.0
      IF(IX.EQ.1)X=0.0
      IF(IX.EQ.MAX)DELTA=0.0
      DO 1 I=1,16
      GO TO (2,3),N
    2 T=AW1(I)*DELTA
      Q=Q+F1(I)*T
      IF(MTH.EQ.1) GO TO 1
      QP=QP+T
      GO TO 1
    3 T=AW1(I)*X
      Q=Q+G1(I)*T
      IF(MTH.EQ.1) GO TO 1
      QF=QP+T
    1 CONTINUE
      RETURN
      END


      SUBROUTINE GCOEFF
      COMMON THICK,DELTA,X,CONST1,CONST2,GAMMA,CORINT,IX,MAX,MTH,U1(16),
     1U2(32),PHINP1(110),PHINP2(110),XX(110),P0(110),P1(110),P2(110),
     2P3(110),Q0(110),Q1(110),Q2(110),Q3(110),F1(16),F2(32),G1(16),
     3G2(32),GRAND2(16),XPY1(16),XPY2(32),XMY1(16),XMY2(32),GX1(16),
     4GRAND1(16)
      COMMON/GAUSQ/W1(16),W2(16),AW1(16),AW2(32)
      READ 1,(W1(I),I=1,16)
      READ 1,(AW1(I),I=1,16)
C     W1(I),AW1(I) - GAUSS QUADRATURE ORDINATES(W1) AND COEFFICIENTS
C                     (AW1) FOR THE LOGARITHMIC INTEGRAL.
C                     THESE ARE OBTAINED FROM *GAUSSIAN QUADRATURE
C                     FORMULAS* BY A.H. STROUD AND D. SECREST,
C                     PRENTICE HALL (1966), PAGE 304 AND ARE READ IN
C                     ASCENDING ORDER OF W1.
      READ 1,(W2(I),I=1,16)
      READ 1,(AW2(I),I=1,16)
C     W2(I),AW2(I)- GAUSS QUADRATURE ORDINATES(W2) AND COEFFICIENTS(AW2)
C                     FOR THE NON-LOGARITHMIC INTEGRALS.
C                     THESE ARE OBTAINED FROM *GAUSSIAN QUADRATURE
C                     FORMULAS* BY A.H. STROUD AND D. SECREST,
C                     PRENTICE HALL (1966), PAGE 105 AND ARE READ IN
C                     ASCENDING ORDER OF W2.
    1 FORMAT(4F20.0)
      DO 2 I=1,16
      GRAND1(I)=AW2(I)
    2 CONTINUE
      RETURN
      END
```

```
      SUBROUTINE START
      COMMON THICK,DELTA,X,CONST1,CONST2,GAMMA,CORINT,IX,MAX,MTH,U1(16),
     1U2(32),PHINP1(110),PHINP2(110),XX(110),P0(110),P1(110),P2(110),
     2P3(110),Q0(110),Q1(110),Q2(110),Q3(110),F1(16),F2(32),G1(16),
     3G2(32),GRAND2(16),XPY1(16),XPY2(32),XMY1(16),XMY2(32),GX1(16),
     4GRAND1(16)
      COMMON/GAUSQ/W1(16),W2(16),AW1(16),AW2(32)
      DELTA=THICK-X
      IFLAG=1
      IF(IX.EQ.1) IFLAG=2
      IF(IX.EQ.MAX)  IFLAG=3
      DO 1 I=1,16
      U1(I)=W1(I)
      U2(I)=W2(17-I)
      U2(I+16)=-W2(I)
      AW2(I)=GRAND1(17-I)
      AW2(I+16)=GRAND1(I)
    1 CONTINUE
      GO TO (4,5,6), IFLAG
    4 U0=X/DELTA
      CONST1=GAMMA+ALOG(DELTA)
      CONST2=GAMMA+ALOG(X)
      GO TO 3
    5 U0=CONST2=0.0
      CONST1=GAMMA+ALOG(DELTA)
      GO TO 3
    6 U0=CONST1=0.0
      CONST2=GAMMA+ALOG(X)
    3 DO 2 I=1,16
      XPY1(I)=DELTA*(U1(I)  +U0)
      XMY1(I)=X*(1.-U1(I))
      F1(I)=E2(XPY1(I))
      G1(I)=E2(XMY1(I))
    2 CONTINUE
      DC 8 I=1,32
      XPY2(I)=DELTA*(0.5*(1.+U2(I))+U0)
      XMY2(I)=X*(1.-0.5*(1.+U2(I)))
      F2(I)=E2(XPY2(I))
      G2(I)=E2(XMY2(I))
    8 CONTINUE
      DO 7 I=1,16
      GX1(I)=THICK*W2(I)
      GX2=THICK-GX1(I)
    7 CONTINUE
      RETURN
      END
```

```
      SUBROUTINE TYPE2(N,Q,QP)
      COMMON THICK,DELTA,X,CONST1,CONST2,GAMMA,CORINT,IX,MAX,MTH,U1(16),
     1U2(32),PHINP1(110),PHINP2(110),XX(110),F0(110),P1(110),P2(110),
     2P3(110),Q0(110),Q1(110),Q2(110),Q3(110),F1(16),F2(32),G1(16),
     3G2(32),GRAND2(16),XPY1(16),XPY2(32),XMY1(16),XMY2(32),GX1(16),
     4GRAND1(16)
      COMMON/GAUSQ/W1(16),W2(16),AW1(16),AW2(32)
      DIMENSION F(32),U(32)
      IF(IX.EQ.1)X=0.0
      IF(IX.EQ.MAX)DELTA=0.0
      GO TO (100,200),N
  100 DO 101 I=1,32
      F(I)=F2(I)
      U(I)=U2(I)
  101 CONTINUE
      D=DELTA
      C=CONST1
      GO TO 10
  200 DO 201 I=1,32
      F(I)=G2(I)
      U(I)=U2(I)
  201 CONTINUE
      D=X
      C=CONST2
   10 Q=0.0
      QP=0.0
      IF(C.EQ.0.0) RETURN
      DO 1 I=1,32
      Q=Q+AW2(I)*F(I)
      IF(MTH.EQ.1) GO TO 1
      QP=QP+AW2(I)
    1 CONTINUE
      Q=Q*D*C*0.5
      QP=QP*D*C*0.5
      SUMPR=0.0
      I1=I2=0
      SUM=0.0
      FAC=D
      DO 2 J=1,60
      IF(I1.EQ.1.AND.I2.EQ.1) GO TO 5
      FJ=FLOAT(J)
      ENTGL=0.0
      ENTGL1=0.0
      DO 3 I=1,32
      T=AW2(I)*(0.5*(1.+U(I)))**J
      IF(I1.EQ.1) GO TO 31
      ENTGL=ENTGL+F(I)*T
   31 IF(MTH.EQ.1.AND.I1.EQ.1) GO TO 5
      ENTGL1=ENTGL1+T
    3 CONTINUE
      FAC=-FAC*D/FJ
      FIC=FAC/FJ
      SUM=SUM+FIC*ENTGL
      SUMPR=SUMPR+FIC*ENTGL1
      IF(I1.EQ.1) GO TO 32
      SUMF=ABS(SUM)
      DIF=ABS(FIC*ENTGL)
```

```
      IF(DIF.LE.(SUMP*1.E-9)) I1=1
   32 SUMPRP=ABS(SUMPR)
      DIFP=ABS(FIC*ENTGL1)
      IF(DIFP.LE.(SUMPRP*1.E-9))I2=1
    2 CONTINUE
    5 Q=Q+0.5*SUM
      QP=QP+0.5*SUMPR
      RETURN
      END
```

```
      FUNCTION E2(Z)
      CALL EXPI(Z,RES)
      E2   =EXP(-Z)-Z*RES
      RETURN
      END
```

```
      SUBROUTINE EXPI(X,RES)
      IF(X-1.)2,1,1
    1 Y=1./X
      AUX=1.-Y*(((Y+3.377358E0)*Y+2.052156E0)*Y+2.709479E-1)/((((Y*
     11.072553E0+5.716943E0)*Y+6.945239E0)*Y+2.593888E0)*Y+2.709496E-1)
      RES=AUX*Y*EXP(-X)
      RETURN
    2 IF(X+3.)6,6,3
    3 AUX=(((((((7.122452E-7*X-1.766345E-6)*X+2.92843[illegible]*X-2.335379E-4
     1)*X+1.664156E-3)*X-1.041576E-2)*X+5.555682E-2)[illegible]00001E-1)*X
     2+9.999994E-1
      RES=-1.E75
      IF(X)4,5,4
    4 RES=X*AUX-ALOG(ABS(X))-5.772157E-1
    5 RETURN
    6 IF(X+9.)8,8,7
    7 AUX=1.-((((5.176245E-2*X+3.061037E0)*X+3.243665E1)*X+2.244234E2)*X
     1+2.486697E2)/((((X+3.995161E0)*X+3.893944E1)*X+2.263818E1)*X
     2+1.907837E2)
      GOTO 9
    8 Y=9./X
      AUX=1.-Y*(((Y+7.659924E-1)*Y-7.271015E-1)*Y-1.080693E0)/((((Y
     1*2.518750E0+1.122927E1)*Y+5.921405E0)*Y-8.666702E0)*Y-9.724216E0)
    9 RES=AUX*EXP(-X)/X
      RETURN
      END
```

```
      SUBROUTINE PROC(NTHK,NT,THKNSS,ITER,NSK)
      DIMENSION TRAN(50),BACK(50)
      DIMENSION XX(101),PHI(101,51),DPHI(101,50),THKNSS(5),ITER(5)
      DIMENSION PHO(101,51)
      DIMENSION IK(6)
      COMMON/FLX/ETRAN(101),EBACK(101),TFAC(101),BFAC(101)
      PRINT 4
      IT=ITER(NT)+1
      KCR=0
      PRINT 11,THKNSS(NT)
   11 FORMAT(1X,*THICKNESS=*,E12.5///)
      READ (1) MAX
      READ (1) (XX(I),I=1,MAX)
      H=XX(2)-XX(1)
      THICK=THKNSS(NT)
      IT1=ITER(NT)
      DO 91 K=1,IT1
      TRAN(K)=BACK(K)=0.0
   91 CONTINUE
      DO 1 K=1,IT
      READ(1)(PHI(I,K),I=1,MAX)
      READ(1)(PHO(I,K),I=1,MAX)
    1 CONTINUE
   38 KCR=KCR+1
      IF(KCR.EQ.1) GO TO 40
      IF(NSK.EQ.0) RETURN
      DO 30 I=1,MAX
      DO 30 K=1,IT
      PHI(I,K)=PHO(I,K)
   30 CONTINUE
      PRINT 14
   14 FORMAT(*1*,1X,*FLUX (SOKOLOV METHOD)*/)
      GO TO 39
   40 CONTINUE
      PRINT 12
   12 FORMAT(1X,*FLUX*/)
   39 K1=-5
   15 K1=K1+6
      K2=K1+5
      DO 10 I=1,MAX
      MK=6
      IK(1)=K1-1
      DO 60 L=2,6
      IK(L)=IK(L-1)+1
      IF(IK(L).GE.IT) GO TO 62
   60 CONTINUE
      GO TO 63
   62 MK=L-1
      K2=IT
   63 IF(I.EQ.1) PRINT 61,(IK(L),L=1,MK)
   61 FORMAT(7X,*X*,6X,*N =*,4X,I8,5I16)
      PRINT 21,XX(I),(PHI(I,K),K=K1,K2)
   10 CONTINUE
      PRINT 3
      IF(K2.LT.IT)GO TO 15
   21 FORMAT(1X,E12.5,5X,6E16.9)
    3 FORMAT(/////)
```

```
 4 FORMAT(*1*)
   PRINT 4
   I1=IT-1
   IF(KCR.EQ.2) GO TO 50
   PRINT 13
13 FORMAT(1X,*FLUX OIFFERENC
16 FORMAT(1X,*(SOKOLOV METHC
   DO 5 K=1,I1
   OO 6 I=1,MAX
   IF(K.GT.1) GO TO 17
   OPHI(I,1)=PHI(I,1)
   GO TO 18
17 OPHI(I,K)=PHI(I,K)-PHI(I,K-1)
18 ETRAN(I)= TFAC(I)*OPHI(I,K)
   EBACK(I)= BFAC(I)*OPHI(I,K)
 6 CONTINUE
   KOOE=2
   CALL TYPE3(H,KODE,TR)
   KOOE=3
   CALL TYPE3(H,KOOE,BK)
   TRAN(K+1)=TR
   BACK(K+1)=BK
   TRAN(1)=0.5*(EXP(-THICK)-THICK*E2(THICK))
   BACK(1)=0.0
 5 CONTINUE
   K1=-5
25 K1=K1+6
   K2=K1+5
   IF(K2.GE.I1)K2=I1
   DO 7 I=1,MAX
   PRINT 21,XX(I),(DPHI(I,K),K=K1,K2)
 7 CONTINUE
   PRINT 3
   IF(K2.LT.I1) GO TO 25
   PRINT 4
   PRINT 95
95 FORMAT(1X,*OROER OF SCATTERING*,10X,*NUMBER TRANSMITTED*,10X,*NUMB
  1ER BACKSCATTEREO*//)
   OO 96 K=1,IT
   TRAN(K)=0.5*TRAN(K)
   BACK(K)=0.5*BACK(K)
   M=K-1
   PRINT 97,M,TRAN(K),BACK(K)
96 CONTINUE
97 FORMAT(1X,I10,20X,E16.8,16X,E16.8)
   WRITE(5)THKNSS(NT),IT
   WRITE(5)(TRAN(K',K=1,IT)
   WRITE(5)(BACK(K),K=1,IT)
   GO TO 38
50 RETURN
   END
```

```
      SUBROUTINE INTERP(X,Y,P0,P1,P2,P3,NMAX)
      DIMENSION X(1),Y(1),P0(1),P1(1),P2(1),P3(1)
      DIMENSION JSAVE(4),KSAVE(4),S(4)
      DATA IDBG/0/
      IF(NMAX.GE.5) GO TO 1
      PRINT 100,NMAX
  100 FORMAT(1X,*NMAX(*,I1*) LESS THAN 5*)
      RETURN
C     ENDPOINTS
    1 NTEMP=NMAX+4
      X3=X(NMAX)
      X2=X(NMAX-1)
      X1=X(NMAX-2)
      Y3=Y(NMAX)
      Y2=Y(NMAX-1)
      Y1=Y(NMAX-2)
      X(NTEMP-1)=X3+X2-X1
      Y(NTEMP-1)=(X2-X1)*(2.*(Y3-Y2)/(X3-X2)-(Y2-Y1)/(X2-X1))+Y3
      X(NTEMP)=X(NTEMP-1)+X3-X2
      Y(NTEMP)=(X3-X2)*(2.*(Y(NTEMP-1)-Y3)/(X(NTEMP-1)-X3)-
     1           (Y3-Y2)/(X3-X2))+Y(NTEMP-1)
      NM=NMAX+1
      DO 2 N=1,NMAX
      X(NTEMP-N-1)=X(NM-N)
      Y(NTEMP-N-1)=Y(NM-N)
    2 CONTINUE
      X1=X(5)
      X2=X(4)
      X3=X(3)
      Y1=Y(5)
      Y2=Y(4)
      Y3=Y(3)
      X4=X3+X2-X1
      Y4=(X2-X1)*(2.*(Y3-Y2)/(X3-X2)-(Y2-Y1)/(X2-X1))+Y3
      X5=X4+X3-X2
      Y5=(X3-X2)*(2.*(Y4-Y3)/(X4-X3)-(Y3-Y2)/(X3-X2))+Y4
      X(1)=X5
      Y(1)=Y5
      X(2)=X4
      Y(2)=Y4
      IF(IDBG.EQ.0) GO TO 53
      PRINT 52
   52 FORMAT(*1*)
      DO 50 I=1,NTEMP
      PRINT 51,X(I),Y(I)
   50 CONTINUE
   51 FORMAT(1X,2E16.8)
C     ENDPOINTS FINISHED,, GET SLOPES
   53 T2=0.0
      NM=NTEMP-2
      DO 3 N=3,NM
      T1=T2
      DO 4 J=1,4
      JJ=N+J-2
      JK=N+J-3
      S(J)=(Y(JJ)-Y(JK))/(X(JJ)-X(JK))
    4 CONTINUE
```

```
      IQUALS=0
      DO 5 J=1,3
      JJ=J+1
      DO 5 K=JJ,4
      IF(S(J)-S(K))5,6,5
    6 IQUALS=IQUALS+1
      JSAVE(IQUALS)=J
      KSAVE(IQUALS)=K
    5 CONTINUE
      IF(IQUALS.EQ.0) GO TO 8
      IF(IQUALS.EQ.2) GO TO 7
      GO TO 9
    7 T2=S(2)
      GO TO 20
    9 IF(IQUALS.GE.3) GO TO 7
      IF(IQUALS.NE.1) GO TO 17
      GO TO 10
   17 PRINT 18,IQUALS
   18 FORMAT(1X,*IQUALS=*,I5)
   10 JS=JSAVE(IQUALS)
      KS=JS+KSAVE(IQUALS)
      IF((KS-2*(KS/2)).EQ.0)  GO TO 11
      T2=S(JS)
      GO TO 20
   11 W2=ABS(S(4)-S(3))
      W3=ABS(S(2)-S(1))
      GO TO 12
    8 W2=SQRT(ABS((S(1)-S(3))*(S(3)-S(4))))
      W3=SQRT(ABS((S(1)-S(2))*(S(2)-S(4))))
   12 T2=(W2*S(2)+W3  *S(3))/(W2+W3)
   20 IF(N.EQ.3) GO TO 3
      NN=N-1
      P0(NN)=Y(NN)
      P1(NN)=T1
      P2(NN) =(3.0*(Y(N)-Y(NN))/(X(N)-X(NN))-2.*T1-T2)/(X(N)-X(NN))
      P3(NN) =(T1+T2-2.*(Y(N)-Y(NN))/(X(N)-X(NN)))/((X(N)-X(NN))**2)
    3 CONTINUE
      DO 30 N=1,NMAX
      X(N)=X(N+2)
      Y(N)=Y(N+2)
      P0(N)=P0(N+2)
      P1(N)=P1(N+2)
      P2(N)=P2(N+2)
      P3(N)=P3(N+2)
   30 CONTINUE
      P0(NMAX)=0.
      P1(NMAX)=0.
      P2(NMAX)=0.
      P3(NMAX)=0.
      RETURN
      END
```

A4. Monte Carlo Code for Scattering in the Slab Geometry

PRECEDING PAGE BLANK-NOT FILMED

```
      PROGRAM MCTRN(INPUT,OUTPUT,TAPE2,TAPE3)
C
C     THIS PARTICULAR VERSION OF THE MONTE CARLO CODE WAS USED FOR THE
C     NEUTRON SCATTER IN CARBON CALCULATION
C
      COMMON/MC/STO(7,1024),NCOLL,CTHO,CTH,STH,PHI,CPHI,SPHI,EGY,CPHIO,
     1SPHIO,EO,SIGO,AMBDA,N,IRA,IRB,IRC,IRD,IFLAG,MAXCOLL,SIG(20),LCHR,
     2ENRGY(20),LMAX,XO,YO,ZO,X,Y,Z,ECUT,CLAB,THICK(11),NMAX,ZMIN,ZMAX
     3,NPRNT,AMASS,RATIO,CTHC
      DATA IGO/0/
    1 REWIND 2
      IGO=IGO+1
C     SUBROUTINE SETRUN READS IN THE NECESSARY PARAMETERS TO START THE
C     CALCULATION
      CALL SETRUN(IGO)
    5 N=N+1
      CALL SETHIS
      CALL SCORE
   20 CALL PENET
      IF(IFLAG.NE.0) GO TO 6
      CALL ENERGY
      IF(IFLAG.NE.0) GO TO 6
      CALL SCORE
      CALL ANGLES
      GO TO 20
    6 CALL SCORE
      IF(N-NMAX)5,100,100
  100 WRITE(2)((STO(K,L),K=1,7),L=1,LMAX)
      IF(NPRNT.NE.0) PRINT 2,((STO(K,L),K=1,7),L=1,LMAX)
    2 FORMAT(1X,7E16.9)
      DO 7 K=1,7
      DO 7 L=1,LMAX
      STO(K,L)=0.0
    7 CONTINUE
      WRITE(2)((STO(K,L),K=1,7),L=1,LMAX)
      REWIND 2
      CALL SUMRY(IGO)
      PRINT 50,IRA,IRB,IRC,IRD
   50 FORMAT(1X,4O22)
      IF(IGO.LT.2) GO TO 1
      STOP
      END
```

```
      SUBROUTINE SETRUN(IGO)
      COMMON/MC/STO(7,1024),NCOLL,CTHO,CTH,STH,PHI,CPHI,SPHI,EGY,CPHIO,
     1SPHIO,EO,SIGO,AMBDA,N,IRA,IRB,IRC,IRD,IFLAG,MAXCOLL,SIG(20),LCHR,
     2ENRGY(20),LMAX,XO,YO,ZO,X,Y,Z,ECUT,CLAB,THICK(11),NMAX,ZMIN,ZMAX
     3,NPRNT,AMASS,RATIO,CTHC
      DATA CPHIO,SPHIO,PI,ZMIN,ZMAX,N/1.0,0.0,3.14159265,0.0,1000.0,0/
      DATA ECUT/0.0/
      DATA SIG/.201,.217,.233,.241,.249,.257,.297,.321,.329,.361-.369,
     1.377,.385,.385,.385,.385/
      DATA ENRGY/1.0,0.9,0.8,0.7,0.6,0.5,0.4,0.3,0.2,0.1,0.09,0.08,0.06,
     10.05,0.01,0.25E-7/
      IF(IGO.GT.1) GO TO 10
      READ 1,NMAX,LMAX,MAXCOLL,NPRNT
C     NMAX - TOTAL NO. OF MONTE CARLO HISTORIES
C     LMAX - SIZE OF COLLISION SITE CHARACTERISTIC BLOCK TO EE
C     STORED ON TAPE OR DISK UNTIL PROCESSING TIME
C     MAXCOLL - MAXIMUM NO. OF COLLISIONS PER HISTORY TO BE ALLOWED
C     NPRNT - DEBUG PRINT CONTROL PARAMETER
C             NPRNT EQUAL TO ZERO SUPPRESSES DEBUG PRINTOUT
C             NPRNT NOT EQUAL TO ZERO ACTIVATES DEBUG PRINTOUT
      READ 2,IRA,IRB,IRC,IRD
C     IRA,IRB,IRC,IRD - STARTING RANDOM NUMBERS
C                       THESE  ARE USED IN CONJUNCTION WITH A CDC
C             SUPPLIED RANDOM NUMBER GENERATOR
      READ 3,EO,XO,YO,ZO,SIGO
C     EO - INITIAL PARTICLE ENERGY
C     XO,YO,ZO - INITIAL PARTICLE COORDINATES
C     SIGO - INITIAL MACROSCOPIC CROSS SECTION
      READ 3,AMASS
C     AMASS -  MASS OF SCATTERING CENTER OR TARGET NUCLEUS
      PRINT 4,NMAX,LMAX,MAXCOLL
      PRINT 5,IRA,IRB,IRC,IRD
      PRINT 6,EO,XO,YO,ZO
      PRINT 6, AMASS
    2 FORMAT(4O20)
    1 FORMAT(4I10)
    3 FORMAT(5F10.0)
    4 FORMAT(1X,3I10)
    5 FORMAT(1X,4O22)
    6 FORMAT(1X,5F10.0)
   10 N=0
      LCHR=0
      DO 7 M=1,7
      DO 7 L=1,LMAX
      STO(M,L)=0.0
    7 CONTINUE
      RETURN
      END
```

```
      SUBROUTINE SETHIS
      COMMON/MC/STO(7,1024),NCOLL,CTHO,CTH,STH,PHI,CPHI,SPHI,EGY,CPHIO,
     1SPHIO,EO,SIGO,AMBDA,N,IRA,IRB,IRC,IRD,IFLAG,MAXCOLL,SIG(20),LCHR,
     2ENRGY(20),LMAX,XO,YO,ZO,X,Y,Z,ECUT,CLAB,THICK(11),NMAX,ZMIN,ZMAX
     3,NPRNT,AMASS,RATIO,CTHC
      NCOLL=0
      X=XO
      Y=YO
      Z=ZO
      CPHI=CPHIO
      SPHI=SPHIO
      PHI=0.0
      CALL RN2(IRA,RA)
      CTH=CTHO=RA
      STH=SQRT(1.-CTH**2)
      EGY=EO
      AMBDA=1./SIGO
      IFLAG=0
      RETURN
      ENO
```

```
      SUBROUTINE PENET
      COMMON/MC/STO(7,1024),NCOLL,CTHO,CTH,STH,PHI,CPHI,SPHI,EGY,CPHIO,
     1SPHIO,EO,SIGO,AMBDA,N,IRA,IRB,IRC,IRD,IFLAG,MAXCOLL,SIG(20),LCHR,
     2ENRGY(20),LMAX,XO,YO,ZO,X,Y,Z,ECUT,CLAB,THICK(11),NMAX,ZMIN,ZMAX
     3,NPRNT,AMASS,RATIO,CTHC
      X1=X
      Y1=Y
      Z1=Z
      CALL RN2(IRB,RB)
      S=-ALOG(RB)*AMBDA
      Z=Z1+S*CTH
      IF(Z.GT.ZMIN) GO TO 10
      Z=ZMIN
      S=(ZMIN-Z1)/CTH
      IFLAG=1
   10 X=X1+S*STH*CPHI
      Y=Y1+S*STH*SPHI
      NCOLL=NCOLL+1
      IF(NCOLL.EQ.MAXCOLL) IFLAG=1
      IF(Z.GT.ZMAX)IFLAG=1
      RETURN
      ENO
```

```
      SUBROUTINE ENERGY
      COMMON/MC/STO(7,1024),NCOLL,CTHO,CTH,STH,PHI,CPHI,SPHI,EGY,CPHIO,
     1SPHIO,EO,SIGO,AMBOA,N,IRA,IRB,IRC,IRO,IFLAG,MAXCOLL,SIG(20),LCHR,
     2ENRGY(20),LMAX,XO,YO,ZO,X,Y,Z,ECUT,CLAB,THICK(11),NMAX,ZMIN,ZMAX
     3,NPRNT,AMASS,RATIO,CTHC
      DATA PI/3.14159265/
      CALL RN2(IRD,RO)
      CTHC=2.*RO-1.
      RATIO=(1.+2.*AMASS*CTHC+AMASS**2)/(1.+2.*AMASS+AMASS**2)
      EGY=EGY*RATIO
      IF(EGY.GT.ECUT) GO TO 1
      IFLAG=1
      RETURN
    1 DO 2 I=1,16
    2 CONTINUE
      SIGMA=SIG(16)
      GO TO 4
    3 II=I-1
      SIGMA=(EGY-ENRGY(II))/(ENRGY(I)-ENRGY(II))*(SIG(I)-SIG(II))+
     1SIG(II)
    4 CONTINUE
      AMBDA=1./SIGMA
      RETURN
      END
```

```
      SUBROUTINE ANGLES
      COMMON/MC/STO(7,1024),NCOLL,CTHO,CTH,STH,PHI,CPHI,SPHI,EGY,CPHIO,
     1SPHIO,EO,SIGO,AMBOA,N,IRA,IRB,IRC,IRD,IFLAG,MAXCOLL,SIG(20),LCHR,
     2ENRGY(20),LMAX,XO,YO,ZO,X,Y,Z,ECUT,CLAB,THICK(11),NMAX,ZMIN,ZMAX
     3,NPRNT,AMASS,RATIO,CTHC
      DATA TWOPI/6.283185307/
      COM=(1.+AMASS*CTHC)/((1.+AMASS)*SQRT(RATIO))
      SOM=SQRT(1.-COM**2)
      CALL RN2(IRC,RC)
      RHO=TWOPI*RC
      CRHO=COS(RHO)
      SRHO=SIN(RHO)
      STH1=STH
      CTH1=CTH
      CTH=CTH1*COM+STH1*SOM*CRHO
      STH=SQRT(1.-CTH**2)
      IF(STH1.EQ.0.0.OR.STH.EQ.0.0) GO TO 1
      C1=(COM-CTH*CTH1)/(STH*STH1)
      S1=SRHO*SOM/STH
      CPHI1=CPHI
      SPHI1=SPHI
      CPHI=CPHI1*C1-SPHI1*S1
      SPHI=CPHI1*S1+SPHI1*C1
      GO TO 2
    1 CPHI=CRHO
      SPHI=SRHO
    2 CONTINUE
      PHI=ATAN2(SPHI,CPHI)
      RETURN
      END
```

```
      SUBROUTINE SCORE
      COMMON/MC/STO(7,1024),NCOLL,CTHO,CTH,STH,PHI,CPHI,SPHI,EGY,CPHIO,
     1SPHIO,EO,SIGO,AMBDA,N,IRA,IRB,IRC,IRD,IFLAG,MAXCOLL,SIG(20),LCHR,
     2ENRGY(20),LMAX,XO,YO,ZO,X,Y,Z,ECUT,CLAB,THICK(11),NMAX,ZMIN,ZMAX
     3,NPRNT,AMASS,RATIO,CTHC
      LCHR=LCHR+1
      STO(1,LCHR)=Z
      STO(2,LCHR)=CTHO
      STO(3,LCHR)=CTH
      STO(4,LCHR)=STH
      STO(5,LCHR)=PHI
      STO(6,LCHR)=EGY
      STO(7,LCHR)=FLOAT(NCOLL)
      IF(LCHR.LT.LMAX) GO TO 1
      WRITE(2)((STO(K,L),K=1,7),L=1,LMAX)
      IF(NPRNT.NE.0) PRINT 2,((STO(K,L),K=1,7),L=1,LMAX)
    2 FORMAT(1X,7E16.9)
      LCHR=0
      DO 3 K=1,7
      DO 3  L=1,LMAX
      STO(K,L)=0.0
    3 CONTINUE
    1 CONTINUE
      RETURN
      END
```

```
      SUBROUTINE SUMRY(IGO)
      COMMON/MC/STO(7,1024),NCOLL,CTHO,CTH,STH,PHI,CPHI,SPHI,EGY,CPHIO,
     1SPHIO,EO,SIGO,AMBOA,N,IRA,IRB,IRC,IRO,IFLAG,MAXCOLL,SIG(20),LCHR,
     2ENRGY(20),LMAX,XO,YO,ZO,X,Y,Z,ECUT,CLAB,THICK(11),NMAX,ZMIN,ZMAX
     3,NPRNT,AMASS,RATIO,CTHC
      DIMENSION TRAN(10,41),BACK(10,41)
      DIMENSION EGG(10),EG2(10),COUNT(10)
      DIMENSION SBK(10,41),STR(10,41)
      DIMENSION AVT(10,41),AVB(10,41)
      DATA EPSL/0.0001/
      DATA THICK/2.5,5.0,7.5,10.0,12.5,15.0,17.5,20.0,22.5,25.0,1000./
      DATA ITER/2/
      DATA STR,SBK,AVT,AVB/410*0.,410*0.,410*0.,410*0./
      NFILES=0
    1 FORMAT(I5)
      IF(NFILES.EQ.0) GO TO 1000
      DO 2 K=1,NFILES
      DO 3 I=1,10
      READ(3) II,TK
      DO 4 NC=1,MAXCOLL
      READ(3) NQ,TRAN(I,NC),BACK(I,NC)
    4 CONTINUE
    3 CONTINUE
    2 CONTINUE
 1000 DO 1001 J=1,41
      DO 1001 I=1,10
      EGG(I)=EG2(I)=COUNT(I)=0.0
      TRAN(I,J)=BACK(I,J)=0.0
 1001 CONTINUE
  100 READ(2)((STO(K,L),K=1,7),L=1,LMAX)
      DO 101 L=1,LMAX
      IF(STO(2,L).EQ.0.0.AND.STO(6,L).EQ.0.0)GO TO 500
      IF(STO(7,L).NE.0.) GO TO 5
      IOLD=1
      IF(ITER.EQ.1) WF=STO(2,L)/FLOAT(NMAX)
      IF(ITER.EQ.2) WF=1.0/FLOAT(NMAX)
      IZTOP=1
      GO TO 101
    5 Z=STO(1,L)
      NC=IFIX(STO(7,L)+0.0001)
      EGG(NC)=EGG(NC)+STO(6,L)*WF
      EG2(NC)=EG2(NC)+WF*(STO(6,L))**2
      COUNT(NC)=COUNT(NC)+WF
      IF(Z.GT.ZMIN) GO TO 6
      IF(IZTOP.GE.10) GO TO 101
      DO 11 IB=IZTOP,10
      BACK(IB,NC)=BACK(IB,NC)+WF
   11 CONTINUE
      GO TO 101
    6 DO 10 IZ=1,11
      IF(Z.GT.THICK(IZ)) GO TO 10
      IF(IZ.EQ.1) GO TO 101
      IS=IZ
      IF(IS.LE.IZTOP) GO TO 101
      IZTOP=IS
      IQ=IS-1
      DO 12 IT=IOLD,IQ
```

```
      TRAN(IT,NC)=TRAN(IT,NC)+WF
   12 CONTINUE
      IOLD=IZTOP
      GO TO 101
   10 CONTINUE
  101 CONTINUE
      GO TO 100
  500 PRINT 74
      FLT=FLOAT(ISO)
      DO 801 I=1,10
      DO 801 NC=1,MAXCOLL
      STR(I,NC)=STR(I,NC)+TRAN(I,NC)**2
      SBK(I,NC)=SBK(I,NC)+BACK(I,NC)**2
      AVT(I,NC)=AVT(I,NC)+TRAN(I,NC)
      SBK(I,NC)=SBK(I,NC)+BACK(I,NC)**2
      AVT(I,NC)=AVT(I,NC)+TRAN(I,NC)
      AVB(I,NC)=AVB(I,NC)+BACK(I,NC)
  801 CONTINUE
      DO 501 I=1,10
      IF(ITER.EQ.1)PRINT 75
      IF(ITER.EQ.2)PRINT 76
      WRITE(3)ITER,THICK(I)
      PRINT 503,THICK(I)
      DO 502 NC=1,MAXCOLL
      NQ=NC-1
      AV1=AVT(I,NC)/FLT
      AV2=AVB(I,NC)/FLT
      STD1=SQRT(STR(I,NC)/FLT-AV1**2)
      STD2=SQRT(SBK(I,NC)/FLT-AV2**2)
      PRINT 504,NQ,AV1,STD1,AV2,STD2
      WRITE(3)NQ,TRAN(I,NC),BACK(I,NC)
  502 CONTINUE
  501 CONTINUE
  503 FORMAT(//////,1X,*THICKNESS=*,F5.2/)
  504 FORMAT(1X,I5,4E16.9)
   74 FORMAT(*1*)
   75 FORMAT(1X,*COSINE SOURCE*/)
   76 FORMAT(1X,*ISOTROPIC SOURCE*/)
      MX=MAXCOLL-1
      DO 80 NC=1,MX
      IF(COUNT(NC).LE.EPSL) GO TO 80
      EGB=EGG(NC)/COUNT(NC)
      VAR=EG2(NC)/COUNT(NC)-EGB**2
      STD=SQRT(VAR)
      PRINT 81,NC,EGB,VAR,STD
   81 FORMAT(1X,*ORDER OF SCATTERING =*,I5,2X,*AVERAGE ENERGY =*,E16.9,2
     1X,*VARIANCE=*,E16.9,2X,*STD. DEV. =*,E16.9)
   80 CONTINUE
      REWIND 2
      RETURN
      END
```